With the support of the Erasmus+ Programme of the European Union

University of Évora

ARCHMAT
(*Erasmus Mundus Joint Master in ARCHaeological MATerial Science)*

Mestrado em Arqueologia e Ambiente

Studies of the effect of nanoconsolidants on mural paint layers

Berenice Baiza Martínez
m43716

Penka Ilieva Girginova
(Supervisor - Universidade de Évora)

Milene Gil Duarte Casal
(Co-supervisor - Universidade de Évora)

Paula Cristina Gonçalves Pereira Galacho
(Co-supervisor - Universidade de Évora)

Évora, Portugal, November 2020

Universidade de Évora

ARCHMAT
(*ERASMUS MUNDUS JOINT MASTER in ARCHaeological MATerial Science)*

Mestrado em Arqueologia e Ambiente

Estudos do efeito de aplicação de nanoconsolidantes em camadas cromáticas

Berenice Baiza Martínez
m43716

Penka Ilieva Girginova
(Orientador - Universidade de Évora)

Milene Gil Duarte Casal
(Co-orientador - Universidade de Évora)

Paula Cristina Gonçalves Pereira Galacho
(Co-orientador - Universidade de Évora)

Évora, Portugal, Novembro 2020

ARISTOTLE UNIVERSITY OF THESSALONIKI

UNIVERSIDADE DE ÉVORA

SAPIENZA UNIVERSITÀ DI ROMA

JURY

Chair: Prof. Dr. Nicola Schiavon

Principal Investigator Invited - University of Évora

Examiner: Prof. Dr. António José Estevão Grande Candeias

Associate Professor with aggregation - University of Évora

Advisor: Dr. Penka Ilieva Girginova

Researcher - University of Évora

Member: Prof. Donatella Magri

Associate Professor - Università di Roma La Sapienza

ABSTRACT

This research has been focused on the comparison of the effect and impact of three consolidants on mural paint layers with lack of cohesion. The experiments were carried out *in vitro* with a laboratory synthesized nanolime (HERCULES nanolime), a commercial nanolime (CaLoSiL® IP25), and with commercial acrylic resin (Primal ™ SF-016 ER®). Two sets of replicas of mural paint layers, *buon* fresco and lime fresco, were prepared with red and yellow ochre and smalt pigments. Both pictorial techniques and pigments are found in historical mural paintings in the Alentejo region of Portugal.

The characterization and comparison analysis of the paint layers before and after treatment with the three consolidant materials at different time intervals (right before, in one week and in one moth) were carried out with photographic documentation in visible (Vis) and ultraviolet fluorescence induced in visible (UVF), Optical microscopy (OM-Vis), colorimetry and spectrometry and Scanning Electron Microscopy coupled with Energy Dispersive X-ray Spectroscopy (SEM-EDS). Experimental work also included synthesis of nanolime and its characterization by X-ray diffraction (XRD), Scanning Electron Microscopy (SEM), Fourier-transform infrared spectroscopy (FTIR), Thermogravimetry Analysis (TGA-DTG) and Dynamic light scattering (DLS).

This study has indicated that the HERCULES nanolime has potential to be used effectively for consolidation of fresco paintings affected by lack of cohesion and it represent a viable alternative to organic consolidants.

Key words: *Cultural Heritage, Conservation*, *Nanolime, Synthesis, Consolidation, Frescoes paintings.*

Estudos do efeito de aplicação de nanoconsolidantes em camadas cromáticas - RESUMO

O trabalho apresentado teve como principal objetivo o estudo comparativo do efeito da aplicação de três consolidantes em pintura mural com falta de coesão. Os ensaios foram realizados *in vitro* com uma nanocal sintetizada no laboratório (HERCULES nanolime), uma nanocal comercial (CaLoSiL® IP25) e uma resina acrílica comercial (Primal ™ SF-016 ER®). Foram preparados dois conjuntos de réplicas de pintura mural recorrendo às técnicas de *buon* fresco e fresco em cal, e utilizando, como pigmentos, os ocres vermelho e amarelo e o azul esmalte. Tanto as técnicas pictóricas como os pigmentos utilizados são frequentemente encontrados em pinturas murais históricas da região do Alentejo, em Portugal.

A caracterização e análise comparativa das pinturas murais, após a aplicação dos três materiais consolidantes, realizou-se em três períodos de tempo distintos: imediatamente após a sua aplicação, ao final de uma semana e ao final de um mês. As técnicas de análise utilizadas foram a fotografia no visível (Vis) e a fluorescência de ultravioleta induzida no visível (UVF), a Microscopia Ótica (OM), a Colorimetria e Espectrometria, e a Microscopia eletrónica de varrimento acoplada a espectroscopia de raios X dispersiva de energia (MEV-EDS). O trabalho experimental incluiu a síntese de nanocal e sua caracterização por recurso às técnicas de difração de raios X (DRX), Microscopia eletrónica de varrimento acoplada a espectroscopia de raios X dispersiva de energia (MEV-EDS), Espectroscopia de infravermelho por transformada de Fourier (FTIR), Análise Termogravimétrica (TGA-DTG) e Espalhamento Dinâmico de Luz (DLS).

Este estudo revelou que nanocais apresentam potencial para serem usadas na consolidação de pinturas murais a fresco afetadas pela falta de coesão e representam uma alternativa viável aos consolidantes orgânicos.

Palavras-chave: Património Cultural, Conservação, Nanocal, Síntese, Consolidação, Pintura a fresco.

Acknowledgements

I would like to express my gratitude to my academic supervisors Dr. Penka I. Girginova, Dr. Milene Gil and Prof. Cristina Galacho for their support, guidance and patience during my research and studies in the HERCULES Laboratory. I highly appreciate the opportunity to meet and work with you three, and enrich my learning. They have helped me realize that conservation and material development are the field I would like to work in.

My most sincere gratitude goes to Dr. Penka I. Girginova, who strongly advocated transferring all her knowledge to me with remarkable patience to my mistakes which for I can't be more grateful. She provided constant help over millions of Zoom meetings and became a pushing hand along the way. She helped me develop my critical thinking skills, my writing, my results and understand the knowledge when I did not. Her passion for her work has inspired me and she is definitely a role model for my career.

I would like to thank the master's program the ARCHMAT consortium for providing this incredible and important opportunity to improve my career. And giving me the opportunity of meeting many unique and amazing people.

To the team of HERCULES laboratory, specially Dr. Luis Dias for helping with the settings for SEM equipment which was a crucial part of this research.

To Professor Antony Burke and Dr. Elisabete Caeiro, from the Chemistry Department of Èvora University, for the Dynamic light scattering (DLS) analyses.

To all my colleagues of ARCHMAT 2018/2020 which whom I have shared many wonderful moments. I would like to highlight Letícia Gondim, Deniz Kabil, Athina Trebicka, Islam Shaheen, Luka Bruketa, Degsew Zerihun, Tawanda Mushweshwe and Shivani Rajwade for their love, support and perhaps to some of their unconscious comments that have marked my life in a better way.

Thanks to my family who has always been there for me, encouraged me and for not put limits to the things I want to do but instead helping me achieve them.

TABLE OF CONTENTS

List of symbols and abbreviations

Vis	Visible
UVF	Ultraviolet flourescence
FT-IR	Fourier-transform infrared spectroscopy
TGA-DTG	Thermogravimetry analysis
SEM-EDS	Scanning Electron Microscopy coupled to Energy Dispersive X-ray Spectrometry
XRD	X-ray diffraction
OM	Optical Microscopy
DLS	Dynamic light scattering
NPs	Nanoparticles
CaLoSiL®	CaLoSiL® IP25
Primal®	Primal ™ SF-016 ER®
rLF	Red ochre lime fresco replicas
rBF	Red ochre *buon* fresco replicas
yLF	Yellow ochre lime fresco replicas
yBF	Yellow ochre *buon* fresco replicas
bLF	Smalt lime fresco replica
Ø	diameter
R%	Reflectance

List of Figures

List of Tables

List of Appendices

1. Introduction

1.1. Introductory considerations

Cultural heritage is the bond we have with the past, with knowledge, with culture, with traditions, with nature. It is a book full of mysteries waiting to be discovered and lessons to learn from. Its importance is crucial to us, as it is a testimony of our predecessors. It is evidence of how humanity has evolved, people's achievements and mistakes. The United Nations Educational, Scientific and Cultural Organization (UNESCO) defines heritage as our legacy from the past, what we live with today, and what we pass on to future generations. Our cultural heritage is an irreplaceable source of life and inspiration [1]. Therefore it needs to be protected and cared for.

Mural paintings are a fundamental part of cultural heritage**,** they are expressions of people and societies and have existed even before humanity could write. Their concept has changed through time. From a simple form of communication, they have become artistic expressions that show the ideas, ideals, and issues humanity has experienced. According to the International Council on Monuments and Sites (ICOMOS) mural paintings form an integral part of the monuments and places of patrimonial value and should be preserved *in situ* whenever possible [2].

Mural paintings are influenced by environmental factors that change their structure and composition and cause deterioration. Some of the causes of their decay are excessive moisture, pollution, human interventions, thermal variation, light exposure, wind erosion, biological action, and inherent defects of the materials employed to produce them [3-6]. The resulting alterations can vary from aesthetic modifications (e.g., loss of brightness, discoloration of pigments, dip staining, blackening) to structural damage (e.g., flacking of paint layers, fracturing, loss of cohesion) or even to changes in the mechanical stress of the artwork (e.g., of efflorescence impact) [6-8].

This study aims to address deterioration by lack of cohesion of mural paint layers. Loss of cohesion occurs when pigment particles in a paint layer become exposed and gradually loose from the binder. When this phenomenon is observed it urges the need for a consolidation treatment.

Consolidation in a porous material is an irreversible process; therefore it is a challenge for conservators. Before any intervention takes place it is necessary to respect the integrity and nature of the material, the elaboration technique, and the aesthetic of the masterpiece to treat [9]. Yet, consolidation depends not only on the properties of the decayed substrate, but on different factors concerning the consolidant: type, concentration, solvent, and the application technique [10].

Different types of consolidants have been used in the consolidation of mural paintings for the last century, such as acrylic polymers, organosilicates, baryta water, and lime water [10]. The application of such consolidants has been successfully used but also have caused a number of drawbacks. For example, acrylic resins while being one of the most used consolidants for *in situ* intervention have low penetration that may produce a hard crust that blocks water permeability in the substrate when not used carefully [11,12]. During the last decades [13], nanoconsolidants have been studied as an alternative to traditional consolidants. Having the advantages of nanomaterials, they are expected to have improved properties and open a new field for research [14]. Nanoparticles of calcium hydroxide ($Ca(OH)_2$) dispersed in alcohol, known as nanolime, have become a material of interest for the consolidation of lime-based mural paintings.

The consolidation of paint layers of mural paintings or other architectural surfaces is associated with the notion of material compatibility [15]. In this context, this thesis focuses on the study of nanolime as an effective nanoconsolidants for the conservation and restoration of fresco paintings. For this research, nanolime was selected since both fresco and nanolime are based on

lime. Their main function is to increase the cohesion between the paint layer and the pigment particles of the substrate and to strengthen the porous lime mortar [13,16]. Their size makes nanolime consolidant more reactive in porous media and increases the concentration of active component. The high surface of the nanoparticles (NPs), influences their chemical reactivity producing consistent consolidation of the treated substrates only after a few days of application by the carbonatation of $Ca(OH)_2$ [13]. At a deeper level, the nanolime consolidant can decrease the tendency of the matrix to absorb liquid water, as a consequence of being dispersed in alcohol [13,17]. Which in return, contributes to the prevention of risks related to activation of soluble salts (efflorescence) caused by moisture; in this way overcoming the limitations of lime-water ($Ca(OH)_{2\ (aq)}$) consolidation: low solubility with water (H_2O) limiting the amount of consolidant that enters the porous system of the treated substrate, substrate dissolution, freeze-thaw deterioration, and weathering by salt formation [13,15,17].

1.2. Object of study and research aims

This master thesis research took place in HERCULES Laboratory of the University of Évora, Portugal, as a part of the Erasmus Mundus Archaeological Materials Science Joint Master's Degree (ARCHMAT).

The thesis research topic has emerged in the frame of ongoing research in Laboratory HERCULES, consisting of the development of novel nanomaterials for Cultural Heritage. In particular, nanoconsolidants for conservation and restoration of lime-based cultural heritage (e.g., mural paintings, stone, and mortars) have been explored.

The overall purpose of this research was to study the effect and impact of three consolidant products; laboratory synthesized nanolime (HERCULES nanolime), commercial nanolime CaLoSiL® IP25 and commercial acrylic resin dispersion Primal™ SF-016 ER®; on the paint layer of fresco paintings and provide knowledge of the usage of nanoconsolidants one of the biggest concerns of conservators-restores. The main goals were: 1) to test, ascertain and compare

the effect of the consolidant products on fresco mural paint layers of natural pigments (ochres and smalt) affected by lack of cohesion, and 2) to synthesize and characterize nanolime consolidants (HERCULES nanolime).

Goal 1 was achieved by recording and analyzing with different complementary techniques if the application of the three consolidants modifies the color of the paint layer or induces other kind of chemical alteration in the paint layer composition. The effect of the HERCULES nanolime was compared to the effect of commercial nanolime CaLoSiL® IP25 and of the commercial Primal™ SF-016 ER®, an acrylic resin world wide used in the past in adhesion and consolidation of mural paintings. The analytical setup comprised photographic documentation in visible (Vis) and ultraviolet fluorescence induced in visible (UVF), Optical Microscopy (OM), Spectra-colorimetry, and Scanning Electron Microscopy coupled to Energy Dispersive X-ray Spectrometry (SEM-EDS).

Goal 2 was approached by using an established synthesis route in the Laboratory HERCULES and using complementary characterization techniques. The characterization of the nanolime was carried out with X-ray diffraction (XRD), Scanning Electron Microscopy (SEM), Fourier-transform infrared spectroscopy (FT-IR), and Thermogravimetry Analysis (TGA).

1.3. Research objectives

In order to achieve the research main goals, several objectives were defined:

- ✦ To make a bibliographic overview of nanolime applied as a consolidant in cultural heritage, specific for consolidation of fresco mural paintings and limestone;

- ✦ To successfully synthesize and characterize a nanolime developed in Hercules laboratory (HERCULES nanolime), consisting of Calcium Hydroxide ($Ca(OH)_2$) nanoparticles (NPs) dispersed in different media/or solvents;

✦ To prepare two sets of mural painting replicas in *buon* fresco and lime fresco techniques using pigments historically found in mural paintings, such as ochres (yellow and red) and smalt pigments;

✦ To apply the three consolidants under study into the paint layers with lack of cohesion-The commercial products, nanolime CaLoSiL® IP25 and the acrylic resin dispersion Primal™ SF-016 ER® were selected for this study for comparison reasons;

✦ To compare the effectiveness and impact of the three consolidants tested on the paint layers;

✦ To assess the suitability of the application of HERCULES nanolime as a consolidant.

1.4. Thesis structure

This thesis will be structured into four parts:

Part 1 (Introduction) provides some introductory considerations, and an overview of the object of study, research aims and objectives, and thesis structure.

Part 2 (Literature review) includes a brief introduction to frescoes and overview of the state of the art of consolidation treatments of mural paintings and nanolime synthesis and application.

Part 3 addresses the methodology, experimental conditions, and main results and their discussion.

Part 4 discusses the conclusions obtained from the comparison of the three consolidant products.

2. Literature review

2.1. Fresco technique (a brief introduction)

"Of all the methods painters employ, fresco painting is the most masterly and beautiful because it consist in doing in a single day that which, in other methods, may be retouched day after day, over the work already done"

Giorgio Vasari, Italian painter, (1511-1574)

According to its etymology, fresco refers to any painting executed on a fresh plaster whilst still moist in such a way that the pigments are fixed by the carbonatation of the lime ($Ca(OH)_2$) contained in the plaster ground [18]. Classical frescoes are commonly composed of three layers: the *arriccio,* the *intonaco* and the paint layer (Figure 1) [19]. The inner coarser layer in contact with the wall structure is called *arriccio.* The intermediate thinner layer, called *intonaco,* represents a plaster composed of a mixture with higher lime content and finer sand than the one found in *arriccio*. The paint layer of a *buon* fresco is executed on the freshly prepared and wet *intonaco*.

Figure 1. *Fresco stratigraphy.*

When the rendering begins to dry, the saturated $Ca(OH)_2$ solution migrates towards the surface where it reacts with the CO_2 to form $CaCO_3$, as water evaporates [Eq.1].

$$Ca(OH)_{2\ (s)} + (H_2O + CO_2)_{(g)} \rightarrow CaCO_{3\ (s)} + 2H_2O_{(g)} \quad \text{Eq.1}$$

During the course of this reaction, the pigments become bounded by the crystallization of the superficial carbonate, which fixes them to the wall making the painted image become permanent [19]. The carbonatation takes place from the surface inwards and after a certain time forms a surface curst which slows down the reaction within [18].

In *buon* fresco the pigments are mixed with pure water, while in lime fresco the pigments are mixed with lime water ($Ca(OH)_{2(aq)}$) or milk of lime. In both cases the pigments are fixed by carbonatation reaction [Eq. 1] but what differentiate the two techniques are the $Ca(OH)_2$ sources. Their main difference, stratigraphical speaking is the thickness of the resultant paint layer (Figure 2).

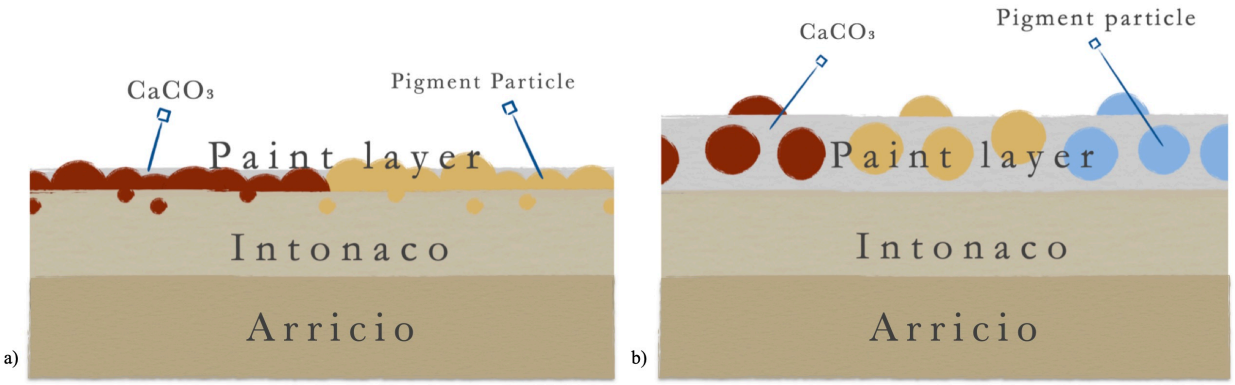

Figure 2. *Stratigraphies of fresco techniques: a) Buon frescos (pigment combined with water), b) Lime fresco (pigment combined with lime water or milk of lime).*

2.2. Mural paintings consolidation

Lime-based materials, such as *fresco* mural paintings and limestone, can be object of constant degradation processes that changes their structure and composition, therefore they should be consolidated. Consolidation is performed to strengthen their crystalline network, to improve the mechanical resistance within their structure, and slowdown their natural decay. In mural paintings, consolidation treatment is performed to correct the stability and durability of different stratigraphic layers that compose them. To choose a suitable treatment, the precise aim for consolidation should be defined. Consolidation treatment depends on the nature and degree of deterioration and may consist of [18]:

- Reinforcement of the adherence of the paint layer to the support, in order to stop flaking;
- Reinforcement of the cohesion of the paint layer itself, weakened by the disintegration of the binding medium or by surface abrasive action of some kind, that leads to the powdering of color;
- Consolidation of the rendering (*intonaco/arriccio*) in depth like falling fragments; render from wall or disintegration of the binder of the renders;
- Temporary consolidation of paint layer in preparation for the cleaning of sulphated regions or to prepare when the detachment (separation) of the mural painting from the wall is necessary for its conservation.

After defining the consolidation purpose, the most suitable consolidant must be carefully selected for the particular task to be performed, remembering that interventions associated to consolidation must be performed always with respect to the individual characteristics of the decayed substrate and the overall characteristics of the mural painting, which is a subject of consolidation [2,17]. Organic and inorganic consolidants have been applied in fluid state by brush, spray, pipette or injection. Once the consolidant is applied, depending on the type of material used, the deposition of the consolidant may occur by different actions, for example by cooling (for the case of organic polymers), by solvent evaporation, by action of a chemical reaction, or by a combination of the enumerated actions [20]. Since the action of consolidation requires the

application of a foreign compound in the substrate, finding a highly efficient consolidant is an interdisciplinary challenge: material scientists have the task of developing the products, which must meet a broad range of requirements made by conservation scientists for suitable *in situ* application.

An effective consolidant must:

- ***Have affinity with the substrate network:*** From a chemical point of view, the consolidant should create strong chemical bonds between minerals and must not affect the crystalline structure on the substrate [8]. In addition, from the physical point of view, the treated substrate must demonstrate similar characteristics as the original material; for example, porosity, elastic modulus, and moisture and thermal expansion must not change after treatment [8], in order to not create additional tensions between treated and untreated areas of the substrate.

- ***Have a good depth penetration:*** Penetration depth is a key factor for the effectiveness of a consolidation treatment [8,17]. For effective consolidation, the consolidant should adhere to the granular structure from the micropores and extend gradually to the micropores without completely covering them. This makes possible to avoid eventual over-consolidation or the formation of a thin skin as the solvent dries out, which would trap the pigment particles instead of fixing them to the paint layer [17,18]. Penetration depends on the micro-structural characteristics of the substrate, the properties of the consolidant (e.g., suitable viscosity, concentration, and solvent volatility and polarity), the application method and environmental conditions [21,22].

- ***Improve the mechanical properties of the substrate,*** to a similar to the original sound substrate compressive strength and abrasion resistance.

- ***Modify pore structure, but not abruptly:*** Pore structure is closely related to the substrate network strength, resistance to salt crystallization, and water ingress and circulation within the structure [23]. When a fresco substrate is weathered, it generally presents higher porosity in the surface, therefore the consolidant should decrease the porosity, contribute to water

permeability, reduce the amount of capillary forces and increase mechanical strength to similar values of the untreated substrate [23,24]. Treatment should reduce the pores with diameter size between approximately 0.1 to 100 micrometers to reduce the structures' absorption of liquid moisture by capillarity and infiltration [25]. However an abrupt change in porosity should be avoided, since it can cause detachment of the surface layers due to salt crystallization [23]. Prior study and observation of the pore size and distribution (pore system), and the water penetration within the substrate is important.

- ***Preserve aesthetic characteristics of the original substrate:*** Consolidation treatments should improve the physical-mechanical properties of the treated material without affecting its aesthetic appearance [2,17]. In the specific case of mural paintings, color change is particularly important as it can alter the entire appearance and perception of a painting [26]. However, a possible side effect of most consolidation treatments is a chromatic variation of the surface caused by the treatment.

- ***Long term performance:*** the consolidant must have resistance to biological and atmospheric agents (e.g., humidity, and ultraviolet light), because any change to its optical or mechanical properties may affect the art work [18].

- Not form harmful by-products in the substrate, because by-products can accelerate degradation during aging. The consolidant should also enable future re-treatment with the same or different consolidant [17,21,27].

- ***Be non-toxic and environmental friendly:*** Consolidants and solvents must be designed and selected with respect to the environmental and human factors.

Both inorganic and organic consolidants have been used in consolidation of lime-based works of art. $Ca(OH)_2$ is the most compatible material for fresco, given the lime-based nature of the paintings. The oldest known treatment used for the protection and restoration of surfaces and maintenance of lime-based historical monuments is lime water ($Ca(OH)_{2(aq)}$), first used by ancient Greeks and more extensively used by Romans [17,28]. The use of lime in cultural heritage is based on the carbonatation reaction to $CaCO_3$ and on the characteristics of obtained $CaCO_3$.

The compatibility between lime and lime-based substrates makes $Ca(OH)_{2(aq)}$ highly suitable for consolidation treatment. However, its effectiveness is limited because of the low solubility of $Ca(OH)_2$ in water [29]. The use of large quantities of water can cause additional damage, such as chromatic alteration, substrate dissolution, freeze-thaw deterioration, weathering by activity of soluble salts formed and swelling clays [13,29].

In the 19th century the development in chemistry introduced other consolidation products for lime-based material (e.g., limestone, and lime mortar renders for mural paintings). Since the 20$^{'s}$ century silica-based materials (e.g., silicic acid esters, alkoxysilanes (e.g., TEOS), fluosilicates, and sodium, potassium and lithium silicates) have been used in the field of conservation of limestone [28]. The usage of thetraethoxysilane (TEOS) was patented by Laurie in 1926 yet, TEOS was not used for mural paintings until the 80s [17,28].

The application of organic compounds in conservation of mural paintings, such as acrylic polymers, epoxy resins and synthetic waxes, dates from the 1940$^{'s}$ century [17,28]. According to literature, acrylic polymeric resins were first applied for the consolidation of mural paintings in the 1940s in the ex-URSS and in Japan [17]. The polymers have been used in the re-adhesion of flaking parts of paint layers of mural paintings, because they were considered to be easy to apply, and because of their hydrophobic properties [29]. At the beginning they were thought to be highly resistant to aging and to be easily removable. However, later on, it was found that synthetic polymers can undergo degradation due to action of temperature (T), relative humidity (RH), saline solutions and UV-Vis light. These factors cause changes in the polymer solubility [27-29] and degradation, consequently accelerating the decay of the works of art by changing its physicochemical properties [13], resulting for example, in aesthetic alteration (discoloration). Furthermore, acrylic polymers have low penetration rate that can produce a hard crust that blocks water permeability in the substrate [11,12]. With the evolution of the treatment some of these drawbacks have been reduced by new formulations or by applying them diluted (e.g., Primal® used as 2%).

Due to the observed drawbacks of the organic consolidants, the traditional inorganic

consolidants have been reconsidered by scientists (e.g., lime water, calcium oxalates and barium hydroxide) [28,27]. Barium hydroxide ($Ba(OH)_2$) has been used as a consolidant for carbonaceous material since the middle of the 19th century. Ferroni-Dini's method was proposed for the use of aqueous solutions of $Ba(OH)_2$ in the consolidation of frescoes seriously damaged in the Florence floods in 1966 [29]. This method has been particularly applied to mural paintings affected by calcium sulphate damage. Yet $Ba(OH)_2$ is not fully compatible with lime-based mural painting matrix, as small amounts of barium (as barium carbonate or sulphate) are introduced to the calcium carbonate matrix after treatment [29].

For the last two decades, nanomaterials have emerged as a good alternative to traditional consolidants; due to their features some of the limitations of traditional consolidants can be overcome [13,31]. These materials exhibit unique properties, which are distinct comparing to their bulk analogues. The smaller dimensions of the nanoparticles ensure higher surface area and enhanced reactivity, which can favor use of smaller amount of consolidant, and good penetration in porous matrixes, when applied as solvent dispersion. Colloidal chemistry and nanotechnology provide effective tools to tailor the nanomaterials properties.

Some examples of nanomaterials used in conservation of lime-based substrates are combined with nanoparticles alkoxisilanes, nanosilica, in situ formed hydroxyapatite, calcium alkoxides ($Ca(OR)_2$) and alkaline earth metal hydroxide NPs dispersions (e.g., of barium ($Ba(OH)_2$), magnesium ($Mg(OH)_2$), strontium ($Sr(OH)_2$), and calcium ($Ca(OH)_2$ nanolime)) [13,28,29].

2.3. Nanolime synthesis and application

The development of nanolime for consolidation in Cultural Heritage has become an excellent approach to overcome the limitations of limewater treatment. Nanolime consists in $Ca(OH)_2$ NPs dispersed in short-chain alcohols (mostly ethanol, n-propanol and 2-propanol) in different concentrations [27,29]. If applied to frescoes and limestone, nanolime can enhance the strength and the cohesion in the porous decayed material. For example, in mural paintings, depending on the damage, it can enable very efficiently the bridging of the flaking parts and increases the

cohesion between the paint layer and the lime substrate [17,29,32]. For a good consolidation, the intake of optimal number of nanolime NPs into the substrate must be ensured. The NPs penetrate into the network as the alcohol carrier evaporates [27] and recreate the decayed network of calcium carbonate ($CaCO_3$) upon carbonatation in the presence of moisture. The overall carbonatation process is identical to the traditional lime carbonatation (see Eq. 1).

Conversion to $CaCO_3$ is fast and very efficient [33], due to the high reactivity of the NPs. Complete carbonatation can be achieved in the time frame between 24 hours and a maximum of 3-4 weeks after application [13,28,34], depending on the environmental conditions, penetration depth, solvent nature, and properties of the nanolime and of the treated substrate. These factors are particularly important as they influence the carbonatation process in terms of both morphology and type of $CaCO_3$ polymorphs (calcite, aragonite and vaterite) [28]. Among the $CaCO_3$ polymorphs, calcite is the most effective for consolidation due to its stability [35]. The polymorphs formation and stability can be influenced also by the alcohol solvent [28].

Self-assembled $Ca(OH)_2$ NPs can be prepared by several synthesis methods based either on the break down of bulk solids (mechanical, grinding or thermal decomposition), known as top-down approach, or on the reaction of different precursors mostly in solution, the bottom-up approach. Top-down approach can lead to large reaction yields, but cannot ensure monodispersity or shape and size control [31]. Several promising bottom-up approaches have been developed and optimized, e.g., precipitation method, homogeneous phase reaction, water/ oil micro emulsions, sol-gel synthesis, solvothermal reaction of metallic calcium, anion-exchange resins [28,29,31,36]. Issue of nanoparticles synthesis can be possible formation of undesirable by-products and possible self-aggregation, which can occur mainly due to electrostatic, dipolar and Van der Waals forces.

The use of short-chain alcohols as dispersing media for $Ca(OH)_2$ NPs brings many benefits to the nanolime comparing to other organic solvents (e.g., toluene, benzene, trichloroethylene, etc.) and inorganic solvents (e.g., water) used in consolidation treatment. Short chain alcohols wet the substrate effectively and allow the NPs diffusion inside the substrate, and improve particles

stability. In addition, they are not expected to dissolve salts of minerals in the substrate, are less toxic and more volatile than other organic solvents. The tendency for NPs agglomeration in short chain alcohol is lower in comparison to other organic solvents and water; in this way the risk of formation of a white haze on the substrate's surface is decreased [16,27,37].

Nanolime is not equally effective if applied to distinct substrates or under different conditions [13]. One of its limitations as a consolidant is in respect to its transport mechanism into the substrate. Laboratory tests have shown that although there might be considerable in-depth penetration of the alcohol, the degree of penetration of the $Ca(OH)_2$ NPs is not the same as of the alcohol [21,28], as the NPs can accumulate at or just under the surface of the treated material [13]. Additionally, their degree of carbonatation in lime-based mortars depends on the size and homogeneity of the colloidal particles, traits related to the degree of dispersion [33]. Moreover, the effectiveness of the application of nanolime has other variables (e.g. porosity of the substrate, T, and RH).

Treatment of frescoes with nanolime has been effective, where strengthening of the paint layer, renewed cohesion of the powdering paint layer and smoothing of the surface have been observed [16,38,39,40,41] (see Table 1). For example, in the blue paint layers of the ancient Roman frescoes of the Casa dei Cervi in Herculaneum excavation site, where the fresco had been previously treated with acrylic resins, the nanolime showed the ability to increase the mechanical strength of the substrate and to limit the decay due to the polymeric treatment [40,42]. There are also other cases in which nanolime has been applied in combination with other consolidants, such as $Ba(OH)_2$ NPs, micro emulsions, and alkoxysilanes with good results [15,43,44,45]. However the use of combinations depends strongly on the state of the art, when mural paintings are affected by soluble salts (e.g., sulphates and nitrates) [38,43,45], have been treated with other consolidants (e.g., acrylic polymers, and casein)[43], or when the nanolime dispersion alone is not enough to strengthen the substrate [15].

Several case studies of *in situ* application of nanolime dispersions (commercial - CaLoSiL® (IBZ-Salzchemie GmbH & Co. KG, Germany) and Nanorestore® (CSGI, Florence, Italy) - or

laboratory prepared) for consolidation of mural paintings have been reported, where pre-consolidation and consolidation have been considered (see Table 1). In most of the case studies the treated mural paintings were affected by flaking and powdering of the paint layer. In the majority of these cases, the application of the nanolime has been carried out by brush over a sheet of Japanese paper to protect the decayed surface [16,38,44,41,46]. Sometimes when the nanolime dispersion was of low concentrations (e.g., of 0.05, and 2.5 g/L) and applied for a minimum of 6 applications or until saturation, the Japanese paper has been previously wetted with ethanol to remove residual moisture in the surface [38,46]. However large amount of application of the $Ca(OH)_2$ NPs has led to negative results due to the appearance of a white haze. In fact, in several cases nanolime has induced chromatic change observed in the form of white haze. Such white haze appearance has been observed after treatment in the surface of discarded fragments of Mayan paintings from Cobá site in Quintana Roo, Mexico, which have been affected by the presence of sulphate salts, loss of cohesion and physical instability within the substrate [46]. Application by syringe has been preferred when the mural painting is affected by plaster loss, fissures or the absorption of the substrate is uneven [15,40]. Application by spray was considered by Vojtěchovský [15] for usage in test panels for the consolidation treatment of the paintings on the sealing of St. Isidor Chapel in Křenov, in Czech Republic [15]. This type of application ensures uniform application and restricts the amount of the fluid applied to the substrate. The highest concentration used was of 25 g/L in a fresco affected by delamination of the paint layer with good results[40].

Although a large range of concentrations can be effective for the enhancement of the mechanical strength of the substrates of different deterioration rates, concentration and number of applications should be considered very carefully in order to avoid enhancement of the white haze in mural paintings. It has been suggested that nanolime should be applied in lower concentration (0.05 to 5 g/L) with several applications [16,21,22,29,47]. However, in spite of concentration and number of applications, the appearance of the white haze might be also due to the characteristics of the nanolime that influence its behavior during consolidation, such as particle size, shape, size distribution (dispersity), nature of the solvents used, crystalline

domains, presence of defects, and particles agglomeration during synthesis [29]. Furthermore, formation of the white haze could also be due to selective migration of the solvent and the NPs during absorption, back migration of the NPs towards the surface during drying or the quick evaporation of the solvent, which does not allow full particles penetration in the substrate [15,28,40].

The total amount of nanolime dispersion to be applied should be preferably defined by preliminary tests, as saturation is not always necessary [23]. If possible, freshly prepared dispersion should be applied, given that the long storage can cause carbonatation before application, formation of alkoxide or particles agglomeration, which can decrease the available area for carbonatation. It is also possible to slow down evaporation of the solvents and the carbonatation rate of the NPs when hydroxypropylcellulose is applied in the first 24 hours after the treatment [40]. In some cases the addition of small amounts of acetone, cyclohexane or water to the nanolime dispersions is suggested to create a destabilizing effect in the kinetics of the colloid and to possibly favor the deposition of the NPs [29,40,48,49]. Concerning white haze formation it has been recently found that wetting the surface with water after application can reduce the effect, yet not eliminate it [15].

Table 1. *Case studies of nanolime application on mural paintings from 2000 to 2017.*

Reference	Mural painting	State of the art	Application method	Nanolime used	Results
Giorgi et al. 2000 [44]	Mural paintings by Andrea da Firenze (14th century) in the Spanish Chapel of the green Cloister of Santa Maria Novella church, Florence Italy	Paint layer affected by flaking and powdering	2 applications by brush over Japanese paper followed by 7-10 days of setting	Slacked lime particles (3-4μ) in 1-propanol (5 g/L) in combination with Ferroni Dini method	*Strengthening of the painting and re-cohesion of upper painted layers* / excellent overall effects
Ambrosi et al. 2001 [16]	Frescoes by Santi di Tito (16th century) Gli Angeli Musicanti on the Counterfacade of the Santa Maria del Fiore Cathedral in Florence, Italy	Paint layer affected by flaking	2 or 3 applications by brush over Japanese paper	Nanolime dispersion in propanol (1- 5 g/L)	*Strengthening and re-adhesion of the painting/* Highly positive effects
Dei 2004 [28]	Mural painting in Avnso Church, Copenhagen, Denmark	—	—	—	—
Dei 2004 [28]	Mural of Conrad Albrizio (1938) found in Stare Exhibit Museum, Shreveport, USA	—	—	—	—

Dei et al. 2005 [47]	14th century fresco of the Chapella del Podestà of Bargello Palace museum in Florence, Italy	Paint layer affected by flaking and powdering	—	$Ca(OH)_2$ dispersions in 2propanol	Cohesion and smoothing effects in the surface/Positive results
Dei and Salvadori 2006 [47]	13th century Medical fresco in the Saint Zeno Church in Verona, Italy	Paint layer affected by flaking and powdering	Applied till saturation by brush over Japanese paper wet with ethanol	$Ca(OH)_2$ dispersions in 2-propanol (0.05 g/L, containing 2% of water by weight)	Cohesion and smoothing effects in the surface/Positive results
Dei et al. 2007 [28]	14th century mural by Agnolo Gaddi in the church of Santa Croce, Florence, Italy	—	—	—	—
Baglioni and Giorgi 2006, Giorgi et al. 2010, Baglioni et al. 2013 [22,29,38]	Mural paintings of early classic Mayan period in Calakmul, Campeche, Mexico	Paint layer extensive powdering and presence of sulphates	Applied by brush over Japanese paper	Nanorestore® (5 g/L) combined with $Ba(OH)_2$ NPs particles (20% of total NPs)	Effective consolidation in environmental conditions (T: 30 ºC and RH 99%)
2007 [28]	Mural painting in Villa del Bene, Verona, Italy	—	—	—	—
Garreau 2007 [43]	Medieval paintings in Vendel Church, Sweden (malachite and azurite pigments)	Paint layer affected by flaking previously consolidated with casein, and presence of salts	Apply ME and purified water compresses over Japanese paper, then take out the paper and while wet add nanolime till saturation, wet surface once or twice and leave to dry slowly	Wet-in-wet system of oil in water ME and nanolime	Most effective treatment
Grimaldi 2008 [46]	Tlaxcaltec Murals *La Batalla y Templo Rojo* of Cacaxtla, Tlaxcala, Mexico	—	—	—	—
Baglioni et al. 2009 [28]	Mural painting of Filippo Lippi in Prato Cathedral, Italy	—	—	—	—
Piaszczynski 2010 [28]	Mural painting in Mersh Luxemburg	—	Injection	—	—
D´Armanda and Hirst 2012 [50]	Medieval mural painting at All Saints Church in Little Kimble, Buckinghamshire, UK	The paintings where quite stable however the walls exhibited many plaster repairs that were in bad conditions and were affected by efflorescence	10 applications, filling fine cracks adjacent to the delaminating plaster and paint layers in need of stabilization	CaLoSiL® dispersed in Ethanol	Positive effects with out any visual changes in the surface
Dahene and Herm 2013 [40]	Ancient Roman frescoes of the Casa dei Cervi in Herculaneum excavation site, Naples, Italy (blue paint layers)	Delamination of the paint layers cause by salt efflorescence, previously treated with acrylic resin	—	CaLoSiL® E25	Surface flattened and consolidated

Dahene and Herm 2013 [40]	Mural painting on dolomitic lime plaster in Leuben Castle, Germany	Plaster loss and fissures	Injection	CaLoSiL® E50 with hidroxilpropylcellulose solution in ethanol and water (1% v/v)	Strengthenig of the mortar, and cohesion in the paint layer
Bartoli 2013 [228]	Roman mural painting in Domus Aurea, Rome, Italy	—	—	—	—
Chelazzi et al. 2013 [45]	Mixtec tomb mural paintings drawn in a carbonate substrate with *a secco* technique using polysaccharide as binder in Ixcaquixtla , Puebla, Mexico	Detachment and flaking of pain layers and severe degradation of pigments due to salts (sulphates and nitrates) and formation of biofilms	—	Nanorestore® (2.5 g/L) in 2 propanol in combination with Ferroni Dini method	Effectively consolidated, fixing the pigments
Natali et al. 2014 [41]	Historical graffiti in Palazzo Chiaromonte-Steri, Palermo, Italy (Ground clay brick red pigment dispersed in organic medium)	Affected by salt efflorescence and pigment was powdering	10 successive applications by brush over Japanese paper	Nanorestore® 0.06% wt/vol %	Surface became more compact and strengthened. No white haze appearance
Natali et al. 2014 [41]	18th century lunettes belonging to Saint Jude and Simon cloister in Carolina, Florence, Italy	With lacunas and powdering of the paint layer	10 successive applications by brush over Japanese paper	Nanorestore® 0.06% wt/vol %	Strengthening on the pictorial surface , the powdering color film was completely re-adhered to the substrate consolidation took place from inner to outer
Alvarez and Nadal 2016 [46]	Parts of Mayan paintings from Cobá site in Quintana Roo, Mexico (green-blue pigment obtained from fresh leaves and stems of *Indigofera suffructicosa* combined with filosilicate)	Lack of cohesion and physical stability within the substrate presence of carbonated and sulphated salts	6 to 12 applications by brush over Japanese paper previously wetted with ethanol	Nanorestore® dispersed in ethanol 2.5 g/L	Increase of mechanical strength, appearance of white haze
Vojtěchovský 2017 [15]	Paintings on the sealing of St. Isidor Chapel in Křenov, Czech Republic (Brunt umber brown pigment)	Severely deteriorated, high RH	6 cycles of lime suspension by syringe/spray	CaLoSiL® E25 diluted to 5 g/L in combination with alkoxysilane	Effective no changes registered
[15]	St. Vitus Church in the submerged village of Zahrádka, Czech Republic	Extremely deteriorated	4 cycles of nanolime suspensions	Pure lime suspension of concentration of 5 g/L	Unsuitable

— : information not found, ME: Micro-emulsions, RH: relative humidity, NPs: nanoparticles

3. Comparison study of three consolidant products

3.1. Methodology

To carry out this research the methodology was divided into the following tasks:

A) Nanolime synthesis and characterization;

B) Selection of two commercial consolidants for comparison:

- **Primal™ SF-016 ER®** Acrylic polymer dispersion, (by Dow Coating Materials, United States of America): 50-51% of solid content. The dispersion was diluted at 2% in water which is a common concentration used the past conservation works. It will be referred as Primal®.

- **CaLoSiL® IP25** Nanolime, (by IBZ Salzchemie GmbH & Co. KG, Germany): concentration of 25 g/L Calcium hydroxide dispersed in iso-propanol. Particle size ≈ 150 nm. This dispersion will be referred as CaLoSiL®.

C) Preparation and aging at ambient conditions for a period of one month a set of 60 replicas of fresco mural paint layers of three layers (two lime mortar renderings layers and a paint layer). Red and yellow ochre, and smalt pigments were selected because they are among the most commonly used pigments in frescos all over the world. Smalt pigment is of particular interest because its presence is found in many 17th century fresco paintings in the Alentejo region showing different signs of physical and chemical deterioration.

D) Application of the three kinds of consolidant dispersions (HERCULES nanolime, CaLoSiL® and Primal®) over the fresco replicas and further analysis in time intervals to determine/and compare their effect on the paint layers.

3.1.1. HERCULES nanolime synthesis

Nanolime was synthesized by precipitation of calcium chloride ($CaCl_2$) aqueous solution in sodium hydroxide (NaOH) aqueous solution at temperature T_r = 90 ºC (**Figure 3a**).

The aqueous solutions of $CaCl_2$ (99.9% pure, Sigma-Aldrich) and NaOH (99.9% pure, Sigma-Aldrich) were prepared with ultra-pure water (Mili Q) with concentrations of 0.4M and 0.8M respectively. All chemicals were used as they were purchased without further purification (Appendix 1, A1-1).

Afterward, equal volumes of the aqueous solutions were heated under constant stirring until they reached the temperature of 90 ºC. During the heating process, 5 g of non-ionic surfactant Triton X-100 (t-Oct-C_6H_4-$(OCH_2CH_2)_xOH$) were added to the solution of $CaCl_2$, in order to reduce the time of synthesis and the agglomeration of the particles during the reaction process [33]. Once the temperatures of the solutions reached 90 ºC, the aqueous solution of NaOH was added drop wise for an hour to the aqueous solution of $CaCl_2$ and Triton X-100 under vigorous stirring. The reaction took place for an hour after the addition of NaOH was completed (Figure 3).

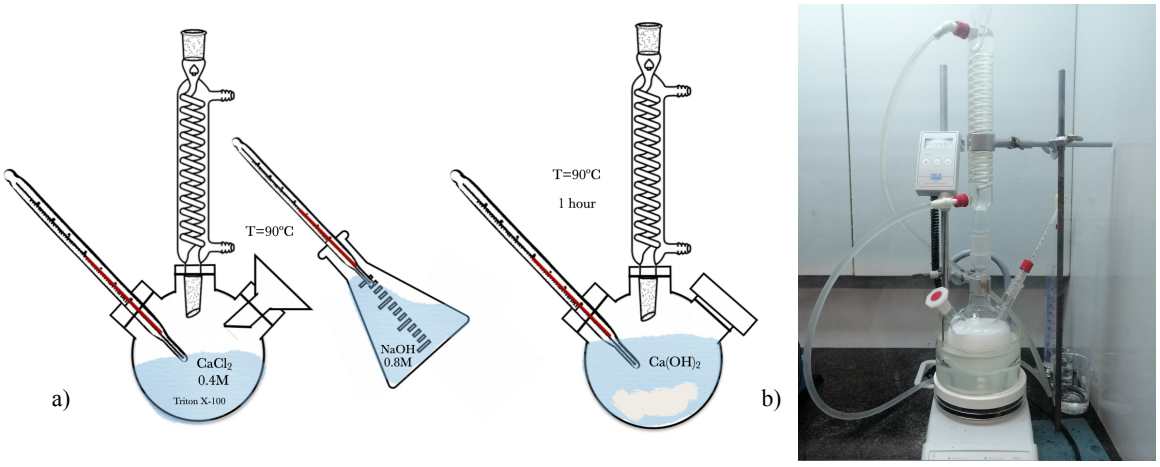

Figure 3. *Synthesis of $Ca(OH)_2$ nanoparticles: a) Synthetic scheme, b) Experimental setup.*

After slow cooling of the reaction mixture to room temperature under normal atmosphere the white precipitate of $Ca(OH)_2$ NPs was washed with Mili Q water with consecutive cycles of

agitation (vortex)/sonication (US bath)/centrifugation/decantation until the by-product of the reaction sodium chloride (NaCl) was removed. The presence or absence of chloride anions was confirmed with a silver nitrate test. Silver nitrate (0.1M $AgNO_3$) drops were added to the supernatant of the fourth wash to determine the absence of NaCl. By the lack of the appearance of a white precipitate due to the formation of silver chloride (AgCl) resulting from the reaction of silver nitrate ($AgNO_3$) and sodium chloride (NaCl) [Eq. 2].

$$NaCl_{(aq)} + AgNO_{3\,(aq)} \rightarrow NaNO_{3\,(aq)} + AgCl_{(s,\,white)} \quad \text{Eq. 2}$$

Once the white precipitation was not observed, Mili Q water was substituted by ethanol for the last wash, followed by a drying process at temperatures of 40-70 ºC. Later the $Ca(OH)_2$ NPs obtained were dispersed and stored in 2-propanol (99.9% pure, Sigma-Aldrich). Dispersions in different solvents were tested before the application in the fresco replicas (see Section 3.2.2).

3.1.2. Fresco replicas preparation

The sixty replicas of mural paintings were prepared under ambient conditions (Tº: 22 ºC and RH: 59%) in three steps:

a) Preparation of an inner layer of mortar with coarse sand and lime putty (*arriccio*);
b) Preparation of a superficial layer of mortar with marble powder and lime putty (*intonaco*);
c) Preparation of the paint mixtures for *buon* fresco (pigments + water) and lime fresco (pigments + lime milk) later laid down over the fresh layer of *intonaco*.

The composition of all materials used for the fresco replicas preparation (sand, marble powder, lime, and pigments) were previously ascertained with X-ray diffraction (XRD) (see Appendix 2, A2-1 to A2-6). In addition, the granulometry of the sand used as an aggregate of the *arriccio* layer was determined through sieving (Appendix 2, A2-7).

Table 2. *Composition of the mortar layers used for the replicas (parts by volume).*

Ariccio	Intonaco
❖ 1 part hydrated lime ❖ 2 parts Sand	❖ 1 part hydrated lime ❖ 2 part marble powder :“cream” of marble (1:1)

The mortar inner layer with coarser aggregates (*arriccio*) was added and compacted in silicon square ice cube moulds (Figure 4a). The plaster was compacted to reduce the water content of the mixture and avoid cracking during de-moulding. The surface of the *arriccio* was scraped while still humid to facilitate the attachment of the *intonaco* layer. After the *arriccio* hardened, the *intonaco* was applied, compacted, and leveled over the surface with the use of a spatula (Figure 4b). The ratio composition of the individual layers of the mortar render by volume can be seen in Table 2.

a) b) c)

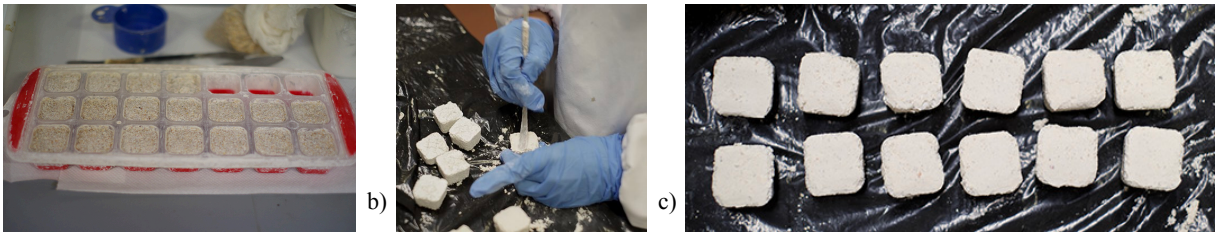

Figure 4. *Mortar render manufacturing process: a) Arriccio drying in the mould; b) Application of the intonaco; c) Lime mortar ready for painting laid down.*

To paint a fresco, the preparation and application of the *intonaco* mortar layer and the paint layer were done in sets of twelve replicas divided by paint mixture and pictorial technique. The paint layer preparation will be described in accordance with each fresco technique, bellow in sub-sections 3.1.2.1 and 3.1.2.2.

3.1.2.1. Buon fresco replicas

For the *buon* fresco painting technique, mixtures of Kremer French Ochre RTFLES - 40020® (red ochre) and Kremer French Ochre JCLES - 40040® (yellow ochre) with tap water were prepared. In this thesis, these replicas will be called red *buon* fresco (rBF) and yellow *buon* fresco (yBF).

Table 3. *Composition of the paint layers of buon fresco replicas.*

Paint layer	
rBF	**yBF**
❖ 4 g red ochre pigment (Kremer French Ochre RTFLES - 40020®) ❖ 10 mL tap water	❖ 4 g yellow ochre pigment (Kremer French Ochre JCLES - 40040®) ❖ 10 mL tap water

The composition used to prepare the paint layer is described in Table 3. To achieve deterioration by lack of cohesion needed for this study, the pigment content mixed with water was intentionally oversaturated. In addition, the paint was applied by three thick brush strokes, in contrast to the *buon* fresco procedure which is normally executed with very diluted brushstrokes.

3.1.2.2. Lime fresco replicas

For the lime fresco painting technique, the red and yellow ochres from Kremer stated above, were instead mixed with lime milk ($Ca(OH)_{2\,(aq)}$). Kremer Smalt - 10010® (smalt pigment) was also prepared in this way according to the findings of previous studies [51]. Similar to the previous case, the paint layers lack of cohesion was achieved by oversaturation of pigment content and by the paint laid down with three thick brush strokes. Table 4 shows the procedure followed by color. These replicas will be referred to in this thesis as red lime fresco (rLF), yellow lime fresco (yLF), and blue lime fresco (bLF).

Table 4. *Composition of the paint layers in lime fresco replicas.*

Paint layer		
rLF	**yLF**	**bLF**
❖ 5 g of red ochre pigment (Kremer French Ochre RTFLES - 40020®) ❖ 4 pp of milk lime	❖ 5 g of yellow ochre pigment (Kremer French Ochre JCLES - 40040®) ❖ 4 pp of milk lime	❖ 5 g of smalt pigment(Kremer Smalt - 10010®) ❖ 4 pp of milk lime

After the paint layers laid down, all the replicas (lime and *buon* fresco) were left to dry in the laboratory under ambient conditions (Tº: 22 ± 2 ºC, RH: 57 ± 9%) for a month (Figure 5).

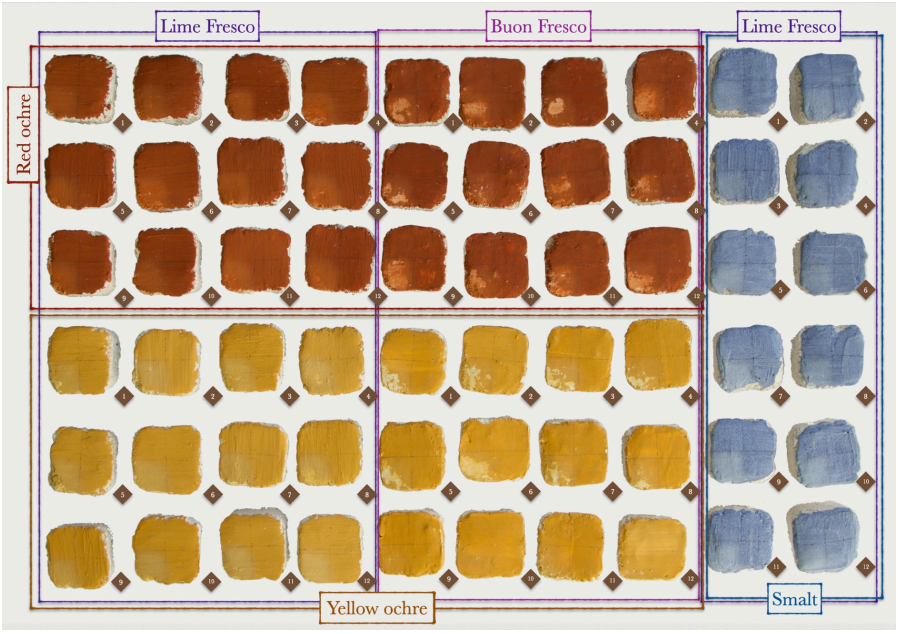

Figure 5. *Overview of the fresco replicas organized according to color and painting technique (before consolidation).*

Afterward, and for further analysis, the paint surface of each replica was divided into four equal areas (Figure 6). Area A was selected as an untreated reference while areas B, C, and D were consolidated. Areas A, B, and C presented natural deterioration in their paint surfaces, while D exhibited an artificially induced degraded paint surface by nail brush. In the *buon* fresco replicas, the induced abrasion also caused flacking of the paint layers. Only areas D in samples 9 to 12 of yBF replicas did not show flaking since the brush strokes were done with less pressure.

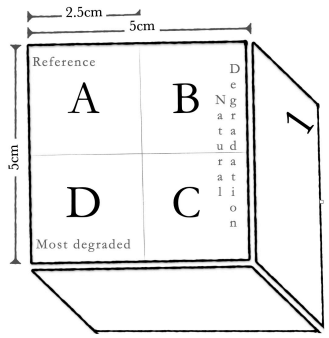

Figure 6. *Scheme of the four replica surface assignments (areas A to D).*

3.1.3. Application of the consolidating products

The three consolidants were applied to the replicas by spray technique after sonication for 10 minutes. Prior to application, several tests were made in order to ascertain the reproducibility of the procedure. During the tests, a white bloom appeared immediately after the HERCULES nanolime was applied to the ochre pigment layer. For these reasons, more tests were carried out in order to mitigate this effect. The tests are described in Section 3.2.2.

CaLoSiL® (25 g/L in 2-propanol) was applied as acquired, without changing its composition while the Primal® was freshly diluted at 2% with tap water. The commercial consolidants were sprayed to the replica surface five times at a distance of circa 5 cm in ambient conditions (Tº: 21 ºC, RH: 46%). During the spraying process, area A was covered with a paper towel. CaLoSiL® was sprayed horizontally, while Primal® was sprayed vertically due to a blockage in the spray when applying the material horizontally. The selected HERCULES nanolime dispersion, 25 g/L in Acetone:Ethanol in proportion 1:10 was applied one week later following the same application procedure as with CaLoSiL® (horizontal spraying, at Tº: 23 ºC, RH: 50%) (Figure 7).

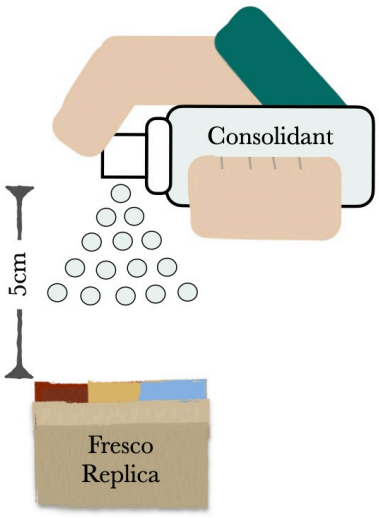

Figure 7. *Nanolime application procedure.*

Each product was applied to the three paint layers of replica sets (red, yellow, and blue). The total number of treated samples was 45: three replicas for each pigment/painting technique/ consolidant (Figure 8). Upon completion, the paint surfaces were held under ambient atmospheric conditions (Tº: 24 ± 3 Cº, RH: 50 ± 4%) and analyzed by the analytical setup one week and one month after the consolidation treatment. The goal was to record and analyze the effectiveness and, in particular the impact on the paint surface materials by comparing it with their initial conditions.

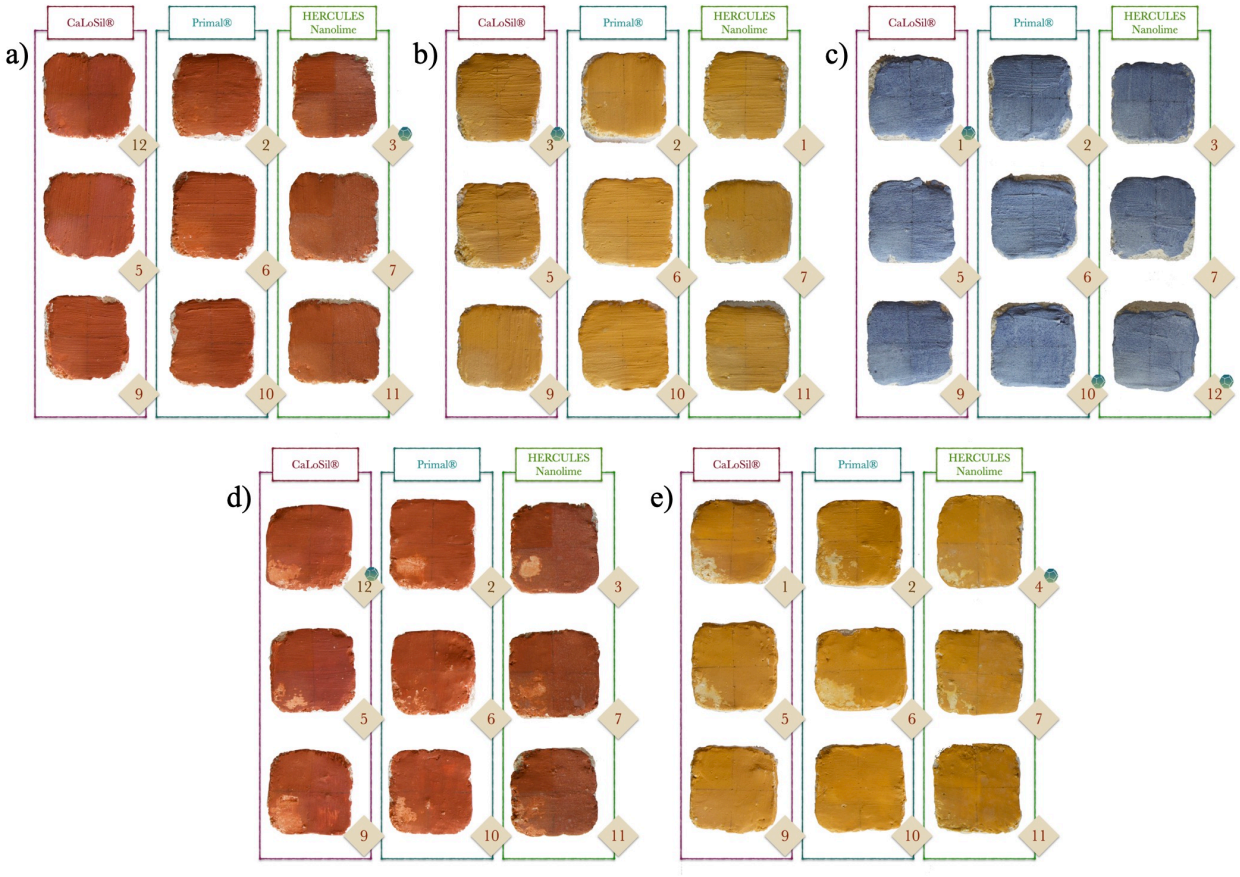

Figure 8. *Schematic representation of the overall 45 lime mortal replicas prepared, describing their division by pigment/painting technique/consolidant, immediately after treatment with the consolidants: a) Red ochre lime fresco replicas (rLF); b) Yellow ochre lime fresco replicas (yLF); c) Smalt lime fresco replicas (bLF); d) Red ochre buon fresco replicas (rBF); and e) Yellow ochre buon fresco replicas (yBF).*

3.1.4. Conditions, instrumentation and sample preparation

3.1.4.1. Nanolime Characterization

Scanning Electron Microscopy (SEM)

Scanning electron microscopy is based on the interaction between a high-energy electron beam and the surface of a solid specimen. The focused electron beam scans the surface of the specimen to create an image. The electrons in the beam interact with the sample, producing various signals that can be used to obtain information about the surface topography and composition [52]. Its magnification ranges from 20X to approximately 30,000X with a spatial resolution of 50 to 100 nm [53]. When SEM is coupled to Energy Dispersive X-ray Spectrometry (SEM-EDS) is possible to acquire elemental maps and/or spot chemical analysis of the chemical composition of the sample.

In this task, the technique was used to study the particle size and morphological characteristics of the HERCULES nanolime and to characterize the commercial lime nanoparticles. SEM samples were prepared by placing a drop (± 0.10 mL) of diluted nanolime dispersions in 2-propanol on to a glass surface placed over carbon film. Once dried the samples were coated with a metallic conductive layer of gold/palladium in Quantum Q150RES / sputter coater SC 7620 Polaron. The effect of the solvents in different dispersions of HERCULES nanolime (Section 3.2.2) was also studied with SEM.

SEM-EDS was used to determine the elemental composition of the CaLoSiL® and HERCULES nanolime. For the EDS analysis, the nanolime powders were placed over carbon film (Appendix 3).

These analyses were carried out in a Variable Pressure Scanning Electron Microscope HITACHI S-3700N operated with an accelerating voltage of 10 kV. EDS analysis was conducted

at an accelerating voltage of 20 kV with the help of Bruker Flash 5010 Silicon Drift Detector (SDD).

X-ray diffraction (XRD)

X-ray diffraction is a non-destructive technique that provides detailed information about the crystallographic structure, chemical composition, and physical properties of materials [54]. XRD peaks are produced by constructive interference of a monochromatic beam of X-rays scattered at specific angles from each set of lattice planes in a sample. The peak intensities are determined by the atomic positions within the lattice planes. Consequently, the XRD pattern is the fingerprint of periodic atomic arrangements in a given material [55].

This technique was used to determine the crystalline and mineralogical composition of the synthesized and commercial lime nanoparticles. XRD samples were prepared by placing dried powder of nanolime on a standard polymeric sample holder. The diffractograms were produced using X-ray diffractometer, Bruker D8 Discovery X-Ray Diffractometer, with Cu Kα radiation (λ = 0.01540598 nm), under the following conditions: scanning between 3º and 75º (2θ), accelerating voltage of 40 kV, and current intensity of 30 mA. The DIFFRAC.SUITE.EVA software was used to identify the mineral phases with Powder Diffraction Files of the International Center for Diffraction Data-2.

Fourier-transform infrared spectroscopy (FT-IR)

Fourier Transform Infrared Spectroscopy is a powerful tool allowing the identification of organic and non-organic compounds [56]. In this study Imaging FT-IR BRUKER Hyperion controlled by OPUS 7.2 software (Copyright© 2012 Bruker Optics and Microanalysis GmbH, Berlin, Germany) was used to obtain the FT-IR spectra of the synthesized and commercial lime nanoparticles and identify functional groups in a range of 400 - 4000 cm^{-1}. The samples were examined in transmission mode in Potassium Bromide (KBr) pellets.

Thermogravimetry Analysis (TGA-DTG)

Thermogravimetric analysis is an analytical technique used to determine a material's thermal stability and its fraction of volatile components by monitoring the weight change that occurs as a sample is heated at a constant rate under inert atmosphere [57]. TGA is one of the most useful techniques for the characterization of NPs and nano-modified formulas [58].

TGA is often used to determine $Ca(OH)_2$ content because is a relative easy and fast procedure. Different phases are distinguished according to the hydrates that decompose as the temperature increases. It is accepted that the decomposition of $Ca(OH)_2$ occurs approximately between 350 °C and 550 °C while $CaCO_3$ decomposes around 550 ºC to 800 ºC [59,60]. When coupled to XRD it has been found to yield very precise information on the phases developed [58].

For this technique, 25 mg of powder nanolime consolidants were placed in a platine (Pt) crucible and analyzed in a Simultaneous Thermal Analyzer STA 449 F3 Jupiter (NETZSCH), under an inert atmosphere of Nitrogen (Air Liquid Alpha gas compressed N_2) with a flow rate of 70 mL/min. The heating program was set to start at 10 °C and then increase it at a constant rate of 20 °C/min until reaching 1000 °C.

Dynamic light scattering (DLS)

Dynamic light scattering (DLS) is a sensitive, non-invasive, powerful analytical technique for measuring the size and size distribution of molecules and particles typically in the sub-micron region [61]. DLS measures the temporal fluctuations of the light scattered due to the Brownian motion of the particles, when a solution containing the particles is placed in the path of a monochromatic beam of light [62]. The size distribution of the small suspended particles is defined by dynamic light scattering with the use of the intensity autocorrelation function [61]. In essence, DLS measures the light scattered from the laser that passes through the colloidal suspension. Then, the hydrodynamic size of the particles is determined via the modulation of scattering light intensity as a function of time.

The dynamic light scattering particle size of the nanolime dispersion of: HERCULES nanolime dispersed in Acetone:Ethanol (1:10), HERCULES nanolime dispersed in Acetone:2-Propanol (1:10), and CaLoSiL® were measured using a Zetasizer NanoSeries from Malvern Instruments.

3.1.4.2. Analysis of the fresco replicas

Photographic documentation in visible (Vis) and ultraviolet fluorescence induced in visible (UVF)

Photographic documentation of the replicas before and after consolidation was acquired to observe if the paint layer presented any visual changes after the application of the consolidation treatment over the replicas.

Visual photography (Vis) was acquired with a Canon EOS 800D with an objective EF-S 18-135 mm f:3.5-5.6 IS STM. Different sets of photos were taken at different time intervals: before, right after, a week and a month after consolidation. In the photos, the presence of the greyscale OPcard101 is crucial to obtain the white balance of each photo. The photographic edition was made in Adobe Photoshop CC.

The ultraviolet photography (UVF) was also acquired with a Canon EOS 800D with an objective EF-S 18-135 mm f:3.5-5.6 IS STM. In a dark room under the light produced by a UV lamp. The use of UV allows the detection and characterization of surface coatings and fluorescent pigments [63]. In this research, UV photography allows to determine if the consolidation treatment produces fluorescence to the paint layer of the replicas.

Spectro-Colorimetry

Colorimetry is a numerical language that describes color unambiguously through three independent variables: hue, saturation (distance from neutral), and lightness. It provides a fingerprint characteristic of the colored material. In the analysis of the works of art, spectro-colorimetry is used for pigment characterization, monitoring of the conservation state and evaluating color value of the pigments before and after interventions and deterioration processes [64].

For this analysis Data Color Check Plus II with the following parameters was used during the analysis: SCE and Standard Illuminant / Observer D65 / 10 and aperture size USAV (Ø25 mm). The analyzed wavelengths were 360-750 nm with the 10 steps between measurements.

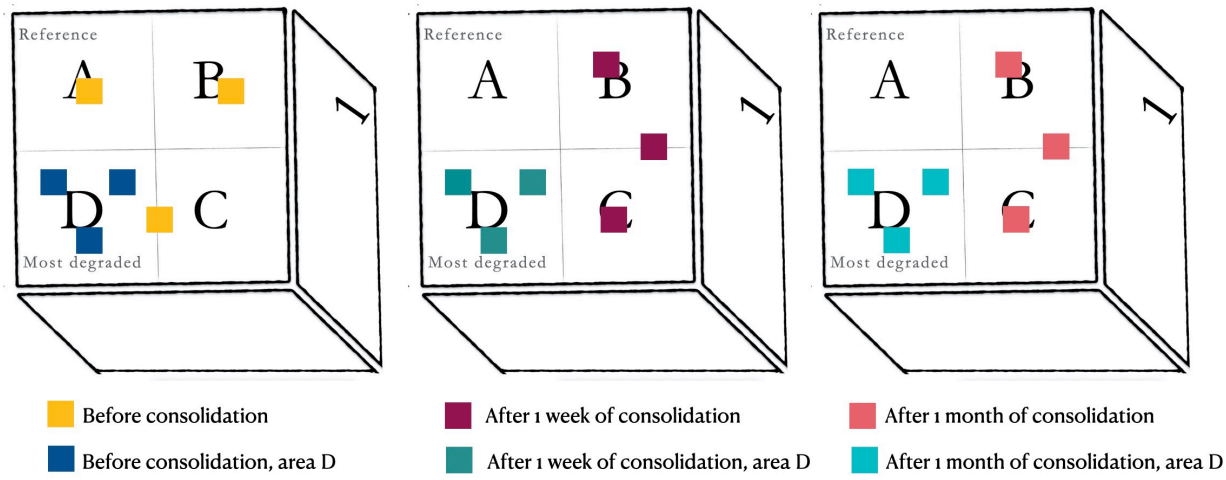

Figure 9. *Scheme of the three points measured to obtain an average colorimetry value for the study of all replicas before, one week and one month after treatment.*

Figure 9 signal the three points measured to obtain an average colorimetry value for the spectro-colorimetry study of all replicas before, one week and one month after consolidation treatment. Description of the color was carried through CEI LAB color space (Commission Internationale de l'Eclairage CIE 1976) [64]. From the obtained coordinates L*, a*, b*, C_{ab}* and h_{ab}* the total color difference ΔE^*_{ab} was determined by the following equation 3:

$$\Delta E^* = ((\Delta L^*)^2 + (\Delta a^*)^2 + (\Delta b^*)^2)^{½} \quad [Eq.\ 3]$$

Where ΔL*, Δa* and Δb* were calculated from the formulas $\Delta L^* = L^*_{sample} - L^*_{standard}$, $\Delta a^* = a^*_{sample} - a^*_{standard}$ and $\Delta b^* = b^*_{sample} - b^*_{standard}$ (sample represents values after consolidation and standard means values before treatment). The meaning of each of the obtained coordinates is describe in Table 5.

Table 5. *Colorimetry coordinates meanings in accordance to CIE system [26,64].*

Coordinate	Meaning
+L*	Sample is lighter than standard
-L*	Sample is darker than standard
+a*	Red
-a*	Green
+b*	Yellow
-b*	Blue
Cab*	Chroma
hab*	Hue angle
ΔE*	Total color difference

The colorimetric data measured for the artificial degraded area D have not been taken in account in the colorimetry analysis, given the strong lime background interference. The results presented in 3.2.3 will only take in consideration the other two painted areas (B and C).

The most important contribution for testing the treatments came from the total color difference (ΔE*), followed by the changes in luminosity (ΔL*). According to compatibility criteria for visual properties concerning consolidants for stone surfaces, mortars and mural paintings found in literature and used in other studies [26,65,66], Table 6 shows the meanings and rating scale of incompatibility risks for the values of ΔE* indicator.

Table 6. *ΔE* values meanings and rating scale of incompatibility risk according to literature [26,65,66].*

ΔE* values	Meaning
ΔE* >3.5	Color variation percieved by eye
ΔE*< 3	Low risk of incompatibility
3<ΔE*<5	Medium risk of incompatibility
ΔE*>5	High risk of incompatibility

Media and standard deviation of ΔE* values of three experiment were compared using two way-ANOVA followed by Bonferroni's multiple comparison test, through the program GraphPad Prism7.00. $P \leq 0.05$; was considered statistical differences between the data in function to pigments and consolidants.

Optical microscopy (OM)

There are several reasons for using microscopy to study paintings. For this research, the replicas and cross-sections before (reference, R) and after consolidation (HERCULES nanolime, Primal®, and CaLoSiL®) were studied under different optical microscopes.

A general examination of the paint layer of the replicas was performed using a Stereozoom microscope Leica M205C coupled to a Nikon DS-Fi1 digital camera. This microscope served to study the macroscopic morphology of the substrate (paint layer). The stereozoom microscope was also used to obtain a general image of the cross-section which became a helpful tool for their further study in SEM.

Reflected light optical microscope Leica DM2005M in dark field illumination mode and ultraviolet fluorescence mode was used to observe the cross-sections of replicas: 1bLF-CaLoSiL®, 4bLF-R, 10bLF-Primal® and 12bLF-HERCULES nanolime. The points in the replicas where the cross-sections were taken are described in Figure 10. The observations were carried at 100x and 200x magnifications. OM study of cross-sections reveals stratigraphy of the painting micro-samples; it helps to describe pigments and mortar particles. In addition, it may provide information about later retouches [67].

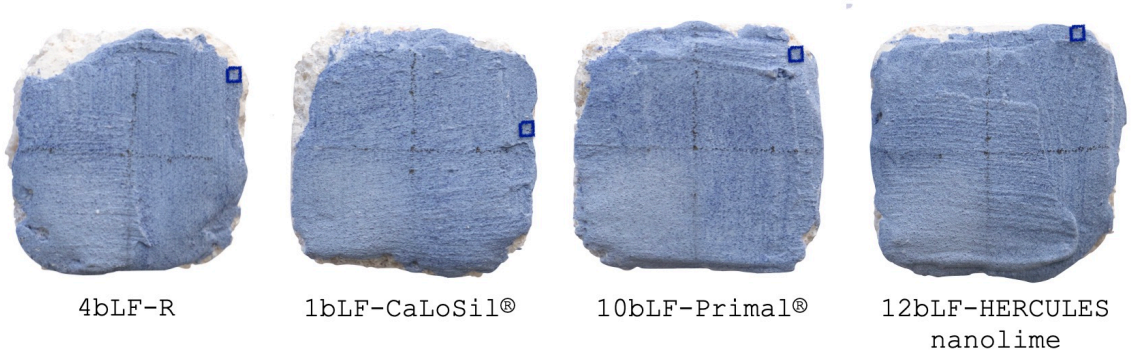

Figure 10. *Cross-sections map of samples extracted for SEM-EDS analysis. Blue colored squares: place were the sample was taken from.*

Cross-section micro-fragments were embedded in an epoxy fix resin (Epofix Fix, Struers A/S, Ballerup, Denmark) and polished with 6000, 8000, and 12000 sandpapers. During polishing a rotating disc, Drehzal Regler (Jean Wirtz, Dusseldorf, Germany) was used.

Scanning Electron Microscopy coupled to Energy Dispersive X-ray Spectrometry (SEM-EDS)

Consolidant penetration and compatibility can be analyzed by obtaining SEM images of the microstructure being treated. Same areas were analyzed with SEM-EDS at four equal magnifications before, one week and one month after treatment (Figure 11). The areas were chosen to represent lack of cohesion in the paint layer of the replicas, where loose pigment particles and pores of different number and sizes were observed. The cross-sections (Figure 10) were also observed under SEM, in order to evaluate the consolidant effects in the paint layer.

Mapping and elemental analyses were done for all the observed areas through SEM-EDS. Variable Pressure Scanning Electron Microscope HITACHI S-3700N operated with an accelerating voltage of 20 kV and chamber pressure of 40 Pa was used.

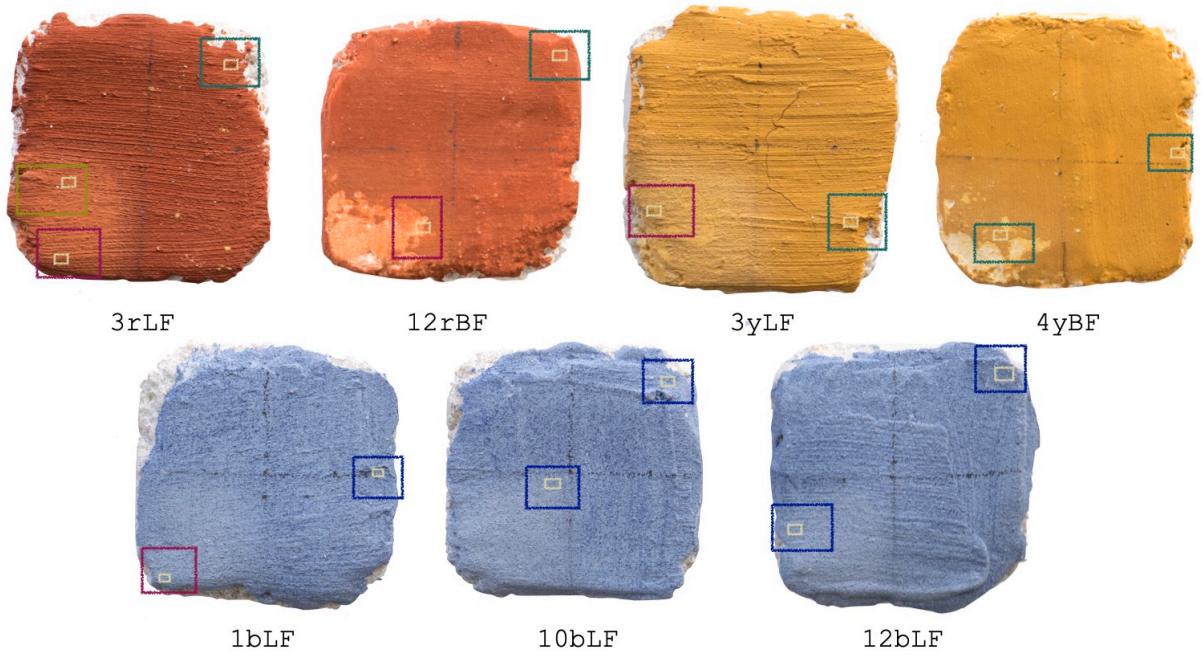

Figure 11. *Selected replicas, surface areas and points for SEM-EDS analysis. Bigger colored squares: studied areas, small yellow square: studied points.*

Cotton swab test of the paint layer of all the replica by groups (pigment/technique/ consolidant) was performed in order to select replicas of highest lack of cohesion for further SEM-EDS analysis. The test consists of passing a cotton swab over the surface of the replicas and visually observe the amount of pigment removed from the paint layer. Overall seven replicas were selected.

3.2. Results and Discussion

3.2.1. Characterization of HERCULES nanolime

The synthesis of nanoparticles of $Ca(OH)_2$ occurs following the reaction [Eq. 4]:

$$CaCl_{2\ (aq)} + 2NaOH_{\ (aq)} \xrightarrow[\text{Triton X-100}]{\Delta\ 90\ ^{\circ}C,\ H_2O} Ca(OH)_{2\ (s)} + 2NaCl_{\ (aq)} \qquad \text{Eq. 4}$$

The average synthesis yield of HERCULES NPs was 47.2 ± 5%. The yields of three reactions were considered in the calculation, where the values support a moderately good reproducibility of the reaction. Details of actual and theoretical yields for each of these three syntheses are shown in Appendix 3 A3-1.

XRD analysis of the powdered sample was performed to identify the crystalline phases. The powdered XRD pattern of HERCULES nanolime is shown in Figure 12. The diffractogram shows the characteristic peaks of the crystalline main phase, portlandite $Ca(OH)_2$, and also the presence of low-intensity peaks characteristic of calcite ($CaCO_3$). The presence of $CaCO_3$ crystalline phase indicates a fast carbonatation of HERCULES nanolime by atmospheric CO_2, when it was exposed to air during the drying process and analysis.

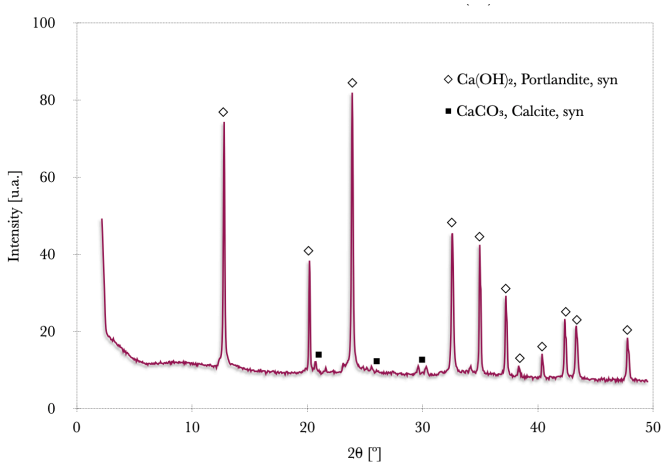

Figure 12. *XRD diffractogram of HERCULES nanolime and identification of the characterization peaks.*

SEM analysis was performed to observe the morphological characteristics (particle shape and dimensions) of HERCULES nanolime. The shape of the NPs is a hexagonal prism. The average particle size is 287 nm, with an observed minimum size of 56 nm and a maximum size of 982 nm (Figure 13).

a)

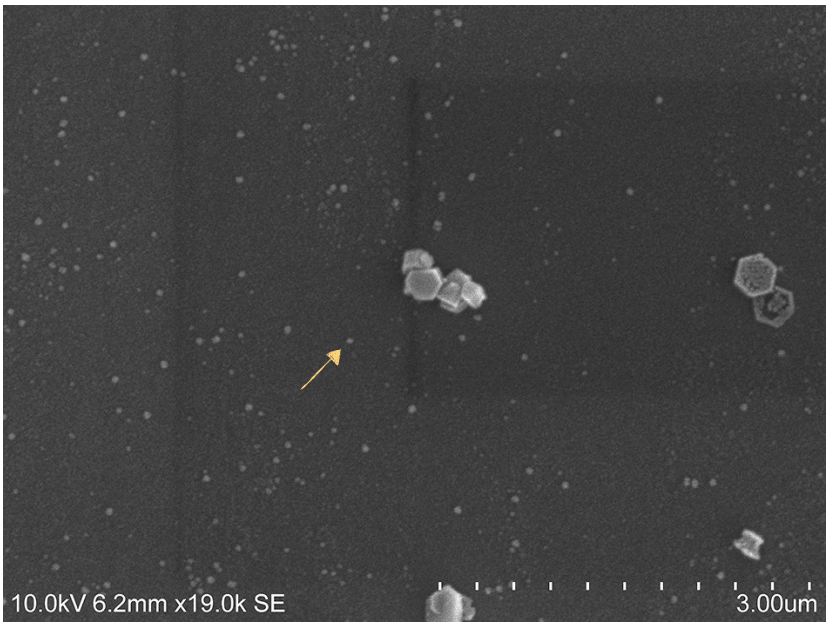

b)

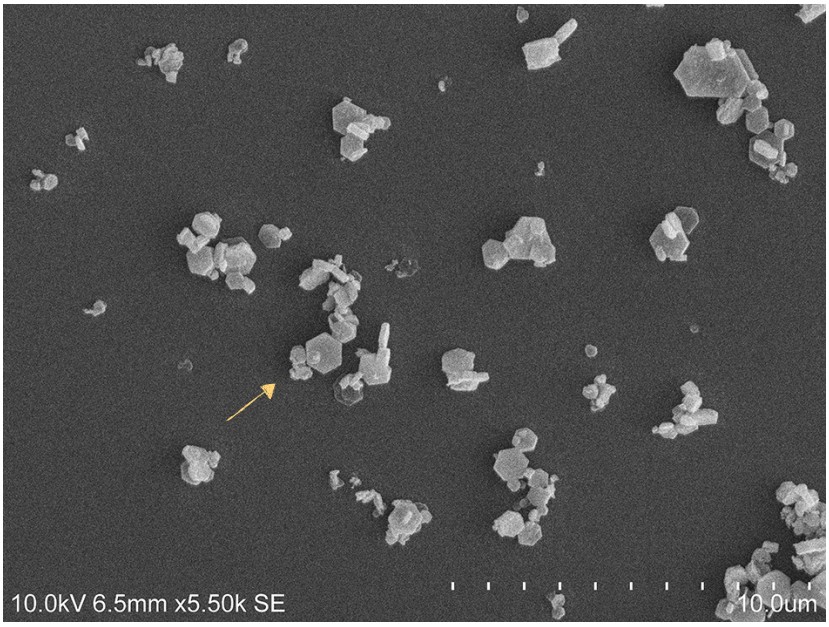

Figure 13. *SEM images of HERCULES nanolime: a) NPs of size <100 nm; b) Characteristic hexagonal shaped crystals of* $Ca(OH)_2$ *NPs.*

FT-IR analysis was realized to check if surfactant residues remain in the $Ca(OH)_2$ NPs. The infrared spectra of the synthesized $Ca(OH)_2$ NPs confirms the existence of $Ca(OH)_2$ (Figure 14). The presence of the bands at 3640 cm^{-1} (s), 3446 cm^{-1} (w), and 1600 cm^{-1} (w) can be assigned to the stretching of O-H and H-O-H [33,68]. The carbonate bands present at 2892 cm^{-1} (w), 2338 cm^{-1} (w), 1459 cm^{-1} (m), and 870 cm^{-1} (w) imply the formation of $CaCO_3$. The corresponding peaks vibration absorption is documented in Table 7. The lack of the characteristic peaks of the surfactant Triton X-100 (Figure 14), confirms the complete removal of the surfactant residues in the product.

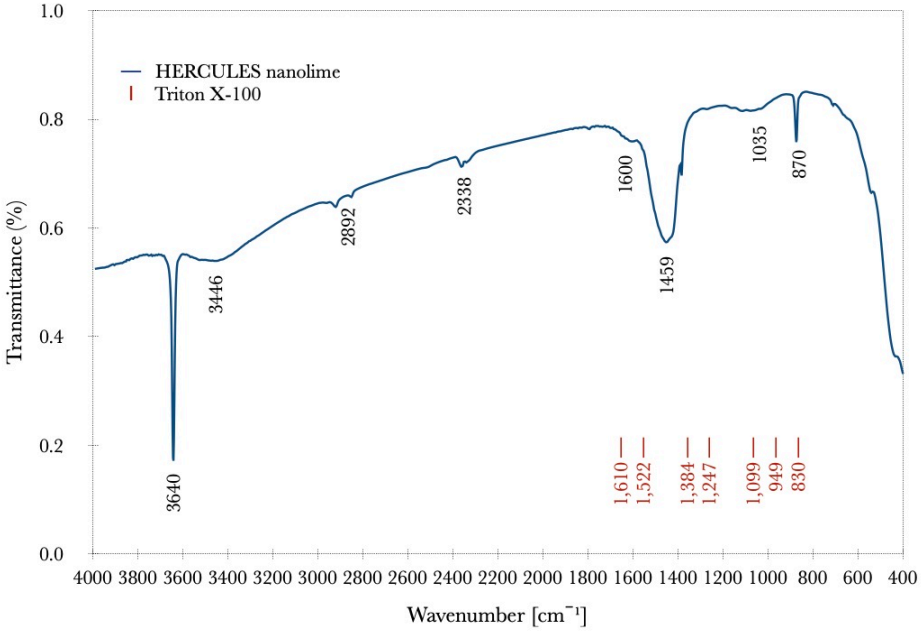

Figure 14. *FT-IR spectra of HERCULES nanolime. In red: characteristic peaks of the surfactant Triton X-100 [33].*

Table 7. *Infrared absorption bands for previous spectra (Figure 14) and the corresponding associated bonds [33,68].*

Band cm^{-1}	Reported Bands cm^{-1}	Intensity	Associated bond	Assignment	Phase
3640	**3640**	sharp	O-H stretching	Hydroxyl group	$Ca(OH)_2$
3446	**3388**	weak	H-O-H stretching	Hydroxyl group	$Ca(OH)_2$
2892	**2646 - 2423**	weak	C-O stretching	Carbonate band	$CaCO_3$
2338	**2646 - 2424**	weak	C-O stretching	Carbonate band	$CaCO_3$
1600	**1600**	stong	O-H stretching	Hydroxyl group	$Ca(OH)_2$
1459	**1444**	medium	C-O stretching, sym	Carbonate band	$CaCO_3$
1035	**1833 -781**	weak	C-O stretching	Carbonate band	$CaCO_3$
870	**875- 830**	sharp	C-O stretching, asym	Carbonate band	$CaCO_3$

The absence of the surfactant was also confirmed by TGA-DTG. Thermogravimetry analysis of HERCULES nanolime was carried out to observe its thermal behavior. The results, shown in Figure 15 present two temperature ranges: 350-550 ºC and 600-850 ºC, where significant weight loss occurred.

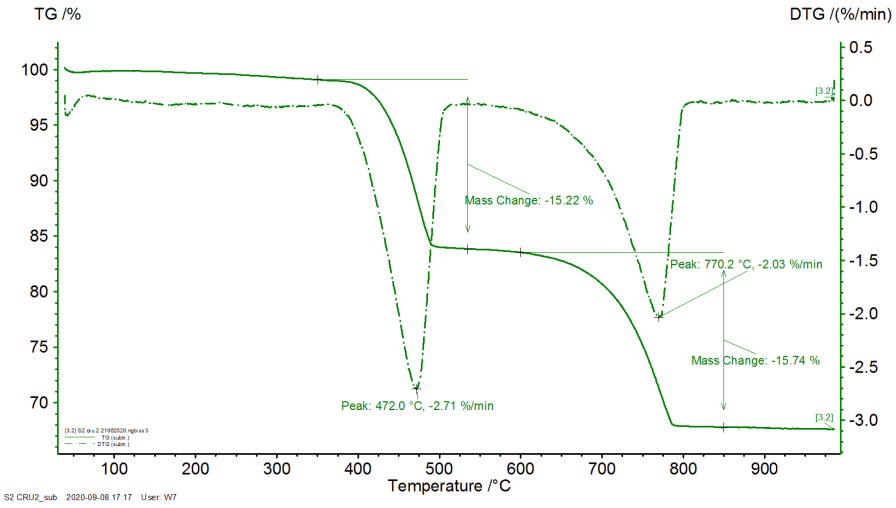

Figure 15*. TGA-DTG results of HERCULES nanolime.*

The weight loss between 350-550 ºC (15.57%) corresponds to the thermal reaction of calcium hydroxide [57,59] according to equation 5, and thus enables the determination of the $CaCO_3$

$$Ca(OH)_{2\ (s)} \rightarrow CaO_{\ (s)} + H_2O_{\ (l).} \quad \text{Eq. 5}$$

The calcium hydroxide content (expressed in % $Ca(OH)_2$) was calculated as follows [Eq. 6]:

$$Ca(OH)_2\ (\%) = [P_{(H_2O)} * M_{(Ca(OH)_2)}] / M_{(H_2O)} \quad \text{Eq. 6}$$

In which $\mathbf{P_{(H_2O)}}$ is the percentage of mass loss between 350 to 550 °C, that corresponds to the decomposition of $Ca(OH)_2$, $\mathbf{M_{(Ca(OH)_2)}}$ represents the molar mass of $Ca(OH)_2$ (74.093 g/mol), and $\mathbf{M_{(H_2O)}}$ the molar mass of water (18.01 g/mol).

The weight loss between 600 and 850 ºC (14.5 ± 2%) corresponds to the loss of CO_2 as a consequence of the decomposition of calcium carbonate, equation 7, and thus enables the determination of the $CaCO_3$ content within the sample.

$$CaCO_{3\ (s)} \rightarrow CaO_{\ (s)} + CO_{2\ (g)} \qquad \text{Eq. 7}$$

Through equation 8 the carbonate content (expressed in % of CaCO3) in the sample was calculated:

$$CaCO_3\ \% = [P_{(CO_2)} * M_{(CaCO_3)}] / M_{(CO_2)} \qquad \text{Eq. 8}$$

In which $\mathbf{P_{(CO_2)}}$ is the percentage of mass loss between 500 to 700 °C, that corresponds to the decomposition of $CaCO_3$, $\mathbf{M_{(CaCO_3)}}$ represents the molar mass of $CaCO_3$ (100.082 g/mol), and $\mathbf{M_{(CO_2)}}$ the molar mass of carbon dioxide (44.02 g/mol).

Table 8. *HERCULES nanolime sample mass losses and calcium hydroxide and calcium carbonate contents (%) obtained by TGA.*

Mass loss (%) between 350-550 ºC	Mass loss (%) between 550–800 ºC	$Ca(OH)_2$ (%)	$CaCO_3$ (%)
15.2	15.7	62.6	35.8
15.9	13.3	65.5	30.3

Table 8 shows the mass losses and the contents of calcium hydroxide and calcium carbonate obtained from the TGA analysis of HERCULES nanolime. TGA of the second pair of results is present in Appendix 3, A3-2. The average percentage of calcite calculated from two syntheses was 33 ± 4%. These results correspond to the amount of $Ca(OH)_2$ NPs that carbonated in the contact atmosphere (carbon dioxide and water vapors) at any stage: synthesis, drying or storage.

3.2.2. Selection of the right dispersion of nanolime

Different dispersions of laboratory synthesized nanolime were tested in order to mitigate the white bloom appearance on the ochre pigment layers. Different concentrations were tested: 25 g/L, 5 g/L, and 2.5 g/L. Several dispersions with varying the type and combination of solvents were formulated (Table 9). In Figure 16 we can observe the visual effect of the application of the HERCULES nanolime in different dispersing media and compared to the untreated surface of the reference, sample C.

Table 9. *Dispersions prepared with laboratory synthesized HERCULES nanolime. For the treated areas see Figure 16.*

Concentration	Solvent	ID of the treated area
5 g/L	Ethanol	Sample A- left side
5 g/L	Ethanol	Sample A- right side
2.5 g/L	2-Propanol	Sample B- left side
5 g/L	2-Propanol	Sample B- right side
"Reference"		Sample C
25 g/L	Acetone	Sample D- left side
25 g/L	H_2O: 2-Propanol (1:10)	Sample D- right side
25 g/L	Ethanol	Sample E- left side
25 g/L	Acetone:2-Propanol (1:10)	Sample F- left side
25 g/L	Acetone:Ethanol (1:10)	Sample F- right side

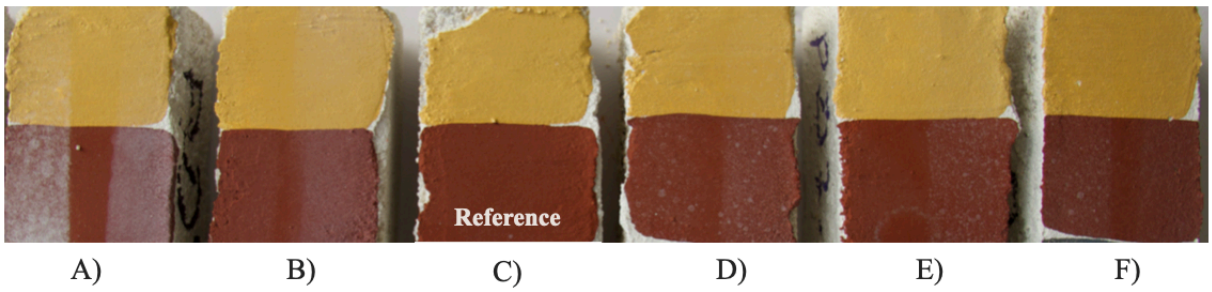

Figure 16. *Visual effect of HERCULES nanolime dispersions over ochre pigments. The image letter and side corresponds to the ID of the treated area column in Table 9.*

The dispersion of HERCULES nanolime dispersed in Acetone:Ethanol (1:10) (Sample F-right side) with a concentration of 25 g/L was selected for the treatment of the fresco replicas since the white haze on the surface was less significant.

In order to explain the whitening effect caused by the HERCULES nanolime on the pigment layer at the time of the application, not observed with the commercial nanolime, further SEM and dynamic light scattering (DLS) studies were carried out to compare the NPs size and texture. In agreement with Figure 17, the NPs of both products have the same shape and are strongly agglomerated, but the commercial NPs show a visually more uniform particle orientation. The average diameters obtained by the DLS analysis suggested smaller average diameters of the commercial nanolime NPs (138 ± 0.4 nm) in comparison to the synthesized NPs (444 ± 7 nm) (see in Table 10).

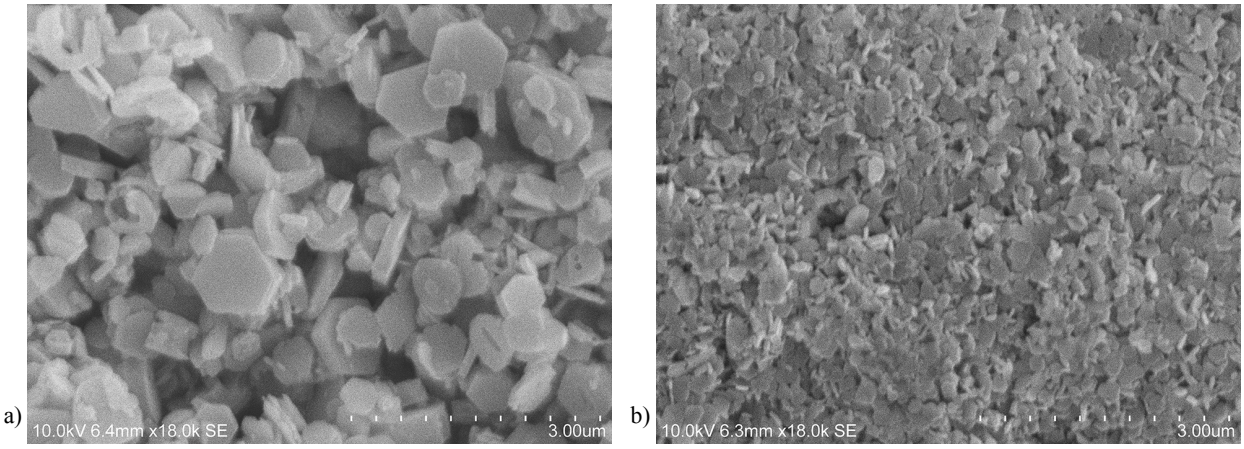

Figure 17*. SEM images of $Ca(OH)_2$ NPs dispersions used for the assays: a) HERCULES nanolime, b) CaLoSiL®.*

Table 10. *DLS results of particle size of HERCULES nanolime dispersions and CaLoSiL®.*

Consolidant	Average hydrodynamic diameter (nm)
HERCULES nanolime in Acetone:Ethanol (1:10)	444 ± 7
CaLoSiL® IP25	138 ± 0.4

The results suggest that a probable reason for the different application effects could be linked to the texture and dimension of the NPs (particle size, orientation and level of NPs agglomeration). One of the reasons for the different textures in both nanoconsolidants is probably due to differences in the exact nature and proportion of the dispersion media. The influence of the dispersion media was also hinted at in the SEM images of all tested HERCULES nanolime dispersions described in Table 10 are shown in Appendix 3 A3-4 to A3-6. The most aleatory oriented NPs were observed for nanolime in Acetone:2-Propanol. The different particles

level of orientation and higher dimension of the HERCULES nanolime NPs is also related to the quantity of the used surfactant used in the synthesis.

3.2.3. Evaluation of treatment

In this section will be presented the effect of the consolidants treatment on the paint layers prepared with *buon* and lime fresco techniques one week and one month after application. The discussion will be made by consolidant and intends to evaluate and compare the aesthetic impacts and treatment effectiveness by technical photography in the visible range, colorimetry, spectrophotometry and SEM-EDS. Colorimetry data was also statistically analyzed by the two-way ANOVA test using the software GraphPad Prism7.00.

HERCULES nanolime

Red ochre pigment

Figure 18 a and b shows an overview of the red paint layers replicas carried out with the *buon* and lime fresco and Figure 18c and d OM-Vis images (x7.8 magnification) of the two paint layers (11rBF and 11rLF) before, one week and one month after treatment. In both types of frescos, the addition of the HERCULES nanolime formed a white haze over the surface at the moment of application. The effect is noticed as a spotted veil over the paint surface. In 11rBF the spots are spread unevenly and are of different sizes and shape (Figure 18c) while in 11rLF the spots seem to be smaller, more uniform in size and spread more evenly (Figure 18d).

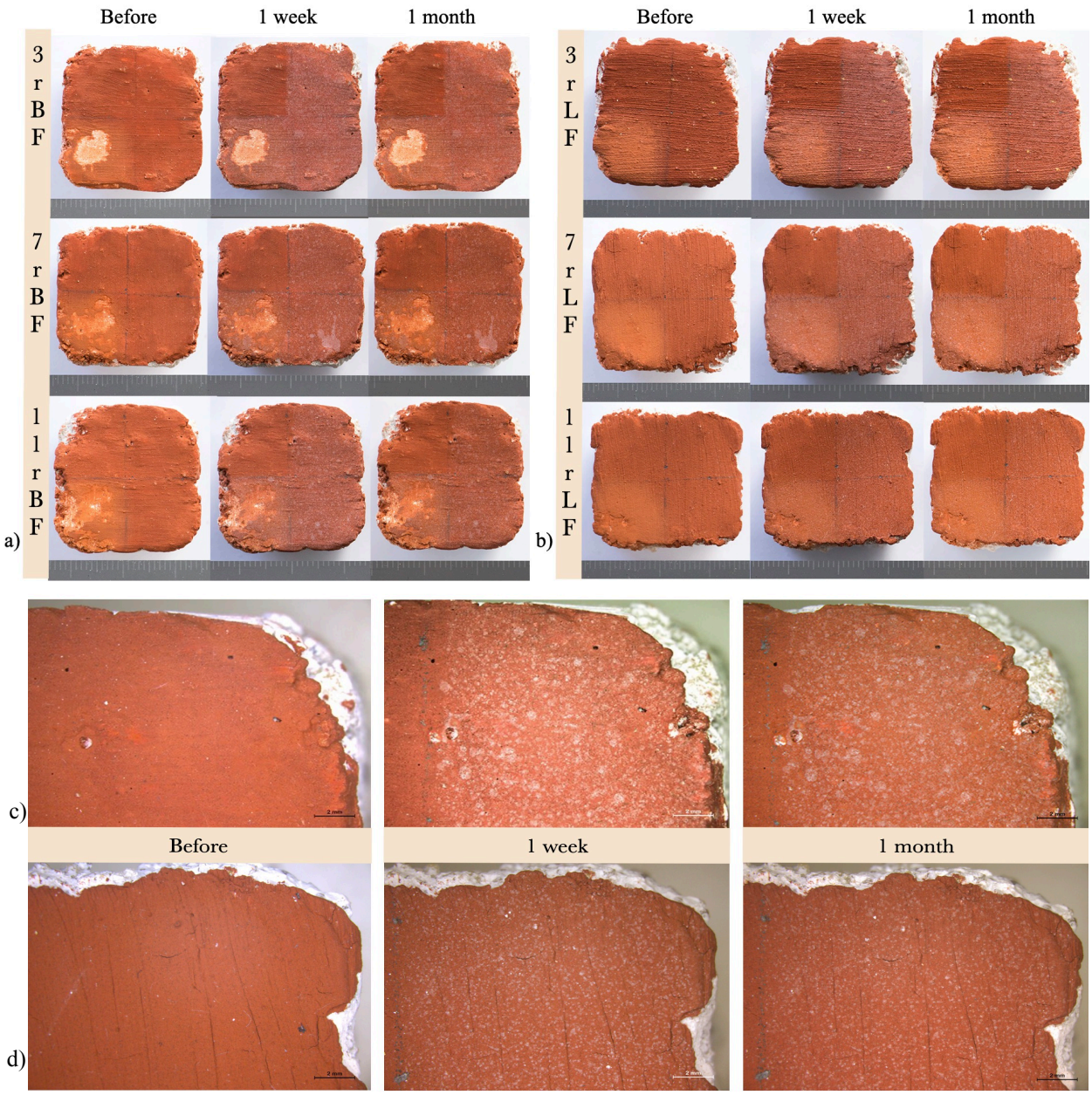

Figure 18. *Photographic documentation of the red replicas before, in one week and in one month after treatment with HERCULES nanolime: a) Buon fresco replicas: 3rBF, 7rBF and 11rBF; b) Lime fresco replicas: 3rLF, 7rLF and 11rLF. OM images (X7.8) of area B of replicas 11rBF (c), and 11rLF (d).*

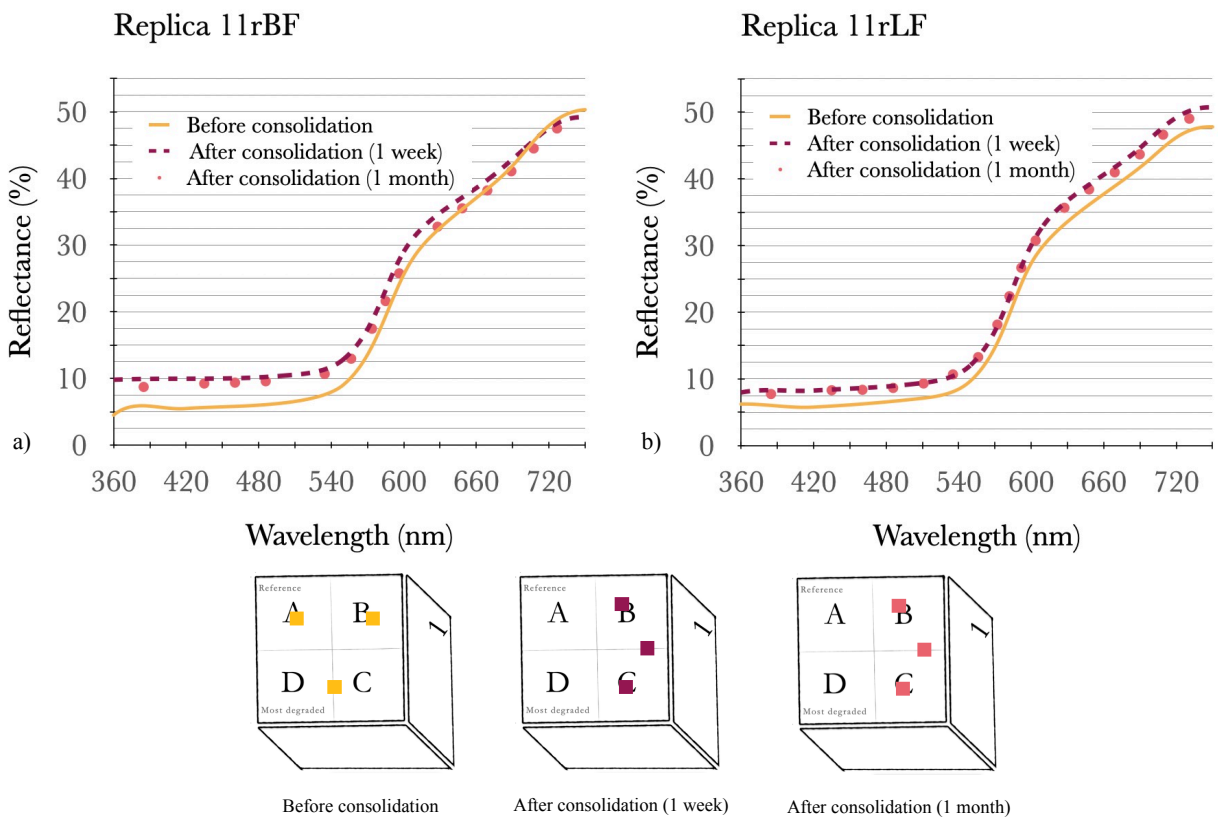

Figure 19. *Reflectance spectral curves of red replicas treated with HERCULES nanolime: a) Buon fresco replica 11rBF; b) Lime fresco replica 11rLF. The small squares under the plots display the three points measured to obtain an average colorimetry value before (yellow), in one week (purple) and in one month (pink) of treatment.*

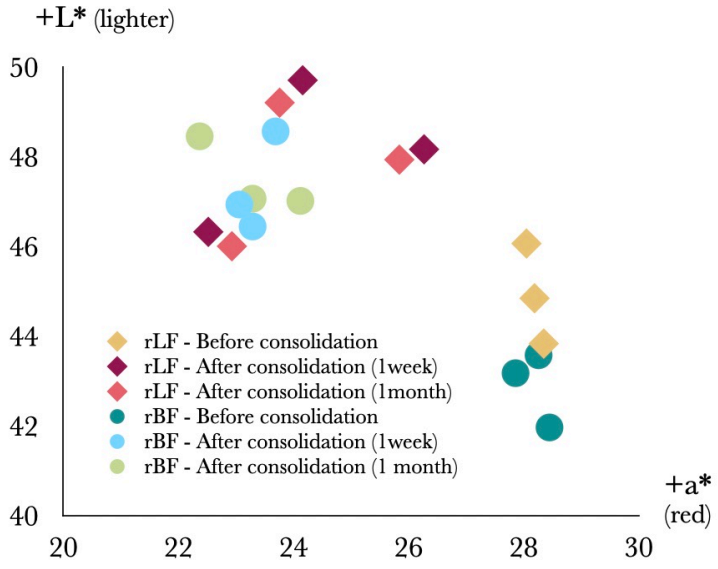

Figure 20. *CIELAB color space plot of all red ochre replicas treated with HERCULES nanolime.*

The presence of the white haze is traduced in an increase of the reflectance (R%) in the spectral curves of the paint layers (Figure 19). No changes in the shape of the curve is detected in both painting techniques made with red ochre showing that the pigment is not affected by the treatment but only the perception of color (Figure 19). The changes are clearly seen in the chromatic coordinates of CIELAB color space plot of Figure 20. In both painting techniques, the values of redness (a*) decreased while lightness (L*) increased. The color fading and lightening effect is more noticed in the *buon* fresco paint layers compared to lime fresco paintings which by nature are already lighter due to the high amount of calcium carbonate in their composition (see section 2.1). The total color difference observed (Table 11) is significant for the red paint layers. ΔE* values were higher than the threshold of detectability by human eye (ΔE* >3.5) and exhibit high risk of incompatibility (ΔE*>5).

Table 11. *Color differences using CIE*L*a*b* coordinates for red paint layers treated with the HERCULES nanolime (one week and one month after replicas treatment).*

	Sample ref.	Color	Painting technique	ΔL*	Δa*	Δb*	ΔE*	Incompatibility risk*
After one week	3rBF	Red	*Buon* fresco	4.48	-5.16	-7.18	9.91	High: color variation perceived by eye
	7rBF	Red	*Buon* fresco	3.76	-4.8	-6.25	8.73	High: color variation perceived by eye
	11rBF	Red	*Buon* fresco	4.99	-4.57	-6.25	9.21	High: color variation perceived by eye
	3rLF	Red	Lime fresco	2.49	-5.83	-8.35	10.48	High: color variation perceived by eye
	7rLF	Red	Lime fresco	3.64	-3.89	-6.04	8.05	High: color variation perceived by eye
	11rLF	Red	Lime fresco	3.32	-1.92	-3.2	4.99	Medium: color variation perceived by eye
After one month	3rBF	Red	*Buon* fresco	5.05	-4.33	-6.2	9.09	High: color variation perceived by eye
	7rBF	Red	*Buon* fresco	5.28	-5.49	-7.62	10.77	High: color variation perceived by eye
	11rBF	Red	*Buon* fresco	3.49	-4.97	-7.02	9.28	High: color variation perceived by eye
	3rLF	Red	Lime fresco	2.17	-5.42	-8.14	10.01	High: color variation perceived by eye
	7rLF	Red	Lime fresco	3.14	-4.29	-6.55	8.43	High: color variation perceived by eye
	11rLF	Red	Lime fresco	3.09	-2.35	-3.62	5.31	High: color variation perceived by eye

* ΔE* values meanings and rating scale of incompatibility risk according to literature [26,65,66]:
Low risk: ΔE*<3; Medium risk: 3<ΔE*<5; High risk: ΔE*>5

Yellow ochre pigment

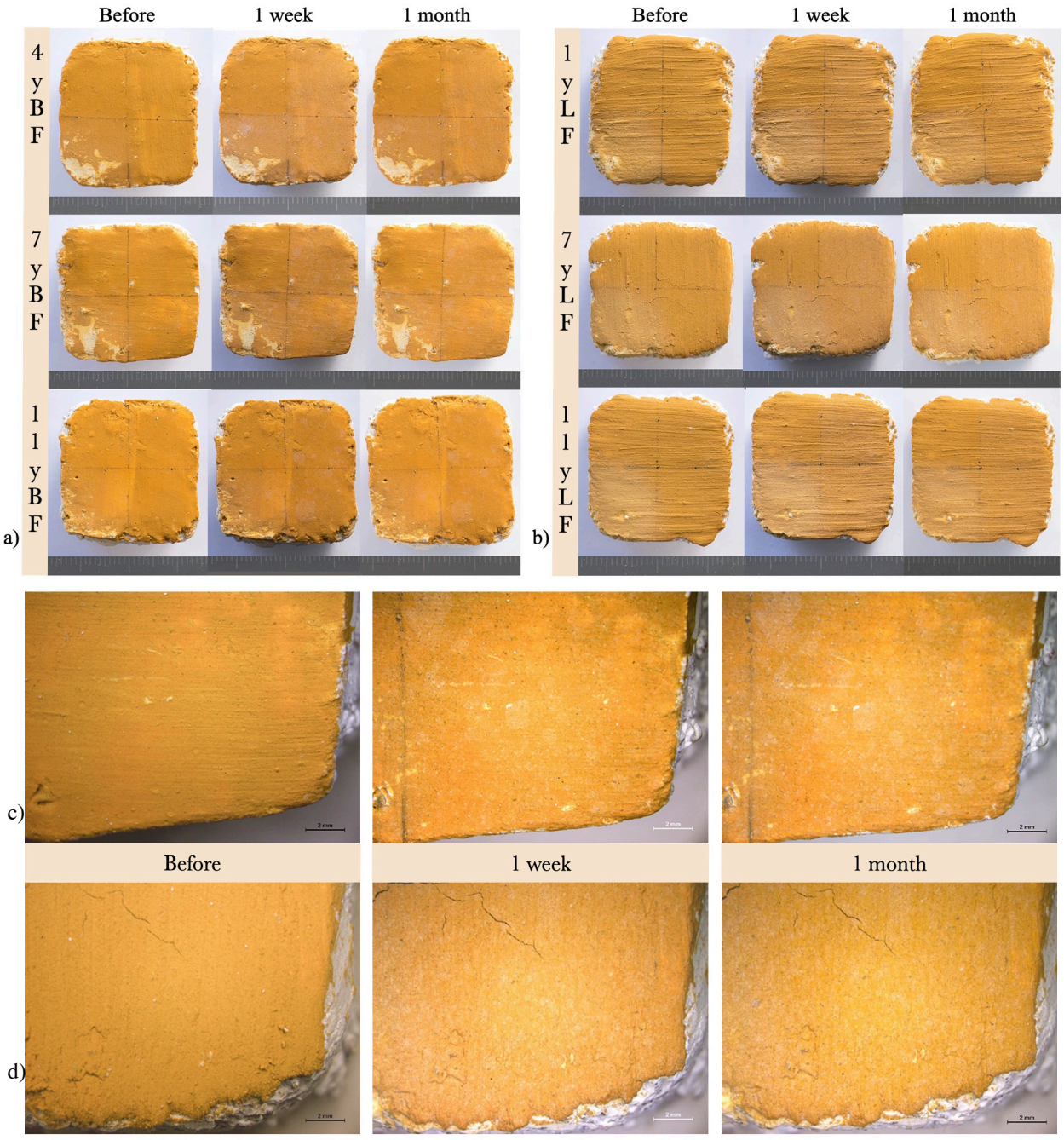

Figure 21. *Photographic documentation of buon and lime fresco replicas painted with yellow ochre; before, in one week and in one month after treatment with HERCULES nanolime: a) Buon fresco replicas: 4yBF, 7yBF, and 11yBF; b) Lime fresco replicas: 1yLF, 7yLF, and 11yLF. OM images (X7.8) of area C of replicas 7yBF (c), and 7yLF (d).*

In agreement with the overall image of all yellow paint layers consolidated with the HERCULES nanolime at the different studied time intervals (Figure 21), the color impact in paint layers made with the ochre pigments is more perceptible at naked eye on the darker tones (red) rather than lighter such as the yellow under study. Only by OM-Vis images and spectro-colorimetric analysis it was ascertain the presence of a white haze on the paint layers carried out with *buon* and lime fresco (Figures 21 - c and d, 22 and 23 and Table 12).

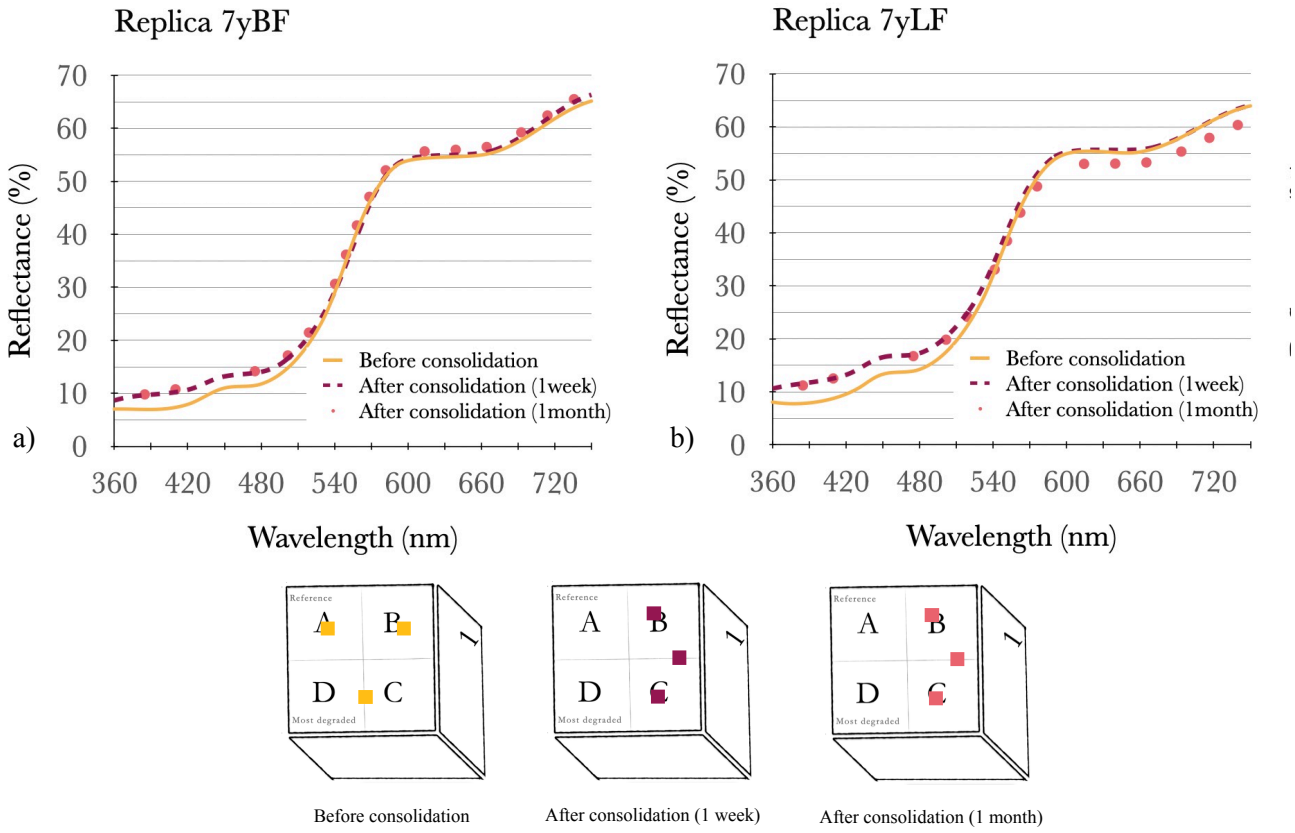

Figure 22. *Reflectance spectral curves of yellow replicas treated with HERCULES nanolime: a) Buon fresco replica 7yBF; b) Lime fresco replica 7yLF. The small squares under the plots display the three points measured to obtain an average colorimetry value before (yellow), in one week (purple) and in one month (pink) after treatment.*

The spectral reflectance curves of the yellow paint layers in Figure 22 show the presence of the white haze by a slight increase in the R%. No change in the shape of the curve is detected in both painting techniques made with yellow ochre showing that the pigment did not suffer any kind of physicochemical alteration, but only a change in the perception of the color. The plot graph for CIE L* and b* coordinates shows a decrease in the value of yellowness (+b*) in all the

yellow replicas after consolidation (Figure 23). For the *buon* fresco lightness (L*) increases, except in replica 11yBF probably due to a differences in the texture of the paint layer in relation to the others (Figure 21a, Table 12). While for the lime fresco replicas lightness decreases from -0.48 to -0.15 in one week and then increases from 0.33 to 1.11 in one month (Figure 23, Tab.12), due to the drying of the consolidant over time, that it is more noticed in light colors (Figure 21b). Even if the white haze is not clearly perceived by naked eye, the total color differences are of ΔE*>5 in the majority of the yellow replicas indicates high risk of incompatibility to the HERCULES nanolime (see Table 12).

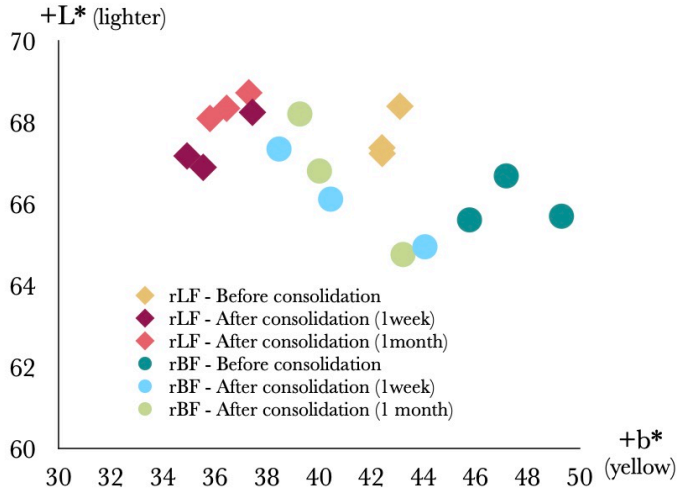

Figure 23. *CIELAB color space plot of all yellow ochre replicas treated with HERCULES nanolime.*

Table 12. *Color differences using CIE*L*a*b* coordinates for yellow paint layers treated with the HERCULES nanolime (one week and one month after replicas treatment).*

	Sample ref.	Color	Painting technique	ΔL*	Δa*	Δb*	ΔE*	Incompatibility risk*
After one week	4yBF	Yellow	*Buon* fresco	0.66	-2.08	-8.72	8.99	High: color variation perceived by eye
	7yBF	Yellow	*Buon* fresco	0.51	-0.3	-5.33	5.36	High: color variation perceived by eye
	11yBF	Yellow	*Buon* fresco	-0.75	-1.78	-5.24	5.58	High: color variation perceived by eye
	1yLF	Yellow	Lime fresco	-0.15	-1.31	-5.66	5.81	High: color variation perceived by eye
	7yLF	Yellow	Lime fresco	-0.06	-1.76	-7.49	7.69	High: color variation perceived by eye
	11yLF	Yellow	Lime fresco	-0.48	-1.61	-6.86	7.06	High: color variation perceived by eye
After one month	4yBF	Yellow	*Buon* fresco	1.52	-1.15	-7.29	8.14	High: color variation perceived by eye
	7yBF	Yellow	*Buon* fresco	1.2	-0.57	-5.76	5.91	High: color variation perceived by eye

11yBF	Yellow	*Buon* fresco	-0.94	-2.44	-6.08	6.61	High: color variation perceived by eye
1yLF	Yellow	Lime fresco	0.33	-1.37	-5.8	5.96	High: color variation perceived by eye
7yLF	Yellow	Lime fresco	1.11	-1.25	-5.97	6.19	High: color variation perceived by eye
11yLF	Yellow	Lime fresco	0.72	-1.41	-6.6	6.78	High: color variation perceived by eye

ΔE values meanings and rating scale of incompatibility risk according to literature [26,65,66].
Low risk: ΔE*<3; Medium risk: 3<ΔE*<5; High risk: ΔE*>5

Smalt pigment

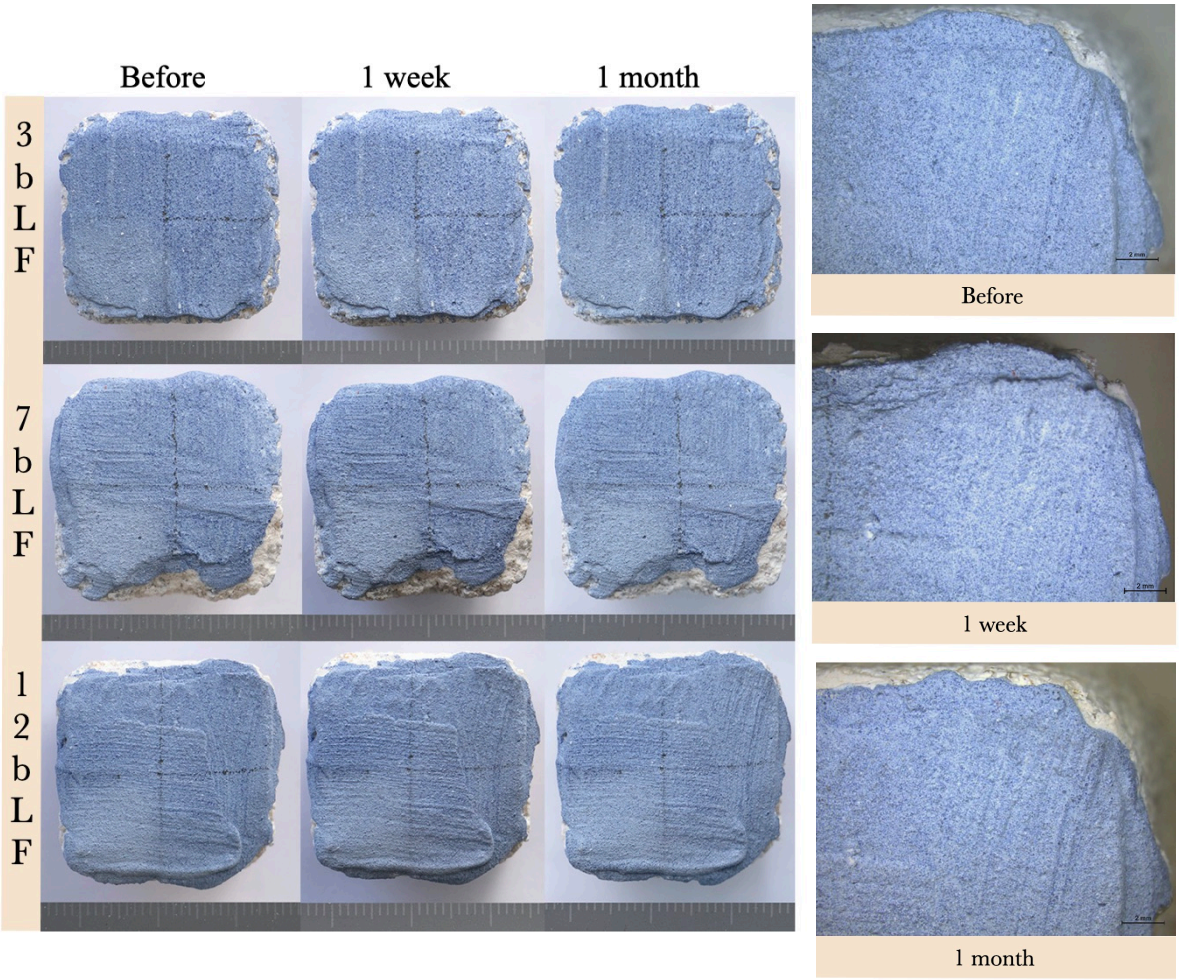

Figure 24. *Photographic documentation of the smalt fresco replicas before, in one week and in one month after treatment with HERCULES nanolime: smalt lime fresco replicas (3bLF, 7bLF and 12bLF) (left side). OM images (X7.8) of area C of 12bLF (right side).*

Unlike the previous paint sets made with ochres, the consolidation treatment with the HERCULES nanolime did not induce changes in the color perception of the blue paint layers

(Figure 24). The spectral curves after one month overlap with the initial ones (Figure 25). Only by colorimetry data is noticed an increase in L* and decrease in blueness (-b*) of the treated replicas, when compared to the values before the treatment (Figure 26 and Table 13). As expected ΔE* indicate low risk of incompatibility (ΔE*< 3) and the changes are undetectable by naked eye ΔE* <3.5 (see Table 13).

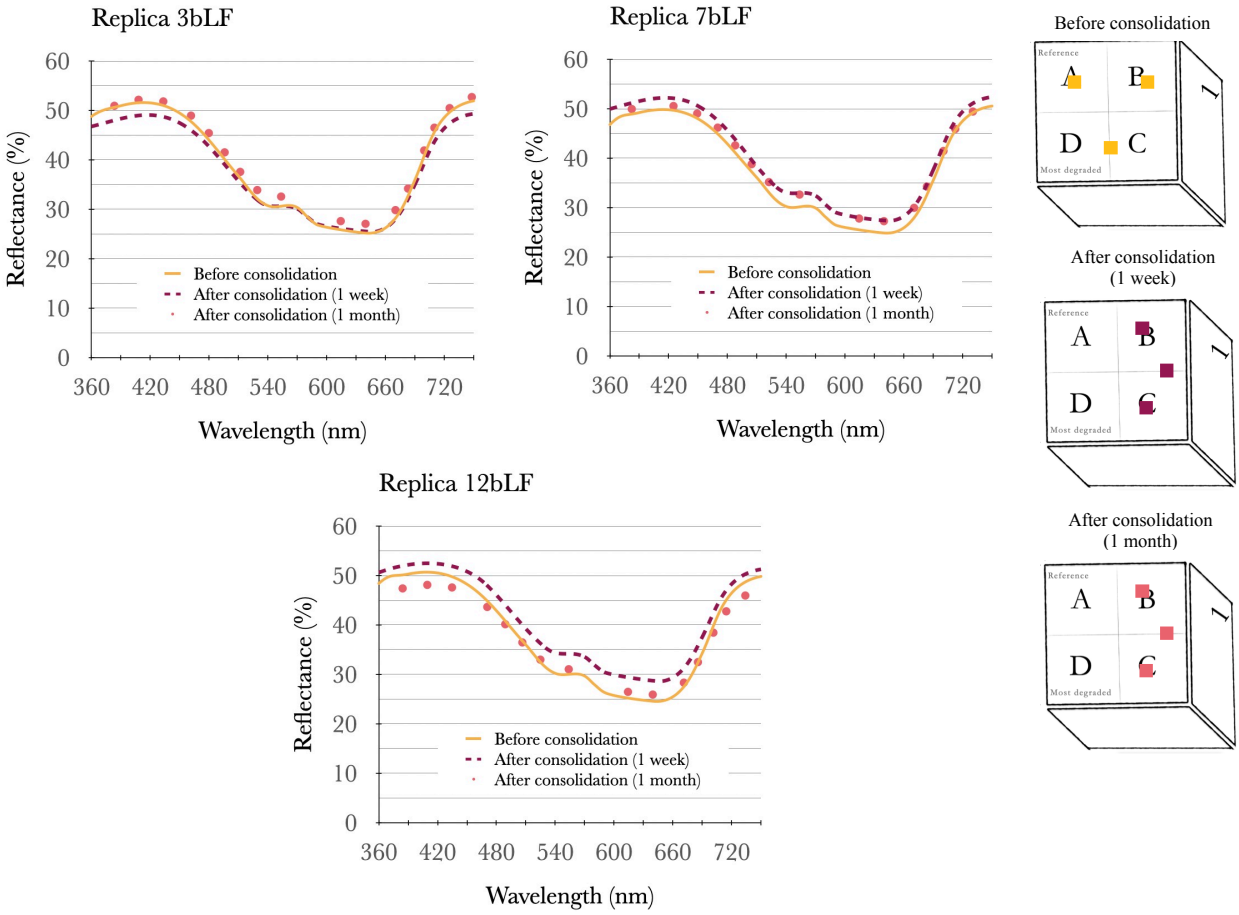

Figure 25. *Reflectance spectral curves of smalt replicas (3bLF, 7bLF, and 12bLF) treated with HERCULES nanolime. The small squares under the plots display the three points measured to obtain an average colorimetry value before (yellow), in one week (purple) and in one month (pink) after treatment.*

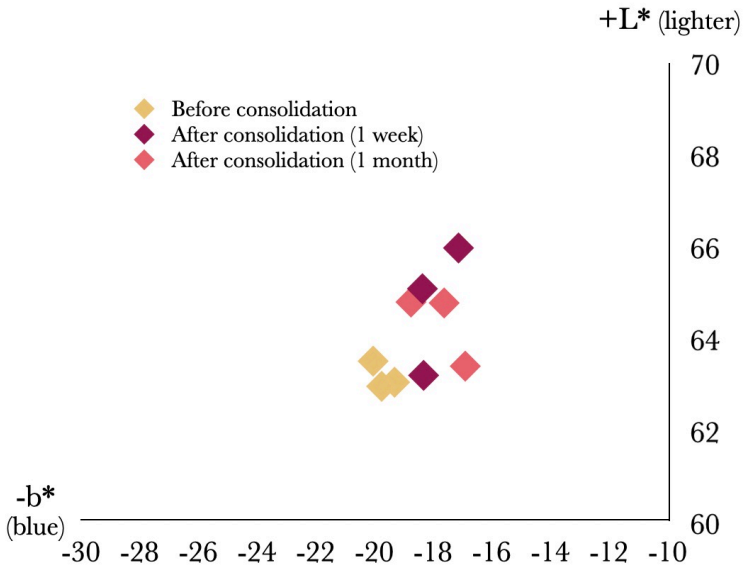

Figure 26. *CIELAB color space of the smalt lime fresco replicas treated with HERCULES nanolime.*

Table 13. *Color differences using CIE*L*a*b* coordinates for blue paint layers treated with the HERCULES nanolime (one week and one month after replicas treatment).*

	Sample ref.	Color	Painting technique	ΔL*	Δa*	Δb*	ΔE*	Incompatibility risk*
After one week	3bLF	Blue	Lime fresco	-0.31	-0.09	1.72	1.75	Low: color variation unperceived by eye
	7bLF	Blue	Lime fresco	2.04	-0.01	0.95	2.25	Low: color variation unperceived by eye
	12bLF	Blue	Lime fresco	3.02	-0.26	2.62	4.0	Medium: color variation perceived by eye
After one month	3bLF	Blue	Lime fresco	1.29	-0.07	1.29	1.8	Low: color variation unperceived by eye
	7bLF	Blue	Lime fresco	1.73	-0.16	1.69	2.42	Low: color variation unperceived by eye
	12bLF	Blue	Lime fresco	0.44	-0.21	2.85	2.89	Low: color variation unperceived by eye

ΔE values meanings and rating scale of incompatibility risk according to literature [26,65,66]:
Low risk: ΔE*<3; Medium risk: 3<ΔE*<5; High risk: ΔE*>5

Statistical comparison of ΔE*

The values for the color variation ΔE* of all the replicas treated with HERCULES nanolime as function of time after one week and one month of consolidation treatment and pigment/technique are shown in Figure 27**.** The overall color variation ΔE* followed the next order in regard to pigment/technique: ΔE*rBF ≥ ΔE* rLF > ΔE* yBF = ΔE* yLF > ΔE* bLF. The ΔE* obtained in smalt paint layers was significantly lower than those made with ochre pigments. It suggests that

ochre pigments are more prone to color changes than the smalt pigment when nanolime is applied.

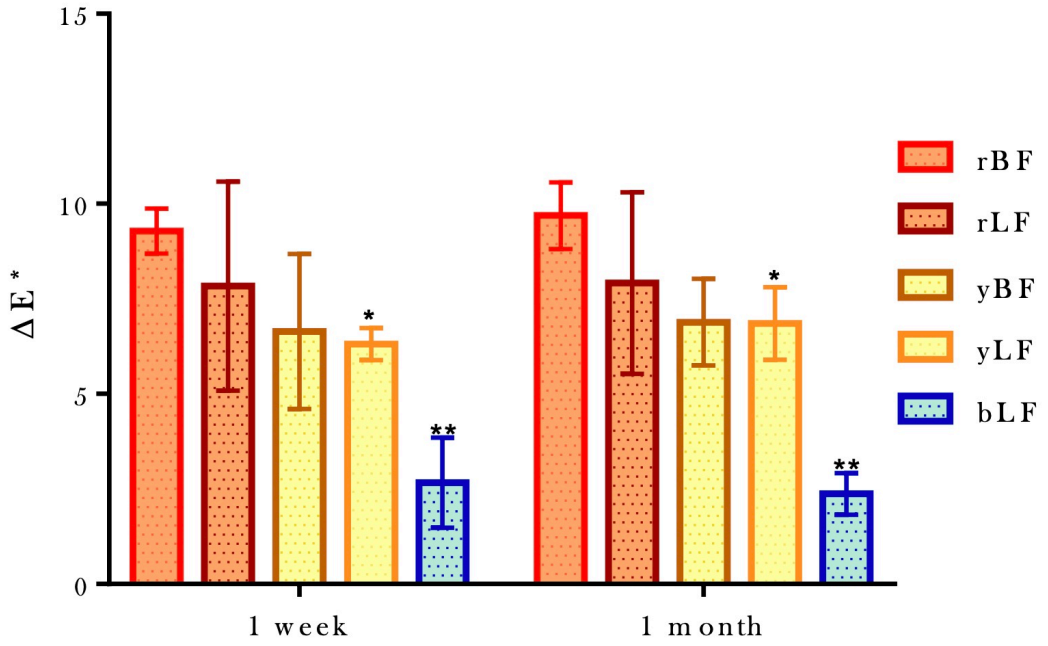

Figure 27*. Average overall color difference for all the replicas (pigment/technique) treated with HERCULES nanolime in one week and in one month after treatment, analyzed by ANOVA followed by Bonferroni's multiple comparison test. * P< 0.05 compared to the red buon fresco replica, **P<0.001 in relation to both ochre pigments. Means and standard deviation of the replicas are shown.*

CaLoSiL®

Red pigment

The images of the red paint layers in *buon* and lime fresco show that in both painting techniques, a white pinkish haze veil is was formed on the paint surface after the addition of CaLoSiL® (Figure 28). The color of the haze is probably the result of the mixture of the consolidant and the pigment particles. In the OM images at 7.8x of 5rBF and 5rLF, it can be seen an evenly spread veil over the surface (Figures 28 c and d). Only in paint layers of 12rBF (Fig 28e) and 9rLF (Figure 28 f) no effect is noticed by naked eye. The effect present in the red ochre replicas treated with the commercial nanolime is different from for the one obtained from the synthesized nanolime, where the veil is spotted (Figure 19).

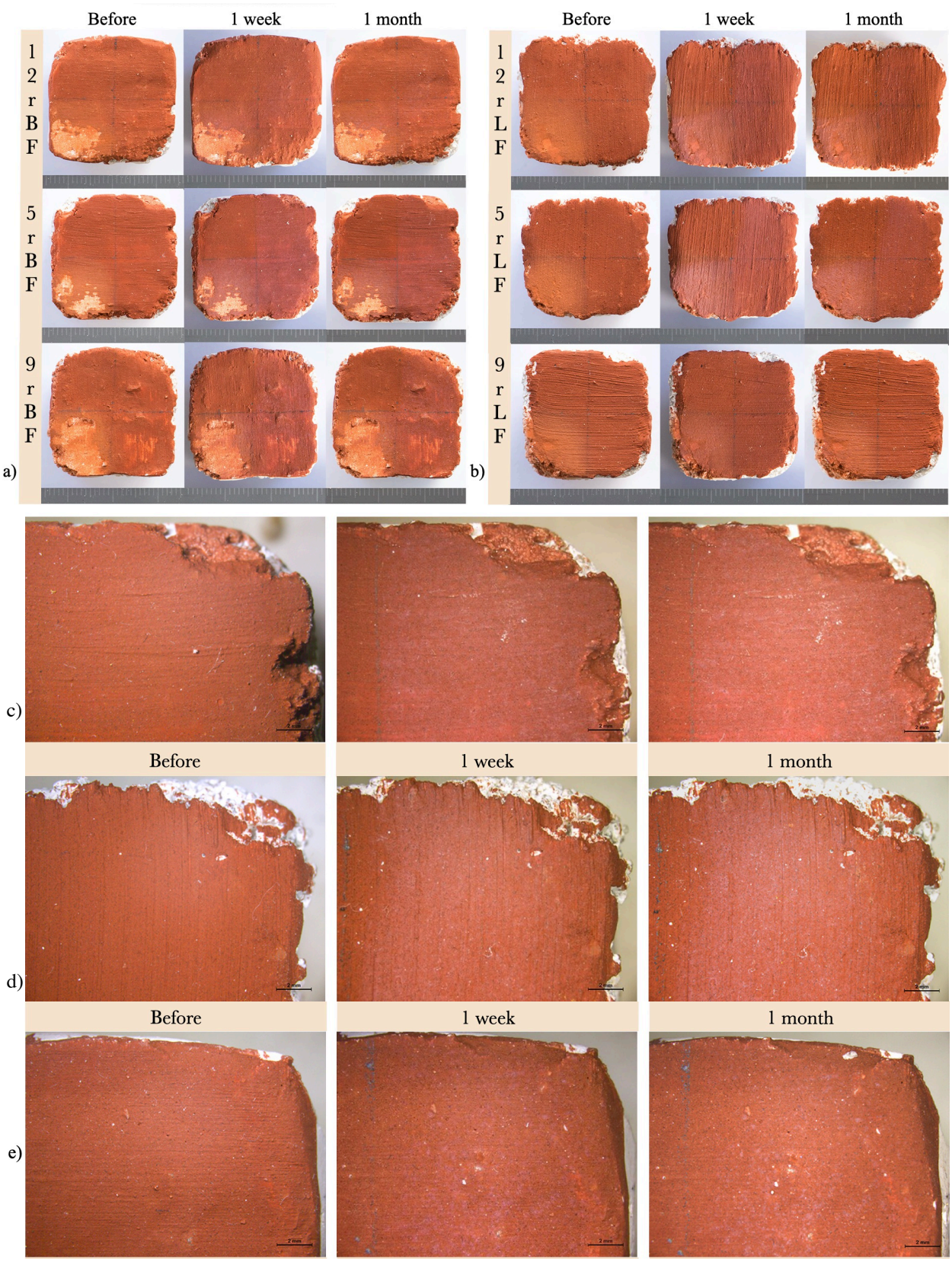
Before
1 week
1 month
12 rBF
5 rBF
9 rBF
a)
Before
1 week
1 month
12 rLF
5 rLF
9 rLF
b)
c)
Before
1 week
1 month
d)
Before
1 week
1 month
e)

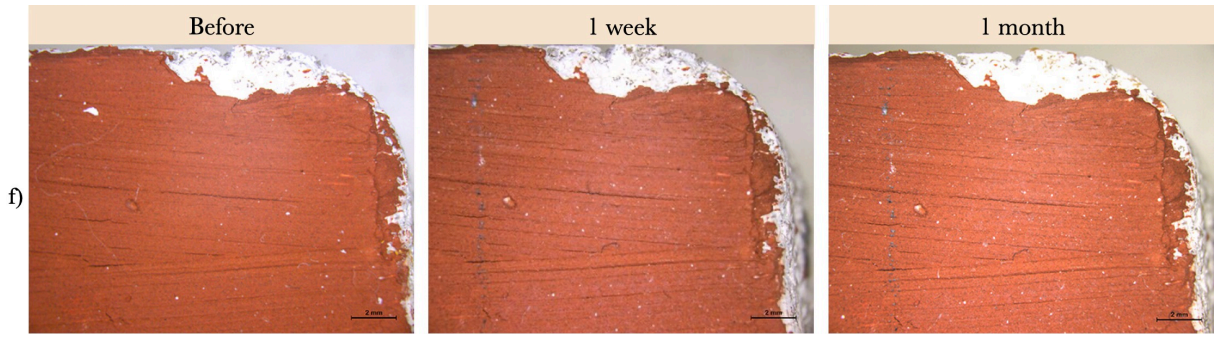

Figure 28. *Photographic documentation of buon and lime fresco replicas painted with red ochre; before, in one week and in one month after treatment with CaLoSiL®: a) Buon fresco replicas: 12rBF, 5rBF and 9rBF; b) Lime fresco replicas: 12rLF, 5rLF and 9rLF. OM images (X7.8) of area B of replicas 5rBF (c), 5rLF (d), 12rBF (e), and 9rLF (f).*

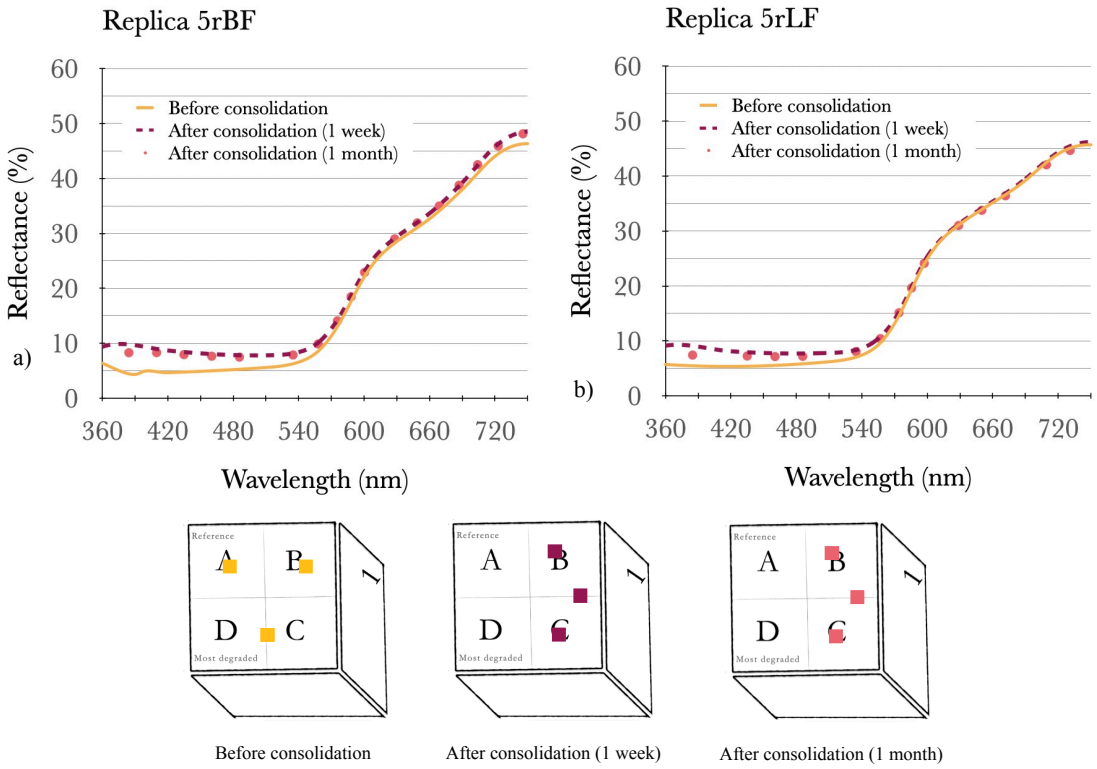

Figure 29. *Reflectance spectral curves of red replicas treated with CaLoSiL®: a) Buon fresco replica 5rBF, b) Lime fresco replica 5rLF. The small squares under the plots display the three points measured to obtain an average colorimetry value before (yellow), in one week (purple) and in one month (pink) after treatment.*

Spectral reflectance curves of the *buon* and lime fresco red replicas consolidated with CaLoSiL® behaved similarly to the ones for HERCULES nanolime (Fig, 29). The same trend is seen on the CIE L* and a* plot in Figure 30. In both painting techniques, the values of L* increased (lightening effect) and most of a* values decreased except for 9rBF, possibly because a slight variability in the measurement location. Similar than with the HERCULES nanolime, CaLoSiL® ΔE* values were higher than the threshold of detectability by human eye (ΔE* >3.5) and exhibit high risk of incompatibility (ΔE*>5) (Table 14). In spite of that the values of ΔE* for the replica 12rBF and 9rLF indicate medium risk of incompatibility, in this replicas no change on the colors was noticed by naked eye and the calculation of ΔE can be influenced by the pinkish haze, which could cause an overestimation in the measurement of reflectance (Table 14, and Figures 28 e and f).

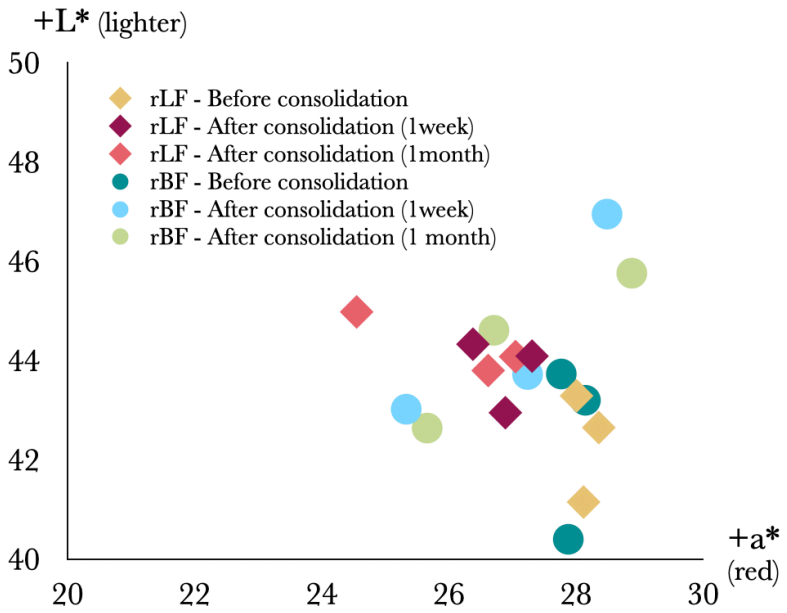

Figure 30. *CIELAB color space plot of all red ochre fresco replicas treated with CaLoSiL®.*

Table 14. *Color differences using CIE*L*a*b* coordinates for red paint layers treated with CaLoSiL® (one week and one month after replicas treatment).*

	Sample ref.	Color	Painting technique	ΔL*	Δa*	Δb*	ΔE*	Incompatibility risk*
After one week	12rBF	Red	*Buon* fresco	-0.01	-0.53	-2.12	2.18	Low: color variation unperceived by eye
	5rBF	Red	*Buon* fresco	2.62	-2.55	-8.71	9.44	High: color variation perceived by eye
	9rBF	Red	*Buon* fresco	3.75	0.34	-4.89	6.17	High: color variation perceived by eye
	12rLF	Red	Lime fresco	1.8	-1.23	-4.84	5.30	High: color variation perceived by eye
	5rLF	Red	Lime fresco	1.68	-1.98	-6.81	7.28	High: color variation perceived by eye
	9rLF	Red	Lime fresco	0.8	-0.7	-2.53	2.74	Low: color variation unperceived by eye
After one month	12rBF	Red	*Buon* fresco	0.88	-1.06	-2.74	3.06	Medium: color variation unperceived by eye
	5rBF	Red	*Buon* fresco	2.24	-2.22	-7.74	8.35	High: color variation perceived by eye
	9rBF	Red	*Buon* fresco	2.56	0.73	-3.69	4.55	Medium: color variation perceived by eye
	12rLF	Red	Lime fresco	3.83	-3.57	-6.09	8.03	High: color variation perceived by eye
	5rLF	Red	Lime fresco	1.15	-1.74	-5.31	5.70	High: color variation perceived by eye
	9rLF	Red	Lime fresco	0.79	-0.96	-2.59	2.87	Medium: color variation unperceived by eye

ΔE values meanings and rating scale of incompatibility risk according to literature [26,65,66]:
Low risk: ΔE*<3; Medium risk: 3<ΔE*<5; High risk: ΔE*>5

Yellow ochre replicas

Similarly to the case of HERCULES nanolime and in agreement with the image of all the yellow replicas consolidated with CaLoSiL® (Figure 31) the color impact in ochre pigments is more perceptible in the darker (red) rather than the lighter (yellow) ochre paint layers. By the overall images no effect of the consolidation was noticed in the *buon* and lime fresco replicas. No white veil is present, however some of the replicas, 9yLF and 5yLF, seem to be visually lighter in comparison to reference area A (Figure 31a, b and d).

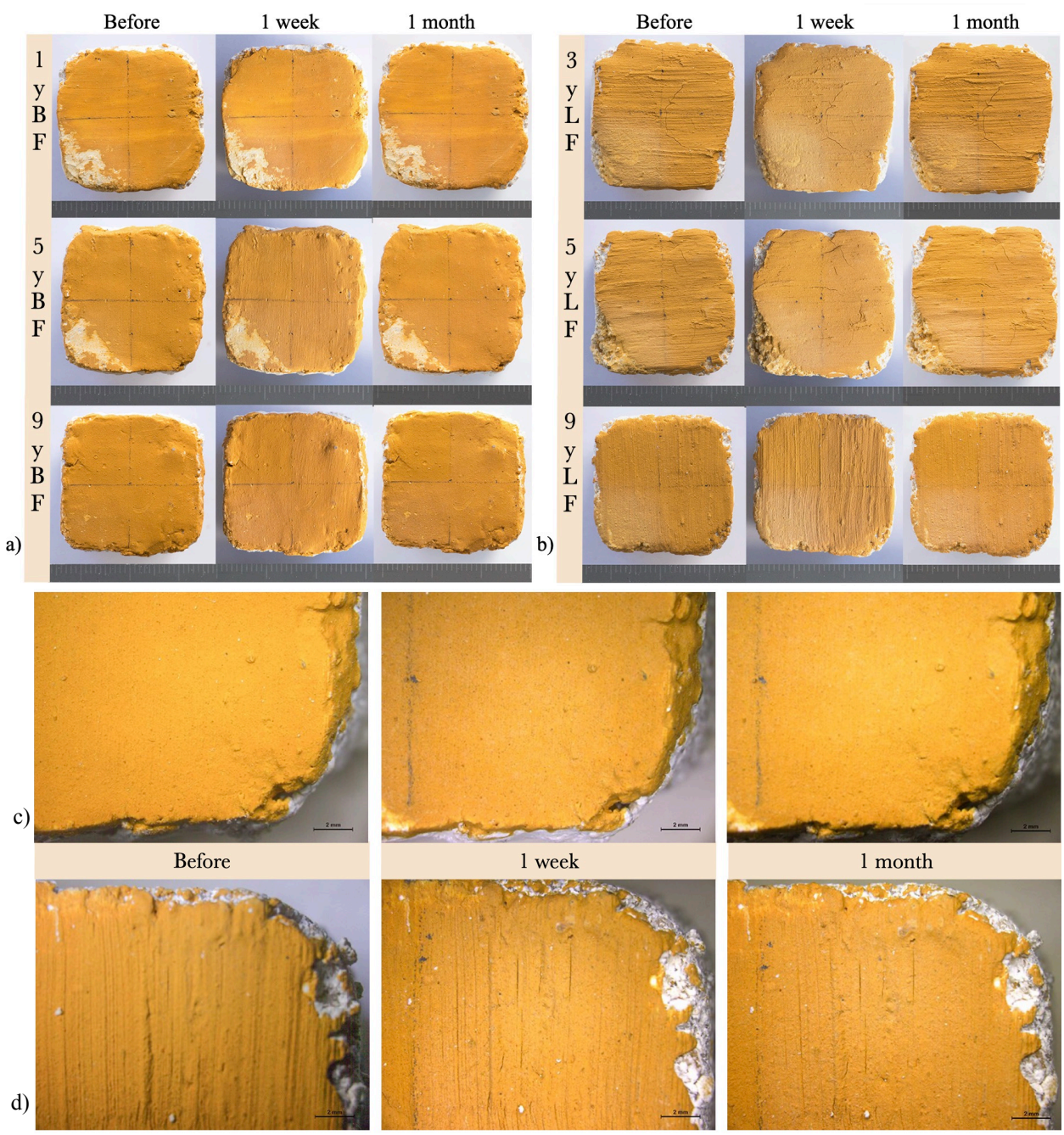

Figure 31. *Photographic documentation of buon and lime fresco replicas painted with yellow ochre; before, in one week and in one month after treatment with CaLoSiL®: a) Buon fresco replicas: 1yBF, 5yBF and 9yBF; b) Lime fresco replicas: 3yLF, 5yLF and 9yLF. OM images (X7.8) of area C of replicas 5yBF (c), and 9yLF(d).*

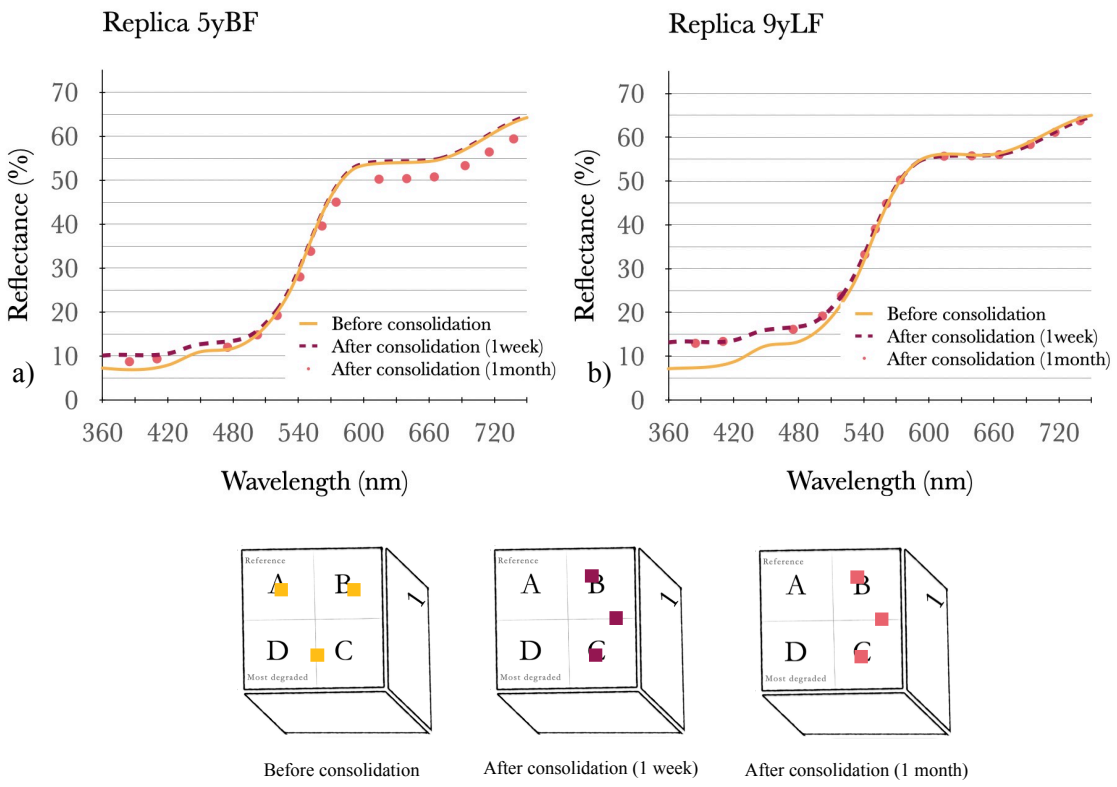

Figure 32. *Reflectance spectral curves of yellow replicas treated with CaLoSiL®: a) Buon fresco replica 5yBF, b) Lime fresco replica 9yLF. The small squares under the plots display the three points measured to obtain an average colorimetry value before (yellow), in one week (purple) and in one month (pink) of treatment.*

The spectral reflectance curves of the yellow replicas (Figure 32) treated with CaLoSiL® had the same behavior as the synthesized nanolime. The plot graph for CIEL L* and b* showed that both techniques exhibit a decrease in yellowness (b*), and an increase in lightness (L*) after one month. However, in the *buon* fresco ΔL* values decreased in one week before increasing in one month, probably due to a change in texture in the surface of the replica as a result of the treatment (Figures 31a, 33, Tab.15). Even if the white haze is not clearly perceived by naked eye, the total color differences of some of the replicas 1yBF, 9yBF and 9yLF have ΔE*>5 which indicates high risk of incompatibility. In *buon* fresco only one replica, 5yBF, presents medium risk of incompatibility, while in lime fresco all replicas presented different ranges of incompatibility (low, medium and high). Probably an overestimation of ΔE* could have been the result of a slight variation in the amount of product deposited when it was sprayed. However, the high values of ΔE obtained for most of the yellow replicas treated with both nanolime need to be further analyzed.

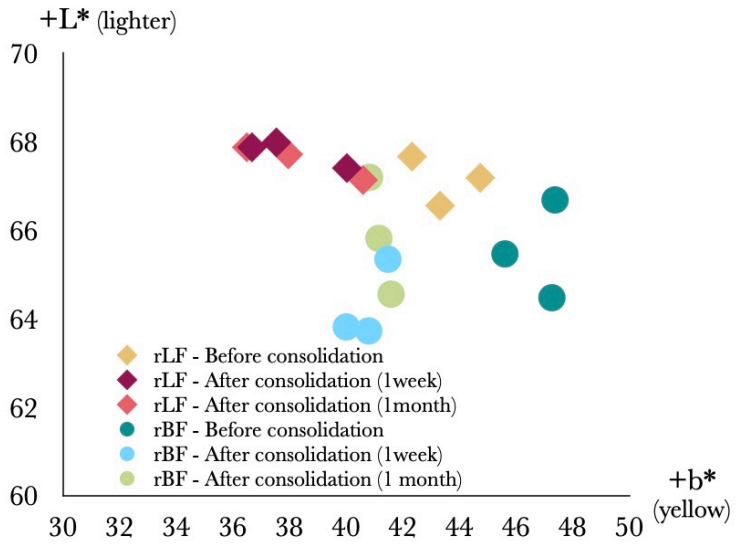

Figure 33. *CIELAB color space plot of all yellow ochre fresco replicas treated with CaLoSiL®.*

Table 15. *Color differences using CIE*L*a*b* coordinates for yellow paint layers treated with CaLoSiL® (one week and one month after replicas treatment).*

	Sample ref.	Color	Painting technique	ΔL*	Δa*	Δb*	ΔE*	Incompatibility risk*
After one week	1yBF	Yellow	*Buon* fresco	-1.34	-0.89	-5.9	6.11	High: color variation perceived by eye
	5yBF	Yellow	*Buon* fresco	-1.65	-0.42	-5.6	5.85	High: color variation perceived by eye
	9yBF	Yellow	*Buon* fresco	-0.75	-0.75	-6.47	6.55	High: color variation perceived by eye
	3yLF	Yellow	Lime fresco	0.85	-0.2	-3.29	3.40	Medium: color variation unperceived by eye
	5yLF	Yellow	Lime fresco	0.32	-0.68	-4.79	4.84	Medium: color variation perceived by eye
	9yLF	Yellow	Lime fresco	0.69	-0.68	-8.06	8.11	High: color variation perceived by eye
After one month	1yBF	Yellow	*Buon* fresco	0.51	-0.94	-6.55	6.63	High: color variation perceived by eye
	5yBF	Yellow	*Buon* fresco	0.35	0.25	-4.45	4.47	Medium: color variation perceived by eye
	9yBF	Yellow	*Buon* fresco	0.08	-0.22	-5.68	5.68	High: color variation perceived by eye
	3yLF	Yellow	Lime fresco	0.58	-0.13	-2.72	2.78	Low: color variation unperceived by eye
	5yLF	Yellow	Lime fresco	0.05	-0.51	-4.37	4.39	Medium: color variation perceived by eye
	9yLF	Yellow	Lime fresco	0.69	-0.71	-8.24	8.29	High: color variation perceived by eye

ΔE values meanings and rating scale of incompatibility risk according to literature [26,65,66]:
Low risk: ΔE*<3; Medium risk: 3<ΔE*<5; High risk: ΔE*>5

Blue pigment

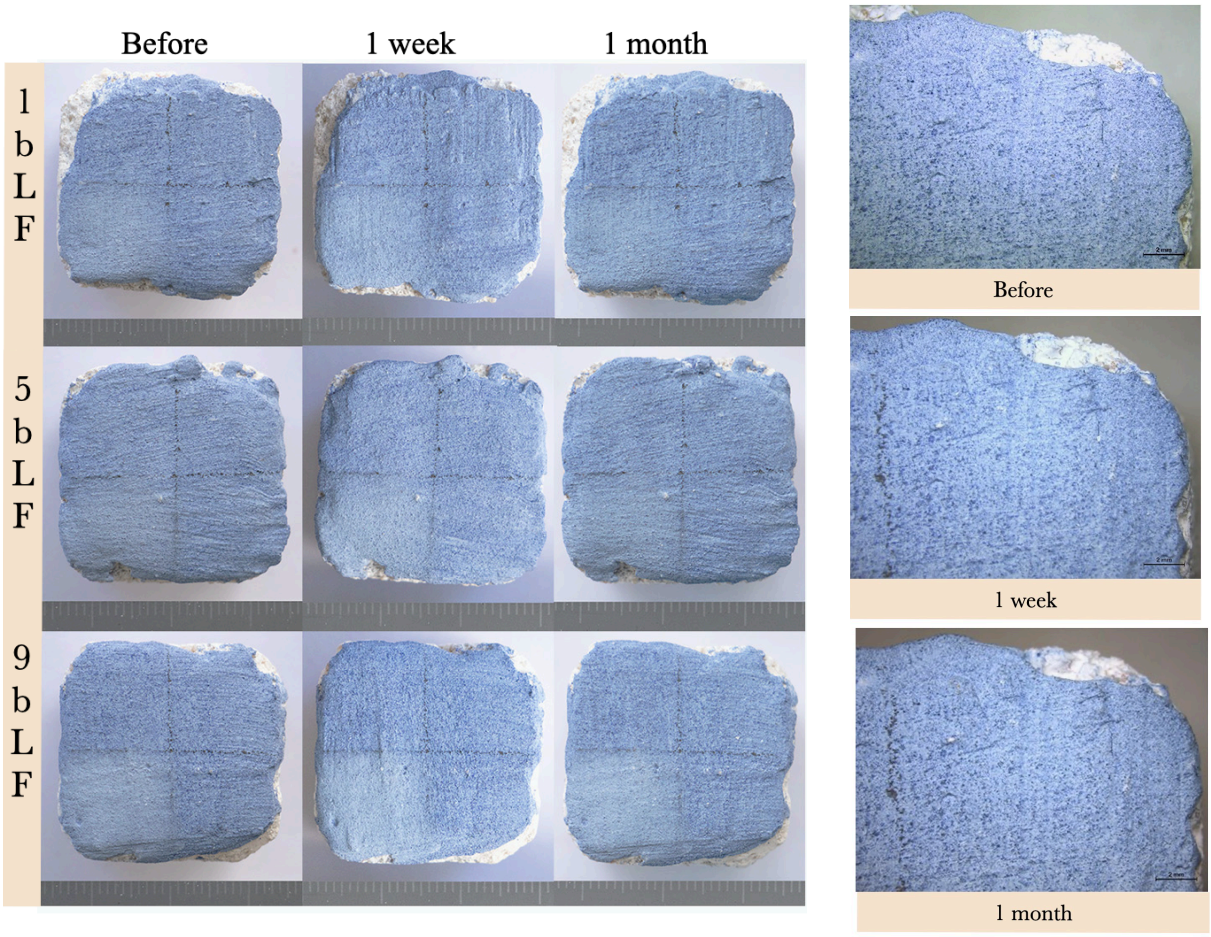

Figure 34. *Photographic documentation of lime fresco replicas painted with smalt before, in one week and in one month after treatment with CaLoSiL®: Left side: lime fresco replicas (1bLF, 5bLF, and 9bLF). Right side: OM images (X7.8) of area B of lime fresco replicas painted with smalt (1bLF).*

Similarly to the results obtained from the HERCULES nanolime, the smalt replicas consolidated with CaLoSiL® (Figure 34) presented no perceptible chromatic variation (ΔE* <3.5) (Table 16). At the same time the behavior of the spectral reflectance curves is the same for both nanolime products (Appendix 4, A4-7 and A4-8) . The chromatic coordinates of CIELAB color space plot shows and a decrease of blueness (-b*) (Figure 35). The majority of ΔL* values were positive signifying a lightening effect after the treatment, only replica 9bLF behaved differently, which could be for unknown reasons that must be further analyzed in the future. The ΔE* obtained indicates low risk of incompatibility (ΔE*< 3).

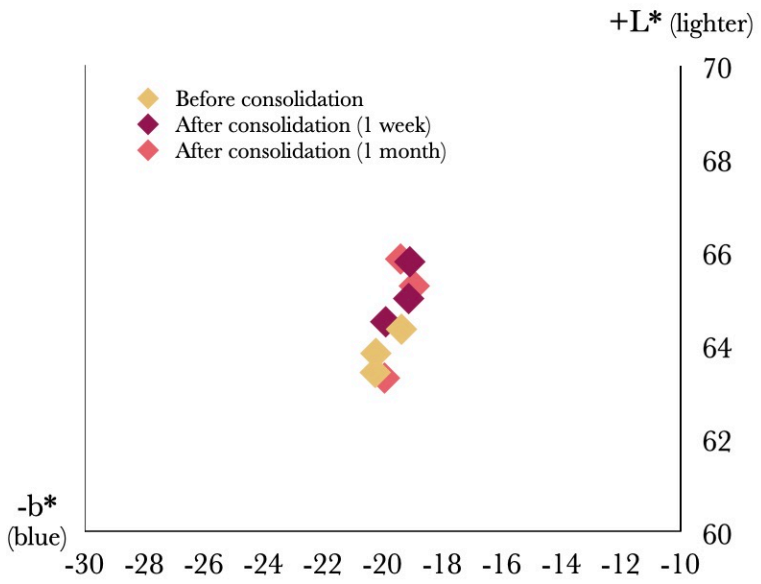

***Figure 35**. CIELAB color space plot of smalt fresco replicas treated with CaLoSiL®.*

***Table 16.** Color differences using CIE*L*a*b* coordinates for blue paint layers treated with CaLoSiL® (one week and one month after replicas treatment).*

	Sample ref.	Color	Painting technique	ΔL*	Δa*	Δb*	ΔE*	Incompatibility risk*
After one week	1bLF	Blue	Lime fresco	2.38	-0.45	1.16	2.68	Low: color variation unperceived by eye
	5bLF	Blue	Lime fresco	1.32	0.01	0.24	1.34	Low: color variation unperceived by eye
	9bLF	Blue	Lime fresco	0.68	-0.22	0.33	0.78	Low: color variation unperceived by eye
After one month	1bLF	Blue	Lime fresco	2.44	-0.49	0.85	2.62	Low: color variation unperceived by eye
	5bLF	Blue	Lime fresco	0.93	-0.12	0.43	1.03	Low: color variation unperceived by eye
	9bLF	Blue	Lime fresco	-0.39	-0.17	0.29	0.51	Low: color variation unperceived by eye

ΔE values meanings and rating scale of incompatibility risk according to literature [26,65,66]:
Low risk: ΔE*<3; Medium risk: 3<ΔE*<5; High risk: ΔE*>5

Statistical comparison of ΔE*

The values for the color variation ΔE* of all the replicas treated with CaLoSiL® as function of the time passed after application of the treatment (one week and one month) and pigment/ technique are shown in Figure 36. The overall color variation ΔE* followed the next order in regard to pigment/technique:ΔE* rBF ≥ ΔE* rLF ≥ ΔE* yLF ≥ ΔE* yBF > ΔE* bLF. No significant differences were found between the ochre paint layers. Similarly to the HERCULES

nanolime the ΔE* obtained in smalt pigment was significantly lower than those of the ochre pigments. Confirming that the ochre pigments are more prone to color changes due to the application of nanolime, this behavior was also observed before by Becherini et al. in 2018 during an aesthetic compatibility assessment of consolidants for mural paintings [69]; and by Zhu et al. while using graphene enhanced nanolime for mural painting protection in comparison to other commercial and synthesized nanolime [70]. It is important to mention that the high color variation, due to white haze by the application of nanolime can substantially be reduced by applying a more diluted dispersion and by using mixed dispersing solvents. For example, by the addition of a small amount of acetone to the short-chain alcohol dispersing the $Ca(OH)_2$ NPs (see Section 3.2.2), reason why preliminary tests, the selected dispersant of the HERCULES nanolime consisted of a mixture of Acetone:Ethanol (1:10). While CaLoSiL® in 2-propanol was applied at 25 g/L, same concentration as HERCULES nanolime.

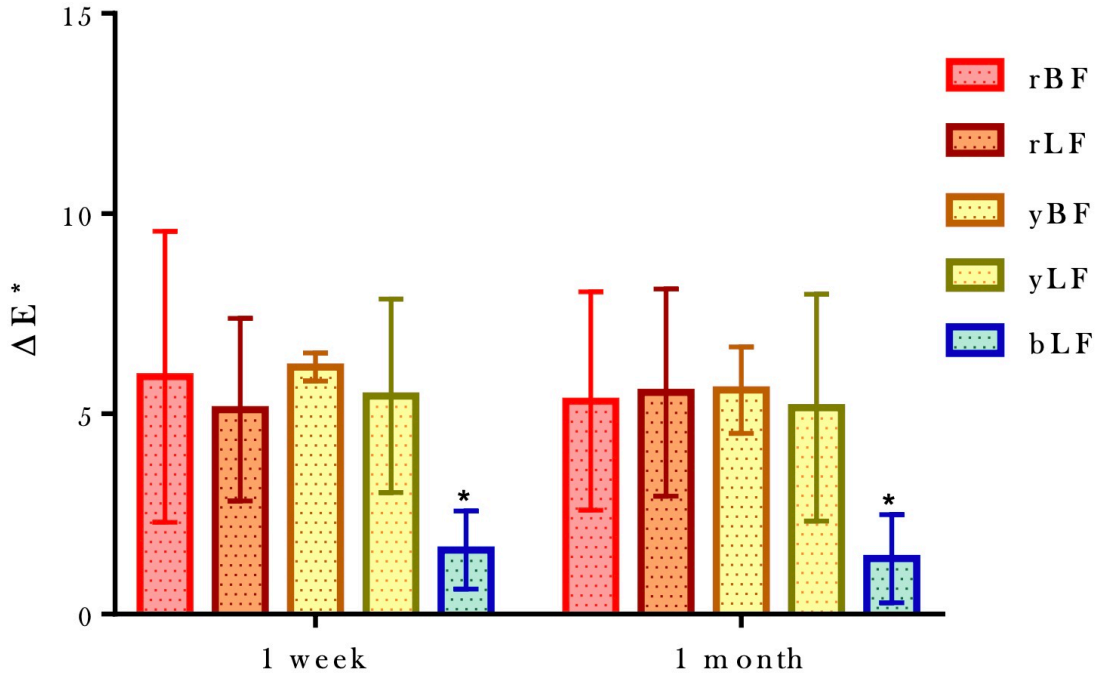

***Figure 36**. Average overall color difference for all the replicas (pigment/technique) treated with CaLoSiL® one week and one month after consolidation, analyzed by two-way ANOVA followed by Bonferroni's multiple comparison test. * P< 0.001 compared to the ochre pigments. Means and standard deviation of the replicas are shown.*

The comparison of the histograms of CaLoSiL® (Figure 36) and the histogram of HERCULES nanolime (Figure 27) showed that ΔE* values are higher after treatment with HERCULES nanolime. Another difference between the histograms was the variability. CaLoSiL® presented higher variability in all variables except for yBF replicas, while HERCULES nanolime presents different degrees of variability independently of pigment and technique. The variable behavior of both nanolimes indicates that a higher number of replicas are required and could depend on uneven cover (texture, and brush stoke direction) in some replicas, due to variation in the paint laid down.

Primal®

Primal® did not produce aesthetic change in most of the fresco replicas, ΔE*<3.5 (see Table 17), except for replica 6yBF (see table 17) because the surface texture of the replica is irregular in comparison to the others and could have affected the colorimetric measurement. Figures 37, 38, and 39 display all the replica sets treated at the different studied intervals (in one week and in one month). The UVF images of an example of each replica group (pigment/technique) after a month of treatment did not show fluorescence in the samples after they were consolidated (Figure 40). It means that the dispersion of 2% commonly used in conservation works is the optimum concentration.

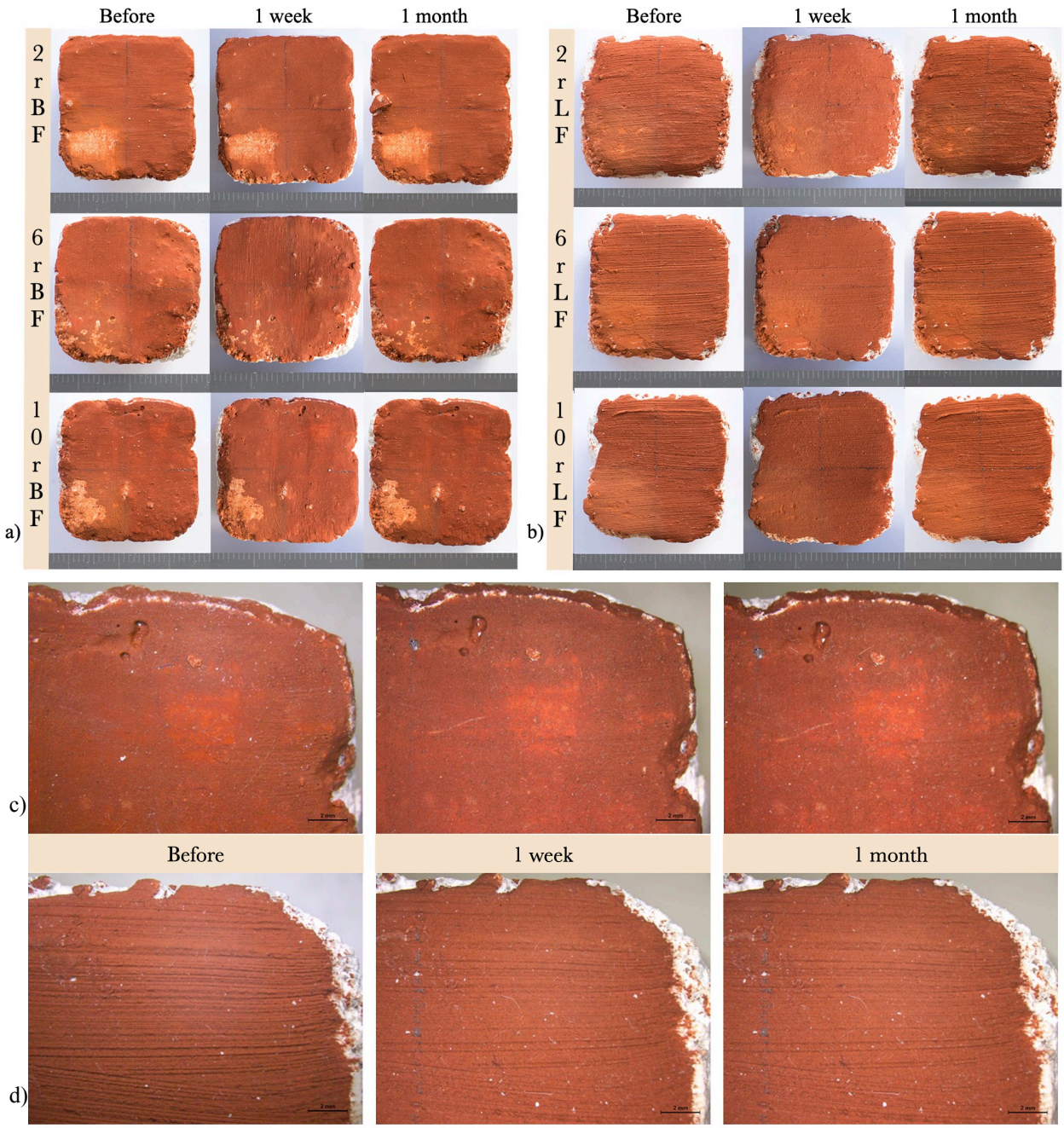

Figure 37. *Photographic documentation of buon and lime fresco replicas painted with red ochre; before, in one week and in one month after application of Primal®: a) Buon fresco replicas: 2rBF, 6rBF and 10rBF; b) Lime fresco replicas:2rLF, 6rLF and 10rLF. OM images (X7.8) of area B of replica 10rBF (c) and replica 10rLF (d)..*

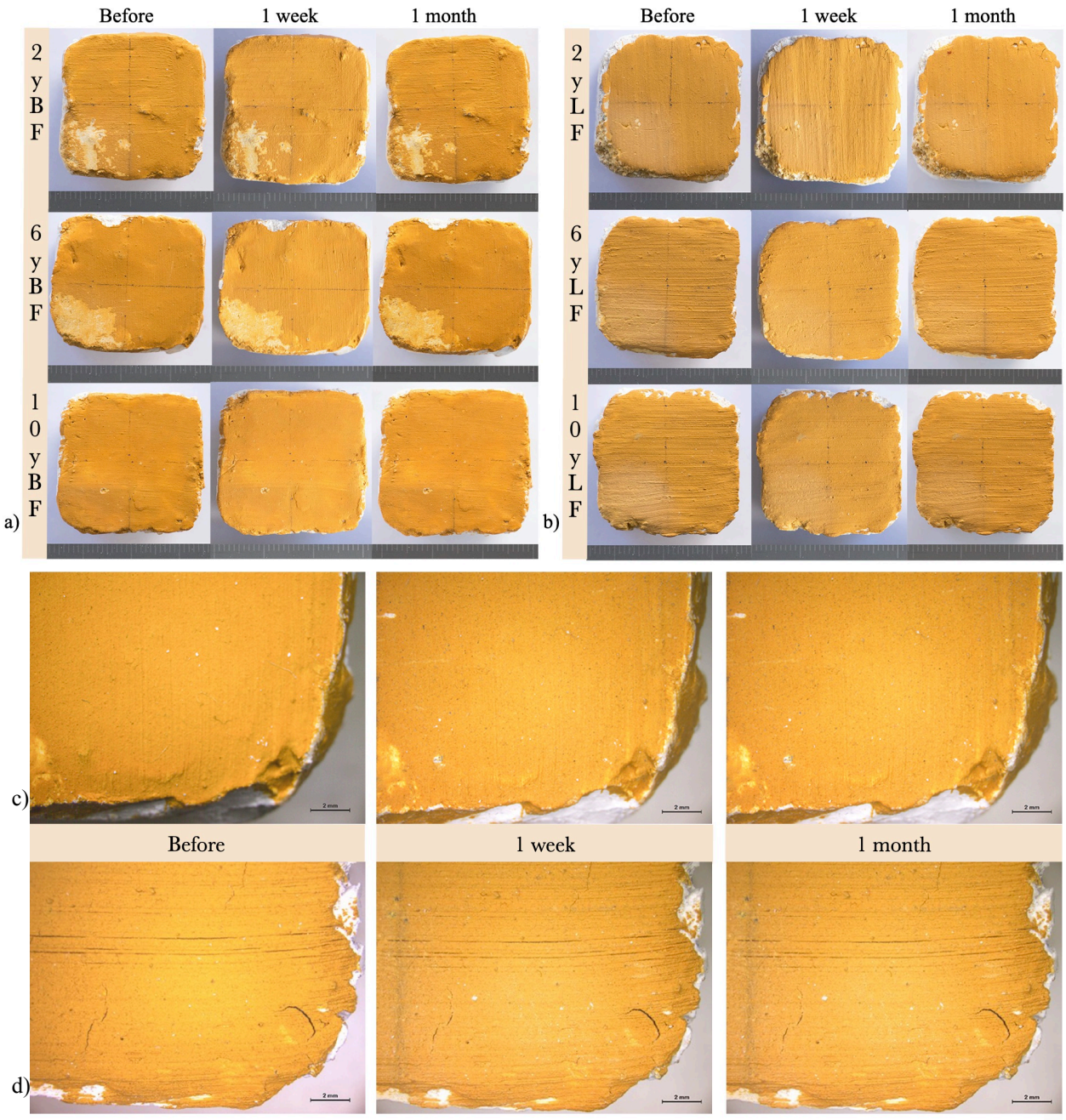

Figure 38. *Photographic documentation of buon and lime fresco replicas painted with yellow ochre; before, in one week and in one month of application of Primal®: a) Buon fresco replicas: 2yBF, 6yBF and 10yBF; b) Lime fresco replicas: 2yLF, 6yLF and 10yLF. OM images (X7.8) of area C of replica 6yBF (c), and 6yLF (d).*

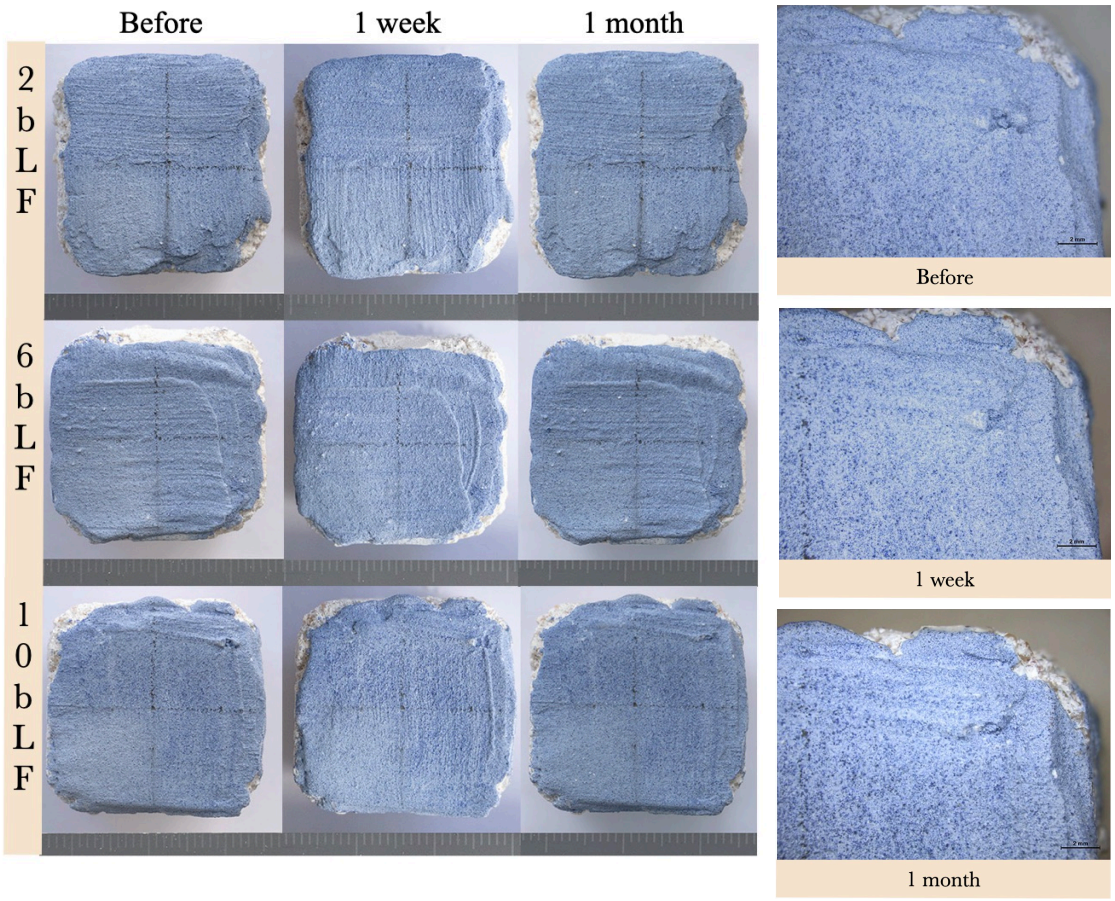

Figure 39. *Photographic documentation of the smalt replicas, before, in one week and in one month after treatment with Primal®: Right side: Photographic documentation of replicas 2bLF, 6bLF and 10bLF; Left side: OM images (X7.8) of area B of fresco replica 10bLF.*

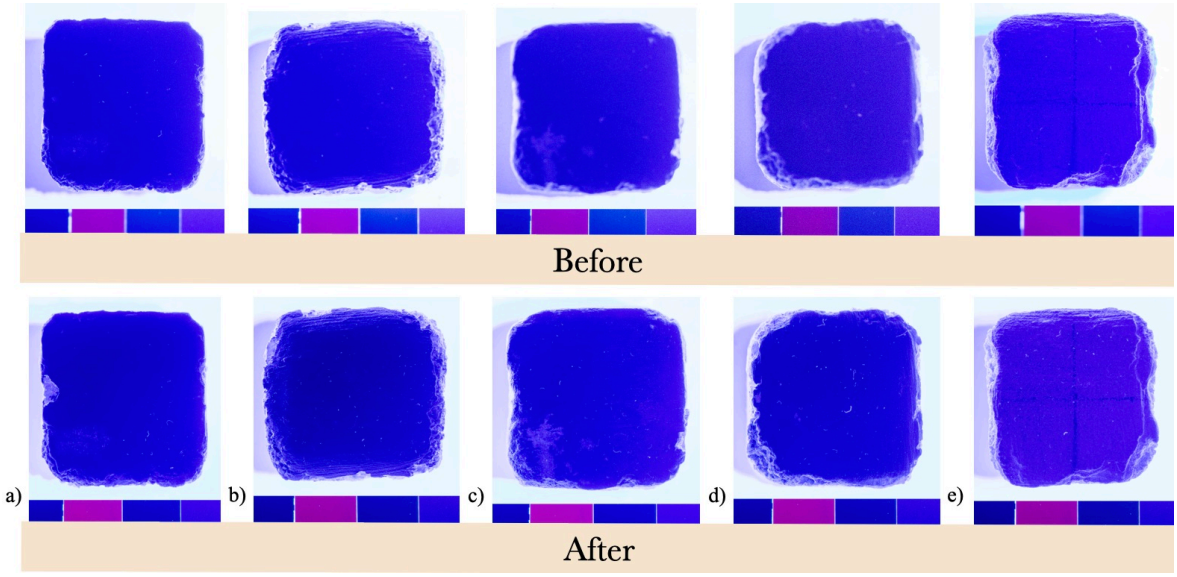

Figure 40. *UV photographic documentation of an example of each replicas by color/technique before and in one month after treatment with Primal®: a) Replica 2rBF; b) Replica 2rLF; c) Replica 2yBF; d) Replica 2yLF; and e) Replica 2bLF.*

The reflectance spectral curves obtained from all replicas (see Appendix 4 and Figure A4-3, A4-6 and A4-8) , the plot graphs for CIEL* and a* (red ochre, Figure 41a) and CIEL* and b* (yellow ochre and smalt, Figure 41b and 41c) showed slight decrease in each of their respective color coordinates a* by -1.5 to -0.15; +b* by -2.52 to -0.45; and -b* by -0.29 to -0.03 (Table 17). In most replicas ΔL* decreased by -0.03 to -2.88, producing a darkening effect that however is not noticed by naked eye. The ΔE* obtained indicates low risk of incompatibility, ΔE*< 3. Only replica 6yBF presented medium risk of incompatibility at the end of the month with ΔE* of 4.38, probably due to the direction of the brush strokes in the surface, which apparently affected the colorimetry measurements (Figure 38a).

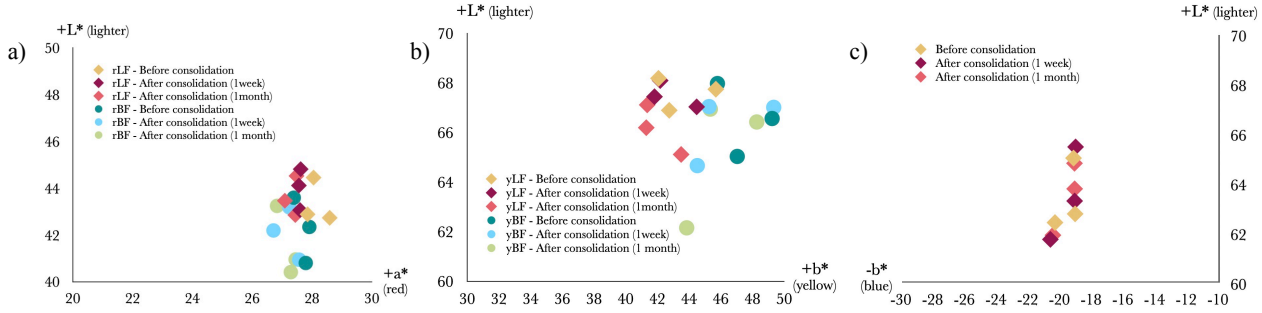

Figure 41. *CIELAB color space plots of all fresco replicas consolidated with Primal®: a) a* versus L*, all red ochre replicas, b) b* versus L* of all yellow ochre replicas; and c) b* versus L* of smalt fresco replicas.*

Table 17. *Color differences using CIE*L*a*b* coordinates for yellow paint layers treated with Primal® (one week and one month after consolidation treatment).*

P	Sample ref.	Color	Painting technique	ΔL*	Δa*	Δb*	ΔE*	Incompatibility risk*
After one week	2rBF	Red	*Buon* fresco	-0.41	-0.15	0.08	0.44	Low: color variation unperceived by eye
	6rBF	Red	*Buon* fresco	-0.15	-1.2	-0.87	1.48	Low: color variation unperceived by eye
	10rBF	Red	*Buon* fresco	0.14	-0.22	-0.23	0.34	Low: color variation unperceived by eye
	2rLF	Red	Lime fresco	0.41	-1.03	-0.62	1.27	Low: color variation unperceived by eye
	6rLF	Red	Lime fresco	0.36	-0.43	-0.42	0.70	Low: color variation unperceived by eye
	10rLF	Red	Lime fresco	0.81	-0.25	-0.19	0.36	Low: color variation unperceived by eye
After one month	2rBF	Red	*Buon* fresco	-0.35	-0.56	-0.74	0.99	Low: color variation unperceived by eye
	6rBF	Red	*Buon* fresco	-1.93	-0.62	-1.05	2.28	Low: color variation unperceived by eye
	10rBF	Red	*Buon* fresco	0.15	-0.34	-0.86	0.93	Low: color variation unperceived by eye
	2rLF	Red	Lime fresco	0.73	-1.5	-1.58	2.29	Low: color variation unperceived by eye

	6rLF	Red	Lime fresco	0.07	-0.57	-0.92	1.08	Low: color variation unperceived by eye
	10rLF	Red	Lime fresco	-0.03	-0.41	-0.64	0.76	Low: color variation unperceived by eye
After one week	2yBF	Yellow	*Buon* fresco	-0.93	-0.08	-0.53	1.07	Low: color variation unperceived by eye
	6yBF	Yellow	*Buon* fresco	-0.37	-0.72	-2.52	2.64	Low: color variation unperceived by eye
	10yBF	Yellow	*Buon* fresco	0.45	-0.07	0.1	0.46	Low: color variation unperceived by eye
	2yLF	Yellow	Lime fresco	-0.09	0.15	0.11	0.20	Low: color variation unperceived by eye
	6yLF	Yellow	Lime fresco	0.55	-0.24	-0.93	1.10	Low: color variation unperceived by eye
	10yLF	Yellow	Lime fresco	-0.71	-0.05	-1.21	1.40	Low: color variation unperceived by eye
After one month	2yBF	Yellow	*Buon* fresco	-1.03	-0.09	-0.45	1.12	Low: color variation unperceived by eye
	6yBF	Yellow	*Buon* fresco	-2.88	-0.87	-3.19	4.38	Medium: color variation perceived by eye
	10yBF	Yellow	*Buon* fresco	-0.14	-0.26	-0.97	1.01	Low: color variation unperceived by eye
	2yLF	Yellow	Lime fresco	-1.07	0.06	-0.71	1.28	Low: color variation unperceived by eye
	6yLF	Yellow	Lime fresco	-0.7	-0.4	-1.45	1.64	Low: color variation unperceived by eye
	10yLF	Yellow	Lime fresco	-2.63	-0.43	-2.19	3.44	Medium: color variation unperceived by eye
After one week	2bLF	Blue	Lime fresco	0.45	0.04	0.13	0.47	Low: color variation unperceived by eye
	6bLF	Blue	Lime fresco	0.52	0.06	-0.03	0.52	Low: color variation unperceived by eye
	10bLF	Blue	Lime fresco	-0.68	0.14	-0.29	0.75	Low: color variation unperceived by eye
After one month	2bLF	Blue	Lime fresco	-0.21	0.06	0.06	0.22	Low: color variation unperceived by eye
	6bLF	Blue	Lime fresco	1.01	-0.02	-0.03	1.01	Low: color variation unperceived by eye
	10bLF	Blue	Lime fresco	-0.51	0.09	0.13	0.53	Low: color variation unperceived by eye

ΔE values meanings and rating scale of incompatibility risk according to literature [26,65,66]:
Low risk: ΔE*<3; Medium risk: 3<ΔE*<5; High risk: ΔE*>5

Statistical comparison of ΔE*

The values for the color variation ΔE* of all the replicas treated with Primal® as function to time (one week and one month of consolidation) and pigment/technique are shown in Figure 42. The overall color variation ΔE* followed the next order in regard to pigment/technique: ΔE* yBF ≥ ΔE* yLF ≥ ΔE* rLF ≥ ΔE* rBF ≥ ΔE* bLF, however, it was not found significant change between each other.

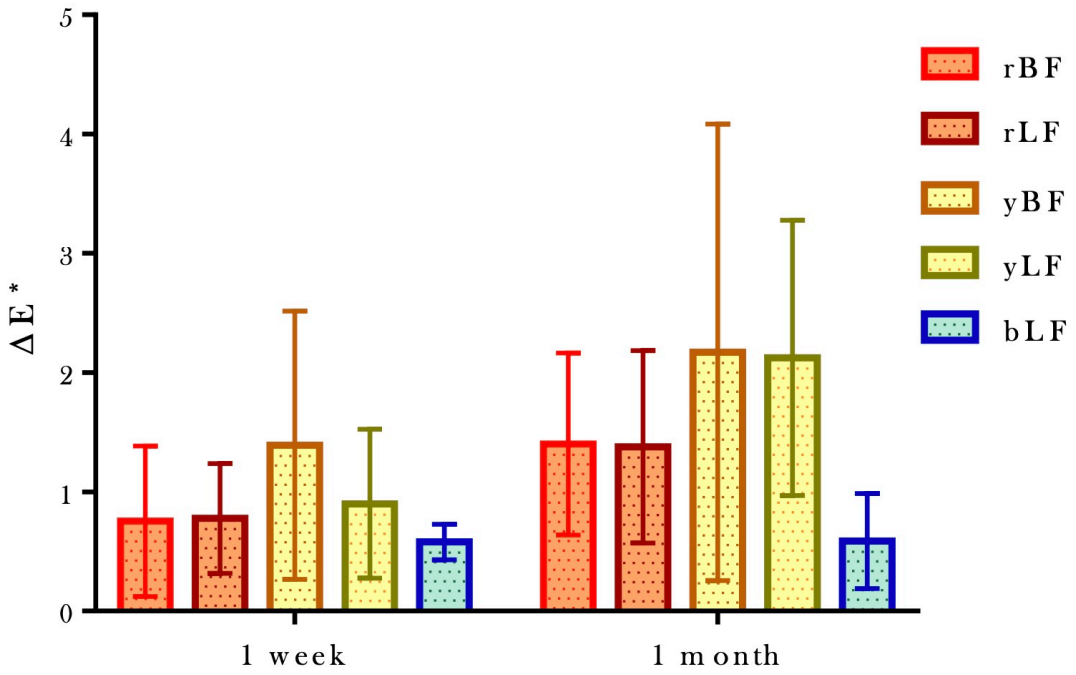

***Figure 42**. Average overall color difference for all the replicas (pigment/technique) treated with Primal® one week and one month after consolidation, analyzed by ANOVA followed by Bonferroni's multiple comparison test. Significative differences between the pigments were not found. Means and standard deviation of the replicas are shown.*

The ΔE* presented by Primal® is lower in all cases in relation to the nanolime products. Primal® presented similar ranges of variation except in the yBF replicas, similarly to the case of CaLoSiL® (Figure 36) as indicated by the standard deviation of all values of ΔE*(Figures 27, 34 and 42), the most probable reason for the difference between the white haze formed by the nanolimes appears to be their different characteristics.

The standard deviation has indicated a uniform behavior in the commercial products. While Primal® and CaLoSiL® have been subject of more laboratory and *in situ* studies, HERCULES nanolime has been still in development stage. As observed previously both nanolimes presented differences in texture, dimension of the NPs (particles orientation, size distribution and level of NPs agglomeration), and in the nature of their solvent (see Section 3.2.2.). The characteristics of the nanolimes could have contributed to produce a difference in the dispersion rate of the particles causing different amounts of nanolime particles to be deposited in the paint layers. At the same time the nanolimes may have followed different consolidation mechanisms or produced different degrees of penetration.

SEM- EDS analysis

Seven replicas were selected for a SEM-EDS comparison analysis of the paint surface before and after consolidation treatment. The location of the analyzed areas on each replica can be seen on section 3.1.4. of methodology. The samples reference, description and consolidant used are listed on Table 18. The blue paint replicas 1bLF, 10bLF and 12bLF made with smalt have shown the higher lack of cohesion on a previous swab test. The high amount of coarse pigments in the surface has also enabled the analysis of the effect of the three products used. The selected ochre replicas 12rBF, 3rLF, 4yBF and 3yLF were used to compare the effects of the nanolimes in *buon* and lime fresco.

Table 18. *Selected replicas for SEM-EDS analysis.*

		Painting Technique	Consolidant	Replicas code
PIGMENT	Smalt	Lime Fresco	**HERCULES nanolime**	12bLF
			CaLoSiL®	1bLF
			Primal®	10bLF
	Red ochre	Lime Fresco	**HERCULES nanolime**	3rLF
		Buon Fresco	**CaLoSiL®**	12rBF
	Yellow ochre	Lime Fresco	**CaLoSiL®**	3yLF
		Buon Fresco	**HERCULES nanolime**	4yBF

Before consolidation the replicas presented inhomogeneous surface texture, as expected for lime mortar paint layers with lack of cohesion. SEM images enabled a morphological comparison of the painted surface before and after the treatment, namely of the pores (number and size), cracks or fracture lines around the pigments. Also it was intended to ascertain the presence and appearance of the white haze and to check how the paint layer is affected by it. Figure 43 shows an example of a selected area of replica 12bLF affected by lack of cohesion on which are visible some of the deterioration features stated for analysis.

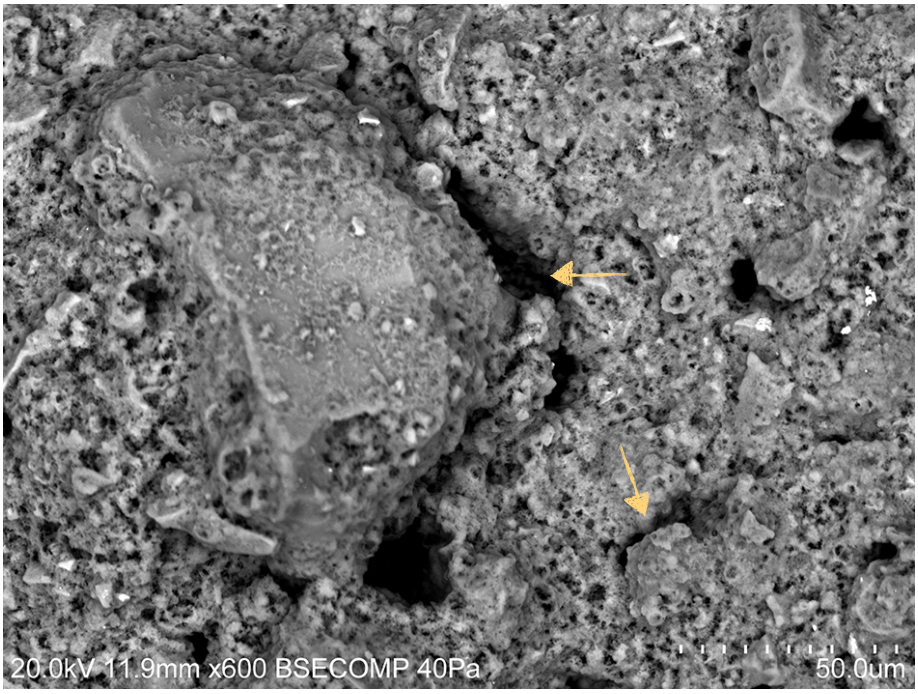

Figure 43. *Untreated paint layer of lime fresco replica 12bLF painted with smalt. Yellow arrows show places on the surface areas, where possible changes have been expected after treatment with the consolidants.*

In turn EDS analysis allowed to carried out elemental mapping and semi-quantitative analysis. By the comparison of the elemental composition of the paint surfaces before and after consolidation it was intended to verify possible changes due to the presence of the consolidant.

Replicas treated with the synthesized, *HERCULES nanolime*

HERCULES nanolime, applied as it was described in 3.1.3, showed nanolime particles deposited on the surface, seen as hexagonal shaped crystals spread over the paint layers of the replicas. The crystals are very similar to the observed in Figure 13 in section 3.2.1. Their shape and small sizes ranging from 1.7 μm to 3.2 μm prove the presence of the $Ca(OH)_2$ NPs in the surface of the replicas (Figure 44). Similar effect has been observed in studies of the effects of the solvents on the nanolime transport mechanism in limestone consolidation [71,72]. Nanolime particles observed have been heterogeneously distributed on the surfaces, isolated and in clusters and the nanolime treatment did not generate a layer, in similarity to historical carbonate stone buildings [73], where no modification of the stone texture was observed. $Ca(OH)_2$ NPs have been

preferentially deposited in similar way, accumulated clusters on certain zones in the surface of earthen samples, where they have been effective for reinforcing the earthen walls [74].

a) 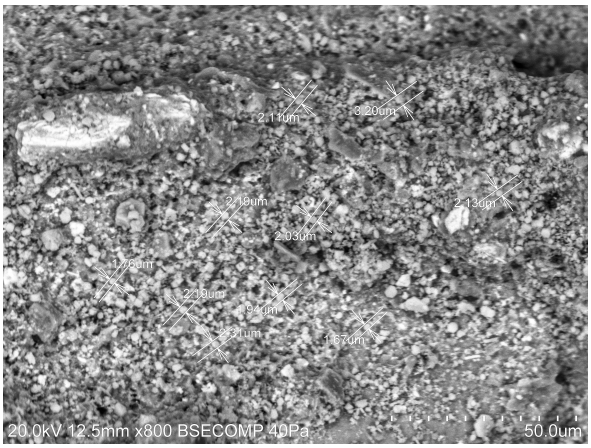

b) 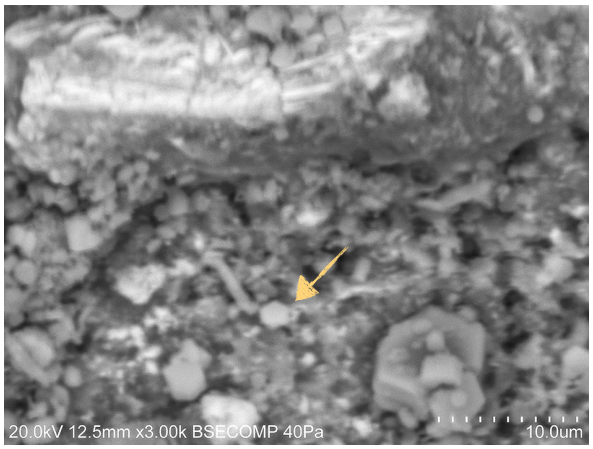

Figure 44. *SEM images of replica 3rLF in one week after treatment with HERCULES nanolime: a) Scale of 50 µm with particles size measured between 1.7 µm and 3.2 µm; b) Scale of 10 µm showing the characteristic hexagonal shaped crystals of* $Ca(OH)_2$ *NPs.*

The isolated and in cluster distribution of the NPs in the surface of the replicas could be a probable reason for the spotted appearance of the white haze in the surface of the ochre replicas treated with the HERCULES nanolime (Figure 45a and b), however the spotted veil was not observed in the colorimetry and spectrophotometry analysis of the smalt pigments. This could be because the composition of the smalt pigment is different from the ochre pigments.

In the yellow *buon* fresco replica, 4yBF in Figure 45a no apparent change in the morphology of the paint layer was observed, suggesting that the performance of the HERCULES nanolime on the paint layer might be stronger in the lime fresco replicas. In the red and blue lime fresco replicas, respectively 3rLF in Figure 45b and 12bLF in Figure 45c a small difference in morphology was also observed after one week of consolidation. The pores surrounding the pigment particles seemed to have reduced in size or have been covered by the NPs present in the paint layers. EDS analysis showed that the chemical composition of the paint layers did not change by the addition of the nanolime to the surface.

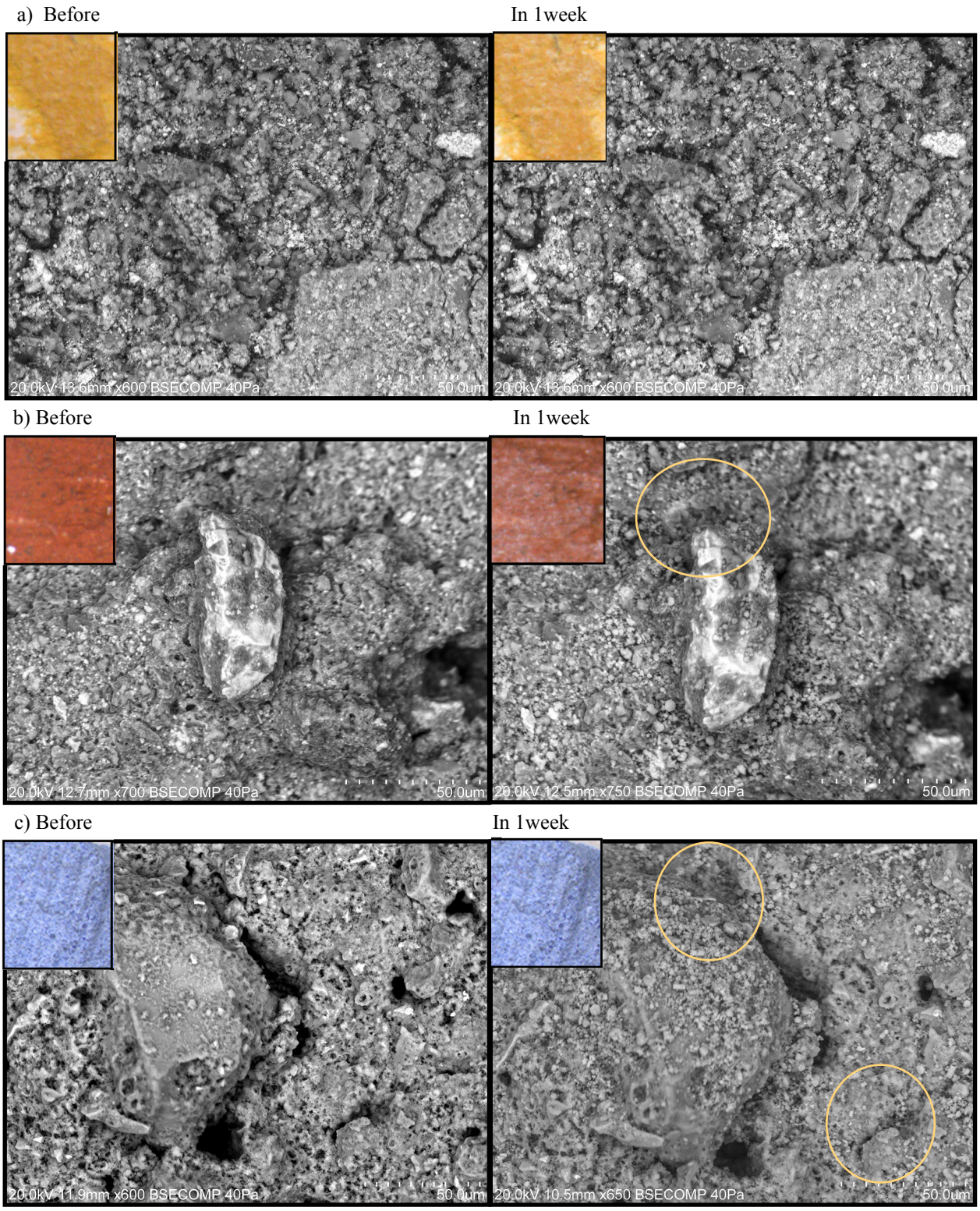

***Figure 45**. SEM images of fresco replicas treated with HERCULES nanolime; before treatment, and in one week after treatment: a) Yellow pigment and buon fresco technique (replica 4yBF area D); b) Red pigment and lime fresco technique (replica 3rLF area B); c) Blue pigment and lime fresco technique (replica 12bLF area B). Circles show the areas where the pores and cracks have been filled. Detail images obtained by OM-Vis of the studied areas are on the left top corner.*

Replicas treated with the commercial nanolime, *CaLoSiL®*

CaLoSiL® applied as it was described in 3.1.3, showed the pigments cohesion has been renewed compared to the untreated areas by the binding of the pigments within the surface due to the coating layer formed by the carbonatation of the $Ca(OH)_2$ NPs. A change in the texture of the painted surfaces has been created, which in turn become smoother (Figure 46). This effects have also been observed by Dei and Salvadori in 2006 during the analysis of the effect of 5 g/L $Ca(OH)_2$ NPs dispersion in 2-propanol (containing 2% of water by weight) over a fresco specimen painted layer of English red pigment simulating degradation by color powdering [47]. The formation of a calcite coating layer as referred to by Zhu J. *et. al* during assays of pure nanolime for mural painting protection [70] could have reduced the amount of $Ca(OH)_2$ NPs making the white haze thinner and more uniformly spread as observed under OM-Vis (Figure 46, see section 3.2.2 CaLoSiL®). The formation of calcite which is of white color could be viable explanation of the appearance of the white haze formed by CaLoSil®.

In the red *buon* fresco, 12rBF (Figure 46a) the thin layer is not continuously spread over the surface, nor appears to be uniformly thick while in the lime fresco replicas 3yLF replica (Figure 46b) and 1bLF (Figure 46b), the layer is more uniform and it is evenly spread over the surface. The formation of the layer does not represent any sort of physicochemical alteration in the pigment particles and to the elemental composition of the replicas. This was confirmed by the spectral reflectance curves of all the paint layers treated with CaLoSiL® (Appendix 4, A4-2, A4-5 , and A4-8) and EDS analysis of the studied areas of the replicas.

In Figure 46a of replica 12rBF, in one week of treatment one zone of smaller granules observed in the right side could be due to the withe haze since in the red ochre replicas the withe haze is visually more apparent as it can be seen in the image and was confirmed by colorimetry and spectrophotometry analysis. However in Figure 46b of replica 3yLF, even though the white haze was not observed in the surface by naked eye, colorimetry and spectrophotometry have indicated high values of total color change ΔE^*, that might indicate that the white haze is present over the surface and could have been masked by the lightness of the yellow color in comparison

to the darker red ochre pigment. However to be sure it is the case further statistical analysis should be carried out with a higher number of samples.

In the case of the smalt pigment replica 1bLF the formed coating layer seems to be more compact since it covers the paint surface completely and the pigment particles are no longer distinguished (Figure 46c), however from previous colorimetry and spectrometry and OM-Vis results is has been proven that there is no visual color alteration $\Delta E^* < 3.5$ (see section 3.2.3 CaLoSiL®). The coating layer created by nanolime consolidation in the blue replica also presented some fractures which could probably have formed during consolidation, as the result of the rapid evaporation of the short chain alcohol (Figure 46b). The differences of the visual density in this replica and larger spreading of the coating layer formed by CaLoSiL® could be because the coarser pigment particles and higher porosity of their paint layer in comparison to the pigment paint layer formed by the ocher pigments might have enabled higher deposition of the $Ca(OH)_2$ NPs within the substrate matrix (mortar layers). Preliminary SEM images of the cross sections (Appendix 4, A4-11 and 12) have shown that a layer seems to have been formed in between the pigment particles which suggests that CaLoSiL® had higher penetration than HERCULES nanolime, which did not show the presence of such formations (Appendix 4, A4-13). However, as the influence of the pigment particles in the porosity of the paint layers has not been previously studied, further research towards this area is recommended.

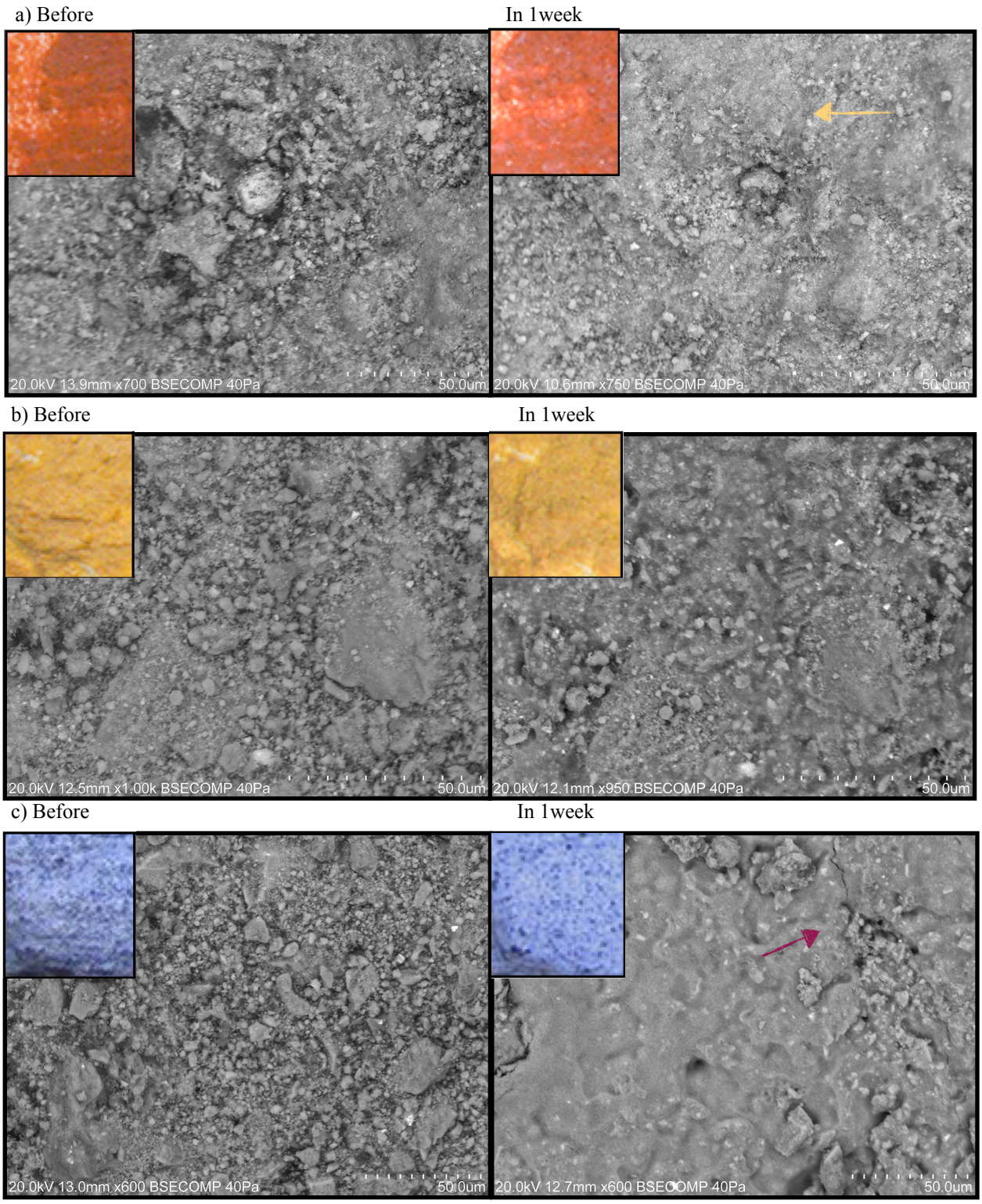

***Figure 46**. SEM images of fresco replicas treated with CaLoSiL®; before treatment, and in one week after treatment: a) Red pigment and buon fresco technique (replica 12rBF area D); b) Yellow pigment and lime fresco technique (replica 3rLF area D); c) Blue pigment and lime fresco technique (replica 1bLF area D). Yellow arrow: layer formed; Purple arrow: Crack formed in the coating layer. Detail images obtained by OM-Vis of the studied areas are on the left top corner.*

Blue paint layers treated with the acrylic resin, *Primal®*

The acrylic resin applied at 2% in water produces little changes in the appearance of the blue paint layers according to OM-Vis images, colorimetry and spectrophotometry results in section 3.2.3. After one week of treatment, a thin film seems to be formed in some cracks around the pigment particles (Figure 47). The use of low concentrations of acrylic resins is to enhance its penetration within the structure and avoid the formation of an hydrophobic film in the surface in order to avoid undesirable effects associated with polymer usage and aging, such as color changes, shrinkage, loss of transparency and accelerated accumulation of dirt on the paint surface, which in turn leads to the loss of readability and integrity of the work of art [75]. The elemental map of carbon (C) present in Figure 48 support that the treatment did not form any organic coating layer in the surface.

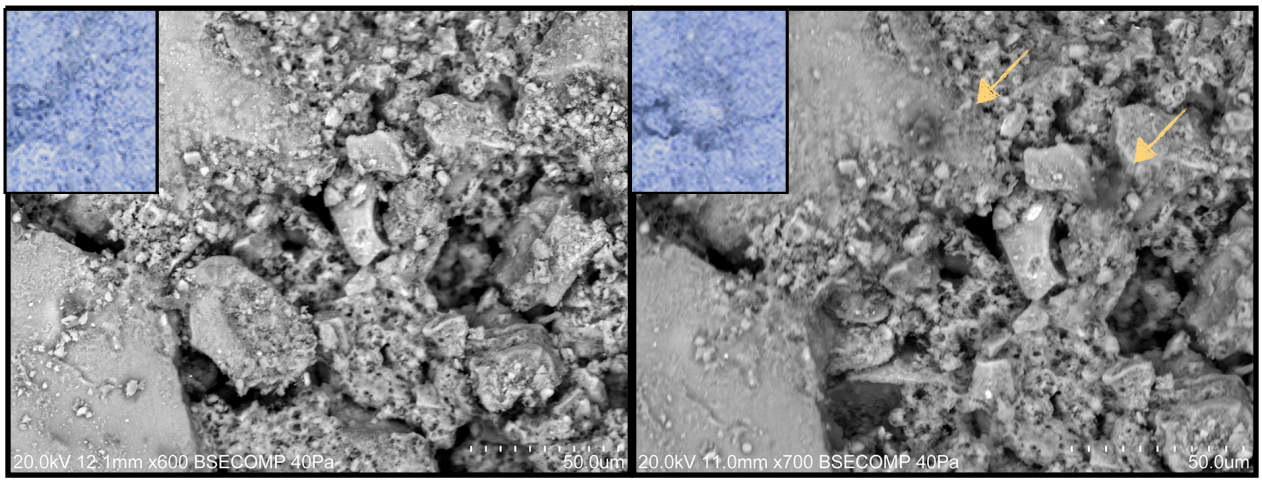

Figure 47. *Smalt lime fresco replica (10bLF) before (left side), in one week (right side) after treatment with Primal®. Arrows: thin film formed. Detail images obtained by OM-Vis of the studied areas are on the left top corner.*

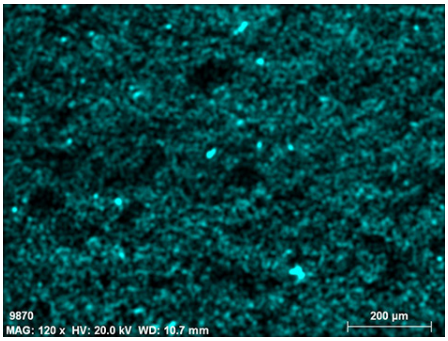

Figure 48. *Elemental map of C of area D of replica 10bLF studied under SEM.*

Comparison of the consolidants

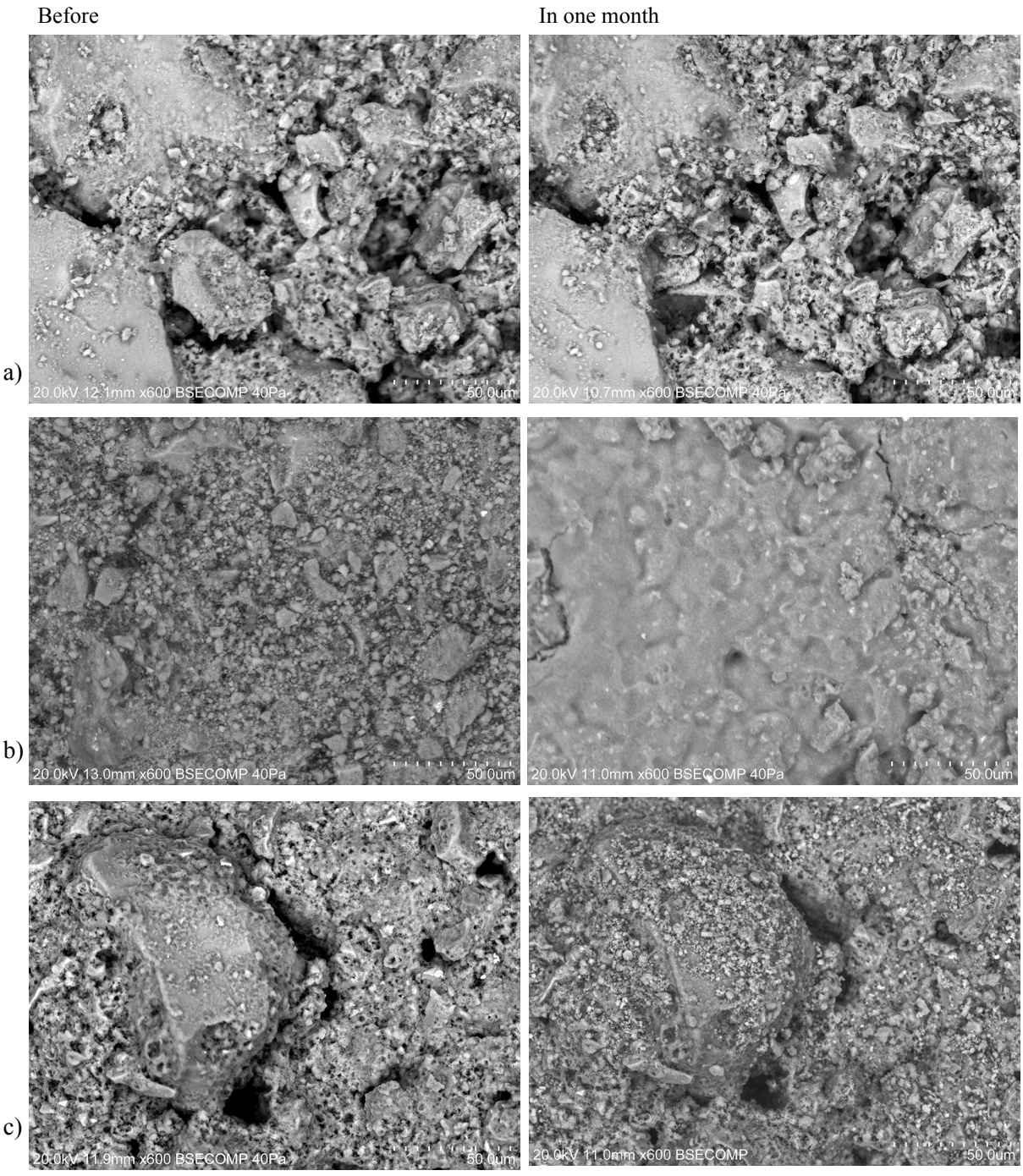

Figure 49. *Smalt lime fresco replicas before (left side) treatment, and in one month (right side) after treatment with the three different consolidant products; a comparison: a) Primal®, b) CaLoSiL®, c) HERCULES nanolime.*

Figure 49 presents a comparison of the effects of the three consolidant products in one month after treatment in the lime fresco replicas painted with smalt pigment. The observed consolidation effect of the nanolimes is stronger in comparison to the effect of Primal®, however it should be noted that the concentration of the Primal® is lower than the HERCULES nanolime and CaLoSiL® which equal to 25 g/L for both. Higher concentrations of Primal® can lead to the formation of a film over the surface that can affect the paint layer dramatically in long term, especially when exposed to aggressive environmental conditions [11,12]. Both nanolimes appear to have a potential to recuperate the physicochemical network of the fresco replicas, yet the changes are faster in the commercial nanolime. This could be to a difference in their degree of penetration, seen by the appearance of the HERCULES nanolime in the paint layers of the replicas, and the nanolimes different carbonatation degree and mechanism shown by the thin film in the surface of the replicas treated with CaLoSiL®. Another possible reason is that the nanolime particles have different reactivity due to the particle dimensions:when applied the smaller nanolime has carbonated more quickly.

4. Conclusions

This study has shown that nanolime has potential to be used effectively for consolidation of fresco paintings affected by lack of cohesion and represent a viable alternative to organic consolidants. However there are still some issues that need to be overcome.

In this research the effects and impacts of three consolidants in the paint layers of frescoes affected by lack of cohesion have been studied. In this comparison efficiency of the nanolime developed in HERCULES laboratory (HERCULES nanolime) was evaluated in relation to two commercial products one nanolime (CaLoSiL®) and an acrylic resin (Primal®) contributing to the knowledge of how nanolime affects the fresco paint layers by its application and the development of this product. Preliminary data has been obtained and they can contribute to further studies on carbonatation process and consolidation mechanism.

In this research it has been shown that:

- The effective preparation of pure phased $Ca(OH)_2$ nanoparticles was obtained by the precipitation of equal volumes of $CaCl_2$ (0.4M aqueous solution) and NaOH (0.8M aqueous solution) at 90 ºC in the presence of Triton X-100 (t-Oct-C_6H_4-$(OCH_2CH_2)_xOH$) as a surfactant. The characterization with SEM of the NPs showed that HERCULES nanolime are hexagonal shaped crystals with an average particle size of 287 nm, with an observed minimum size of 56 nm and a maximum size of 982 nm, and an average synthesis yield of 47.2 ± 5%
- Different dispersions have been prepared and the dispersion of Acetone:Ethanol(1:10) was found more suitable for application due to the reduction of the white haze produced. DLS studies showed that the average diameters of the NPs was 444 ± 7 nm. Further research needs to be carried out towards enhancing the dispersion stability by studies of different solvents proportions and solvent combinations.
- Differences between the two nanolimes: HERCULES nanolime and CaLoSiL® are both composed of hexagonal shaped crystals of $Ca(OH)_2$, however the particles differ in size,

orientation, degree of agglomeration and carbonatation. The NPs in the commercial nanolime have demonstrated to be of more uniform size distribution and visual particles orientation as well as of smaller dimensions. Surfactants or other additives have not been observed by FTIR and TGA analysis. Furthermore, the quantity of calcite is higher in the HERCULES nanolime comparing to CaLoSiL®, as was determined in the TGA analysis.

- All nanolime treatments tend to induce an undesired white haze in the painted layer after application. However, pigment nature and color might have an effect on the visual perception and degree of the haze. The overall total color variation ΔE* was lower in the smalt probably because the coarser pigment particles and higher porosity of their paint layer might have enabled higher deposition of the $Ca(OH)_2$ NPs within the substrate matrix (mortar layers). If nanolime is to be applied towards fresco consolidation the influence of the pigment particles in the porosity of the paint layers need to be further studied as it may affect the nanolime performance. Further cross section analysis should be carried out to observe if the pigments in the paint layers affect the deposition of nanolime.
- Concerning the ochres in the darker color (red) the white haze was higher than in the lighter color (yellow) observed visually and by the spectro-colorimetry analysis performed, however the total color variation ΔE* for the yellow replicas can still be high , meaning that likely the lightness of the yellow pigment may have masked the white haze however further statistical analysis of colorimetry results with higher number of samples are required.
- From colorimetry analysis it was observed that the color variation produced by the consolidants followed the next order: ΔE* HERCULES nanolime > ΔE* CaLoSiL® > ΔE* Primal.
- Both nanolimes produced a lightning effect reflected as an increase in the values of ΔL*. Additionally, the change in ΔE* presented in both the same order in all the pigments used as followed: ΔE* rBF, ΔE* rLF, ΔE* yBF, ΔE* yLF, and ΔE* bLF.
- There was no significative effect of time of treatment (in one week and in one month) since the means of ΔE* stayed at similar values.
- SEM morphological analysis has shown that HERCULES nanolime has been spread unevenly over the treated surfaces and deposited as clusters over pores or cracks. The clusters of the

NPs may be the reason of the white haze in the replicas treated with nanolime it may also explain the reason for the spotted veil appearance of the white haze, observe with the OM-Vis analysis.

- Whereas in CaLoSiL® the formation of a calcite coating layer could have reduced the amount of $Ca(OH)_2$ NPs making the white haze thinner and more uniformly spread as observed under OM-Vis. In this case the white haze could be the formation of calcite which is also white.
- However both of this possible reasons of white haze formation, Ca(OH)2 NPs present in the surface or excess calcite, need to be further analyzed.
- It was confirmed, after 1 month of application, that 2% of the acrylic resin Primal® is an optimum concentration to use in conservation as it has shown not to produce color alteration by spectro-colorimetry analysis and avoids the formation of an organic film in the surface confirmed by the elemental map of carbon and the induced UVF photography.

References

1. UNESCO, (2020), World Heritage. Retrieved from: https://whc.unesco.org/en/about/
2. ICOMOS, (2003), Principios para la preservación, conservación y restauración de pinturas murales. *ICOMOS*, *2.* Retrieved from: http://www.icomos.org/charters/wallpaintings_sp.pdf
3. Mora, P., (2018), Causes of deterioration of mural paintings, *International centre for the study of the preservation and restoration of cultural property (ICCROM).* Retrieved from: https://www.iccrom.org/sites/default/files/2018-02/1974_mora_causes_deterioration_111773_light.pdf
4. Di Tullio, V., Proietti, N., Gobbino, M., Capitani, D., Olmi, R., Priori, S., Riminesi, C., and Giani, E., (2010), Non-destructive mapping of dampness and salts in degraded wall paintings in hypogea's buildings: the case of St Clement at mass fresco in St. Clement Basilica, Rome. *Analytical and bio analytical chemistry, 396*, pp. 1885-1896. DOI: 10.1007/s00216-009-3400-x
5. Charola, A. E., and Ware R., (2002), Acid deposition and the deterioration of stone: a brief review of a broad topic. *Geological society*, *205*, pp. 393-406. DOI: 10.1144/ GSL.SP.2002.205.01.28
6. Spencer, B. N., Rosenthal, A., Podany, J., Larson, J. H., and Zaccari, F., (2017), Art Conservation and Restoration. *Encyclopaedia Britannica.* Retrieved from: https:// www.britannica.com/art/art-conservation-and-restoration
7. Matteini, M., (2008), Inorganic treatments for the consolidation and protection of stone artefacts. *Conservation Science in Cultural Heritage, 8,* pp. 13-27, DOI: 10.6092/ issn.1973-9494/1393
8. Doehne, E., and Price, C. A., (2010). *Conservation in research: Stone conservation, an overview of current research* (2nd ed.). Getty Conservation Institute. DOI: 10.1007/ s10531-016-1233-4
9. Magaloni, K. D., (2011), La pintura mural y su conservación. *Arqueología Mexicana, 108*, pp. 33-37. ISSN 0188-8218

10. Rodrigues, J.D., (2001). *Consolidation of decayed stones. A delicate problem with few practical solutions*. Historical constructions, pp. 3-14. Retrieved from: https://www.researchgate.net/publication/261611619_Consolidation_of_decayed_stones_A_delicate_problem_with_few_practical_solutions

11. Charola, A., Tucci, A., and Koestler, R. (1986). On the Reversibility of Treatments with Acrylic/Silicone Resin Mixtures. *Journal of the American Institute for Conservation, 25*(2), 83-92. doi:10.2307/3179628

12. Becherini, F., Durante, C., Bourguignon, E., Li Vigni, M., Detalle, V., Bernardi, A., Tomasin, P., (2018), Aesthetic compatibility assessment of consolidants for wall paintings by means of multivariate analysis of colorimetric data. *Chemistry Central Journal, 12*(1), pp. 1-10. DOI: 10.1186/s13065-018-0465-7

13. Girginova, P. I., Galacho, C., Mirão, J., Veiga, R., Silva, A. S., and Candeias, A., (2018), Inorganic Nanomaterials for Restoration of Cultural Heritage: Synthesis Approaches towards Nanoconsolidants for Stone and Wall Paintings, *ChemSusChem, 11*(24), pp. 4168-4183. DOI: 10.1002/cssc.201801982

14. Girginova, P. I., Galacho, C., Mirão, J., Veiga, R., Silva, A. S., and Candeias, A., (2016), Estudos preliminares para consolidação de suportes com pintura mural: Sintese e caracterização de nanocais. *Conservar Patrimonio, 23*(23), pp. 103-107. DOI: 10.14568/cp2015046

15. Vojtěchovský, J., (2017), Surface consolidation of wall paintings using nano-suspensions. *Acta Polytechnica, 57*(2), pp. 139-148. DOI: 10.14311/AP.2017.57.0139

16. Ambrosi, M., Dei, L., Giorgi, R., Neto, C., Baglioni, P., (2001), Colloidal particles of Ca(OH)2: Properties and applications to restoration of frescoes. *Langmuir, 17*(14), pp. 4251-4255. DOI: 10.1021/la010269b

17. Gil, M., (2002), Conservação de pintura mural, Estudo e consolidação de argamassas de cal aérea e areia com falta de coesão. DOI: 10.13140/RG.2.2.4036.8880.

18. Mora, P., Mora L., and Philipott, P., (1984), *Conservation of wall paintings.* Butterwoths.

ISBN: 0-408-10812-6

19. Fichner-Rathus, L., (2013), *Understanding art* (10th ed). Wadsworth. ISBN-13:978-1-111-83695-5
20. Young, M., Murray M., and Cordiner P., (2003), Chemical Consolidants and water repellents for sandstones in Scotland. *Historic Environmental Scotland*. Retrieved from: https://www.historicenvironment.scot/archives-and-research/publications/publication/?publicationId=2cb6230e-24b9-4043-a15b-a8eb00b1b885
21. Daehne, A., and Herm, C., (2013), Calcium hydroxide nanosols for the consolidation of porous building materials-results from EU-STONECORE. *Heritage Science, 1*(1), pp. 1-9. DOI: 10.1186/2050-7445-1-11
22. Baglioni, P., Chelazzi, D., Giorgi, R., Carretti, E., Toccafondi, N., and Jaidar, Y., (2014), Commercial $Ca(OH)_2$ nanoparticles for the consolidation of immovable works of art. *Applied Physics A, 114*(3), pp. 723-732. DOI: 10.1007/s00339-013-7942-6
23. Baglioni, P., and Giorgi, R., (2013), Chapter 13 Inorganic nanomaterials for the consolidation of wallpaintings and stone. In P. Baglioni & D. Chelazzi (Eds.), *Nanoscience for the conservation of works of art* (pp. 345-371). RSC Publishing. ISBN: 978-1-84973-566-7
24. Baglioni, P., Carretti, E., Dei, L., and Giorgi, R., (2003). Nanotechnology in wall painting conservation. In B. H. Robinson (Ed.). *Self-Assembly,* pp. 32-41. IOS-Press Omsha. ISBN: 1 58603 382 4.
25. Otero, H., J., (2018), Lime based nanomaterials for the conservation of calcareous substrates in heritage structures. Retrieved from: http://shura.shu.ac.uk/22428/
26. Delgado, J. R., Grossi, A., (2007), Indicators and ratings for the compatibility assessment of conservation actions. *Journal of cultural heritage, 8*(1), pp. 32-43. DOI: 10.1016/ j.culher.2006.04.007
27. Odgers, D., Ball, R., Pesce, G., and Henry, A., (2017). *Nanolime, a practical guide to its use for consolidating weathered limestone.* Historic England. Retrieved from: https:// historicengland.org.uk/images-books/publications/nanolime-use-for-consolidating-

weathered-limestone/

28. Borsoi, G. (2017). *Nanostructured lime-based materials for the conservation of calcareous substrates*. A+BE Architecture and the Built Environment. DOI: 10.7480/abe.2017.8
29. Baglioni, P., Chelazzi, D., and Giorgi, R., (2015), *Nanotechnologies in the conservation of cultural heritage, a compendium of materials and techniques*. Springer. DOI:10.1007/978-94-017-9303-2
30. Melo, M. J., Bracci, S., Camaiti, M., Chiantore, O., Piacenti, F., (1999), Photodegradation of acrylic resins used in the conservation of stone. *Polymer Degradation and Stability. 66*(1), pp. 23-30. DOI: 10.1016/S0141-3910(99)00048-8
31. Rodriguez-Navarro, C., and Ruiz-Agudo, E., (2018), Nanolimes: From synthesis to application. *Pure and Applied Chemistry, 90*(3), pp. 523-550. DOI: 10.1515/pac-2017-0506
32. Gómez-Villalba, L. S., López-Arce, P., Fort, R., Álvarez, M., (2010), La aportación de la nanociencia a la conservación de bienes del patrimonio cultural. *Patrimonio cultural de España, 4*, pp. 43-56. ISSN: 1889-3104
33. Girginova, P. I., Galacho, C., Veiga, R., Santos S. A., and Candeias, A., (2020), Study of mechanical properties of alkaline earth hydroxide nanoconsolidants for lime mortars. *Construction and Building Materials, 239,* pp. 117520. DOI: 10.1016/j.conbuildmat.2019.117520
34. Taglieri, G., Mondelli, C., Daniele, V., Pusceddu, E., Trapananti, A., (2013), Synthesis and X-Ray Diffraction Analyses of Calcium Hydroxide Nanoparticles in Aqueous Suspension. *Advances in materials physics and chemistry, 3*(1), pp. 108-112. DOI:10.4236/ ampc.2013.31a013
35. López-Arce, P., Gómez-Villalba, L. S., Martínez-Ramírez, S., Álvarez de Buergo, M., Fort, R., (2011), Influence of relative humidity on the carbonatation of calcium hydroxide nanoparticles and the formation of calcium carbonate polymorphs. *Powder Technology, 205*(1-3), pp. 263-269. DOI: 10.1016/j.powtec.2010.09.026
36. Taglieri, G., Otero, J., Daniele, V., Gioia, G., Macera, L., Starinieri, V., Charola, A. E., (2017), Nano $Ca(OH)_2$ synthesis using a cost-effective and innovative method: Reactivity study. *Journal of the American Ceramic Society, 100*(2), pp. 5766-5778, DOI: 10.1111/

Jace.15112

37. Ambrosi M., Dei L., Giorgi R., Neto C., and Baglioni P., (2001), Stable Dispersions of Ca(OH)2 in Aliphatic Alcohols: Properties and Application in Cultural Heritage Conservation. *Trends in Colloid Interface Science, 15,* pp.68-72. DOI: 10.1007/3-540-45725-9_15
38. Giorgi, R., Ambrosi, M., Toccafondi, N., Baglioni, P., (2010), Nanoparticles for cultural heritage conservation: Calcium and barium hydroxide nanoparticles for wall painting consolidation. *Chemistry- a European Journal, 16*(31), pp. 9374-9382. DOI: 10.1002/ chem.201001443
39. Baglioni, P., Giorgi, R., and Dei, L., (2008), Soft condensed matter for the conservation of cultural heritage. Comptes Rendus *Chimie, 12*(1-2), pp. 61-69. DOI: 10.1016/ j.crci.2008.05.017
40. Daehne, A., Herm, C., (2013), Calcium hydroxide nanosols for the consolidation of porous building materials - results from EU-STONECORE. *Heritage science, 1*(1), pp. 1-9. DOI: 10.1186/2050-7445-1-11
41. Natali, I., Saladino, M. L., Andriulo, F., Chillura ,M. D., Caponetti, E., Carretti, E., Dei, L., (2014), Consolidation and protection by nanolime: Recent advances for the conservation of the graffiti, Carceri dello Steri Palermo and of the 18th century lunettes, SS. Giuda e Simone Cloister, Corniola (Empoli). *Journal of cultural heritage, 15*(2), pp. 151-158. DOI: 10.1016/j.culher.2013.03.002
42. Carretti, E., Chelazzi, D., Rocchigiani, G, Baglioni, P., Poggi, G., and Dei, L., (2013), Interactions between nanostructured calcium hydroxide and acrylate copolymers: implications in cultural heritage conservation. *Lagmuir, 29*, pp. 9881-9890. DOI:10.1021/ la401883g
43. Garreau, H., (2007), Removal of Damaging Conservation Treatments on Mural paintings, Workshop, Österbybruk, Sweden, Retrieved from: https://www.raa.se/publicerat/ 9789172095540.pdf
44. Giorgi, R., Dei, L., and Baglioni, P., (2000), A new method for consolidating wall paintings based on dispersions of lime in alcohol. *Studies in Conservation, 45* (3), pp. 154-161. DOI:

10.1179/sic.2000.45.3.154

45. Chelazzi, D., Poggi, G., Jaidar, Y., Toccafondi, N., Giorgi, R., Baglioni, P., (2013), Hydroxide nanoparticles for cultural heritage: Consolidation and protection of wall paintings and carbonate materials. *Journal of colloid and Interface Science, 392*(1), pp. 42-49. DOI: 10.1016/j.jcis.2012.09.069
46. Alvarez, A. E., and Nadal, L. F., (2016), Evaluacion del Proceso de Carbonatacion de Nanocales Aplicadas a Pinturas Murales Prehispánicas de Origen Maya. *Intervención, 14*(2016), pp.31-41, DOI: 10.30763/Intervencion.2016.14.163
47. Dei, L., and Salvadori, B., (2006), Nanotechnology in cultural heritage conservation: nanometric slaked lime saves architectonic and artistic surfaces from decay. *Journal of cultural heritage, 7*(2), pp. 110-115. DOI:10.1016/j.culher.2006.02.001
48. Roberts, C., Davis, S. L., Gordon, L. B., and DeRoo, C. S., (2018), Investigatinf approaches to the treatment and preservation of a collection of Egyptian limestone funerary stelae. *Journal of the American Institute for Conservation, 57*(1-2), pp. 19-34. DOI: 10.1080/01971360.2018.1439235
49. CaLoSiL® Colloidal nano-particles of lime for stone and plaster consolidation, Technical leaflet. Available at: https://ibz-freiberg.de/downloads/pdf/produkte/tm/eng/CaLoSiL_E_IP_NP.pdf
50. D'Armata, P., and Hirst, E., (2012), Nano-Lime for Consolidation of Plaster and Stone *Journal of architectural conservation, 18* (1), pp. 63-80. DOI: 10-1080/13556207.2012.10785104
51. Gil, M., Rosado, T., Ribeiro, I., Pestana, J., Caldeira, A. T., Carvalho, M. L., Dias, L., Mirão, J., and Candeias, (2015), Are they fresco paintings? Technical and material study of casas pintadas of vasco da gama house in Évora (Southern Portugal). *X-Ray Spectrometry, 44*(3), pp.154-162. DOI: 10.1002/xrs.2593
52. (2020), Scanning Electron Microscopy. Retrieved from https://www.nanoscience.com/techniques/scanning-electron-microscopy/
53. Swapp, S., (2020) Scanning Electron Microscopy Retrieved from: https://serc.carleton.edu/research_education/geochemsheets/techniques/SEM.html

54. Sima, F., Ristoscu, C., Duta, L., Gallet, O., Anselme, K., and Mihailescu, I. N., (2016), Laser thin films deposition and characterization for biomedical applications. In L. Overend (Ed.), *Techniques and applications* (pp. 77-125). Elsevier. DOI: 10.1016/B978-0-08-100883-6.00003-4

55. Kohli, R., and Mittal, K.L.. (2019). Methods for assessing surface cleanliness. In K. Rajiv & K. L. Mittal (Eds.), *Developments in surface contamination and cleaning* (12th ed., pp. 23-105). Elsevier. DOI: 10.1016/C2017-0-02437-0

56. Derrick, M. R., Stulik, D., Landry, and J. M., (1999). *Tools for conservation: Infrared spectroscopy in conservation science* (pp.1-3). Getty Publications. ISBN: 047126279X

57. Rajisha, K. R., Deepa, B., Pothan, L. A., and Thomas, S., (2011), Thermochemical and spectroscopic characterization of natural fibre composites. In N. E. Zafeiropoulos (Ed.), *Interface Engineering of Natural Fibre Composites for Maximum Performance* (pp. 241-274). Woodhead Publishing, DOI: 10.1533/9780857092281.2.241

58. Papatzani, S., Dimitrakakis, E., (2019), A Review of the assessment tools for the efficiency of nanolime calcareous stone consolidant products for historic structures. *Buildings, 9* (11) pp. 235. DOI: 10.3390/buildings9110235

59. Rodriguez-Navarro, C., Suzuki A., and Ruiz-Agudo E., (2013), Alcohol dispersions of calcium hydroxide nanoparticles for stone conservation. *Langmuir, 29*(36), pp. 11457−11470. DOI: 10.1021/la4017728

60. Kim, T., and Olek, J., (2012), Effects of sample preparation and interpretation of thermogravimetric curves on calcium hydroxide in hydrated pastes and mortars. *Transportation Research Record, (2290),* pp. 10-18. DOI: 10.3141/2290-02

61. (2020), Dynamic Light Scattering (DLS), Retrieved from: https://www.malvernpanalytical.com/en/products/technology/light-scattering/dynamic-light-scattering

62. Nimesh, S., (2013), Tools and techniques for physics-chemical characterization of nanoparticles. *Gene Therapy: Potential applications for nanotechnology* (1st ed., pp. 43-63). Woodhead Publishing. DOI: 10.1533/9781908818645.43

63. Cosentino, A., (2015). Practical notes on ultraviolet technical photography for art examination. *Conservar Património*, *21*, pp. 53-62. DOI: 10.14568/cp2015006

64. Johnston-Feller, R., (2001). *Tools for conservation: Color science in the examination of museum objects, Nondestructive procedures* (1st ed., pp. 5-13). Getty Publications. ISBN:047126279X

65. Pondelak, A., Kramar, S., Kikelj, M. L., and Sever Škapin, A., (2017), In-situ study of the consolidation of wall paintings using commercial and newly developed consolidants. *Journal of cultural heritage, 28,* pp. 1-8. DOI: 10.1016/j.culher.2017.05.014

66. Pozo-Antonio, J. S., Otero, J., Alonso, P., Mas i Barberà, X., (2019), Nanolime- and nanosilica-based consolidants applied on heated granite and limestone: Effectiveness and durability. *Construction and Building Materials, 201,* pp. 852-870. DOI: 10.1016/ j.conbuildmat.2018.12.213 Townsend, J. H., and Keune, K., (2006), Microscopical techniques applied to traditional paintings. *Infocus Magazine, 41*(1). pp. 54-61. DOI: 10.22443/rms.inf.1.2

67. Townsend, J. H., and Keune, K., (2006), Microscopical techniques applied to traditional paintings. *Infocus Magazine, 41*(1). pp. 54-61. DOI: 10.22443/rms.inf.1.2 Nasrazadani, S., and Eureste, E., (2008), Application of FTIR for Quantitive Lime Analysis, Report number 5-9028-01-1. Retrieved from: https://library.ctr.utexas.edu/digitized/texasarchive/ phase2/9028-01-1.pdf

68. Nasrazadani, S., and Eureste, E., (2008), Application of FTIR for Quantitive Lime Analysis, Report number 5-9028-01-1. Retrieved from: https://library.ctr.utexas.edu/ digitized/texasarchive/phase2/9028-01-1.pdf

69. Becherini, F., Durante, C., Bourguignon, E., Li Vigni, M., Detalle, V., Bernardi, A., Tomasin, P., (2018), Aesthetic compatibility assessment of consolidants for wall paintings by means of multivariate analysis of colorimetric data. *Chemistry Central Journal, 12*(1), pp. 1-10. DOI: 10.1186/s13065-018-0465-7

70. Zhu, J., Li, X., Zhang, Y., Wang, J., Wei, B., (2018), Graphene-Enhanced nanomaterials for wall painting protection. *Advanced Functional Materials, 28*(44), pp. 1-10. DOI: 10.1002/ adfm.201803872

71. Borsoi, G., Lubelli, B., van Hees, R., Veiga, R., and Silva, A.S., (2016), Optimization of nanolime solvent for the consolidation of coarse porous limestone. *Applied Physics A*

Material Science and processing, 122(9), pp. 1-10. DOI: 10.1007/s00339-016-0382-3

72. Borsoi, G., Lubelli, B., van Hees, R., Veiga, R., Silva, A. S., Colla, L., Fedele, L., and Tomasin, P., (2016), Effect of solvent on nanolime transport within limestone: How to improve in-depth deposition. *Colloids and surfaces A: Physicochemical and Engineering Aspects, 497,* pp.171-181. DOI: 10.1016/j.colsurfa.2016.03.007
73. Becerra, J., Zaderenko, A.P., Ortiz, R., Karapanagiotis I., Ortiz, P., (2020), Comparidon of the performance of a novel nanolime doped ZnO quantum dots with common consolidants for historical carbonate stone buildings. *Applied Clay Science, 195,* pp.1-9. DOI: 10.1016/ j.clay.2020.105732
74. Lanzón, M., Stefano, V., Gaitán, J. C., Cardiel, I. B., Gutiérrez-Carrillo, M. L., (2020), Characterization of earthen walls in the Generalife (alhambra): Microstructural and physical changes induced by deposition of Ca(OH)2 nanoparticles in original reconstructed samples. *Construction and Building Materials, 232*, pp.117-202. DOI: 10.1016/ j.conbuildmat.2019.117202
75. Kaszowska, Z., kot, M., Bialek-Kostecka, D., Forczeck-Sajdak, A., (2019), Application of micro-identationv tests to asses the consolidation procedure of historic wall paintings. *Journal of cultural Heritage, 36,* pp.286-296. DOI: 10.1016/j.culher.2018.08.005

Appendices

Appendix 1 Materials and chemicals.

A1-1. *Chemicals used in the thesis research.*

Material	Chemical Formula	Molecular weight (g/mol)	Producer	Purity
		Chemicals		
Calcium Chloride	$CaCl_2$	110.98	Sigma-Aldrich	99.9%
Sodium Hydroxide	NaOH	40	Sigma-Aldrich	99.9%
Triton X100	$(C_2H_4O)_nC_{14}H_{22}O$		Sigma-Aldrich	99.9%
Ethanol	C_2H_6O	46.069	Sigma-Aldrich	99.9%
2-propanol	C_3H_8O	60.10	Merck	99.9%
Acetone	C_3H_6O	58.08	Sigma-Aldrich	99.9%
		Pigments		
Kremer French Ochre RTFLES - 40020®	—	—	Kremer	—
Kremer French Ochre JCLES - 40040®	—	—	Kremer	—
Kremer Smalt - 10010®			Kremer	
		Consolidants		
CaLoSiL® IP25	—	—	IBZ Salzchemie GmbH & Co.KG	25 g/L
Primal™ SF-016 ER®	—	—	Dow Coating Materials	50-51%

Appendix 2 Characterization of the materials used in the preparation of the fresco replicas (pigments, sand and lime).

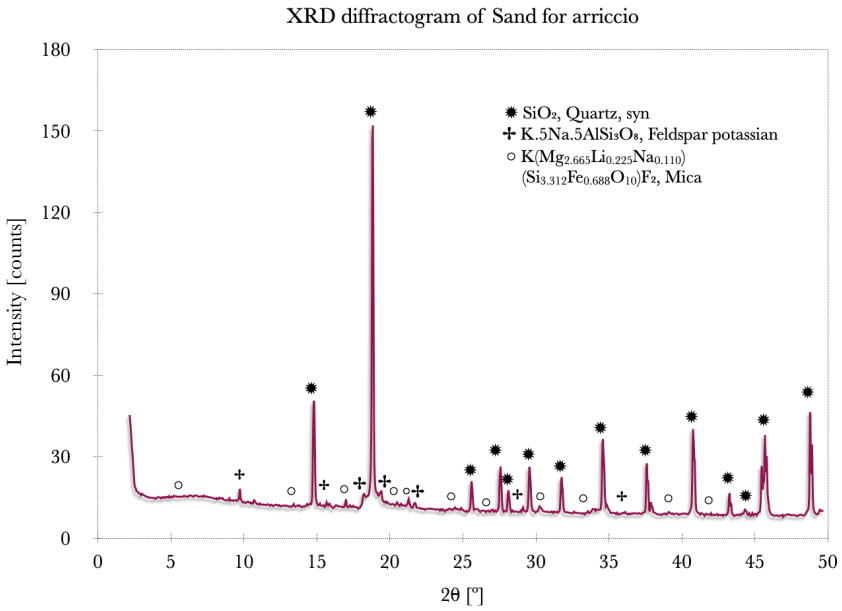

A2-1 *XRD diffractograms of sand used to prepare the arriccio layer.*

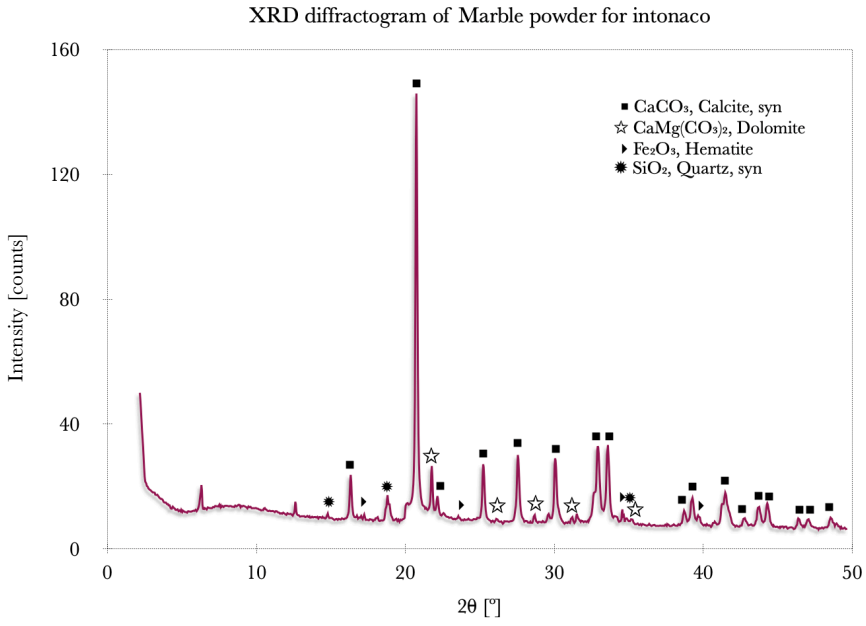

A2-2 *XRD diffractograms of marble powder used to prepare the intonaco layer.*

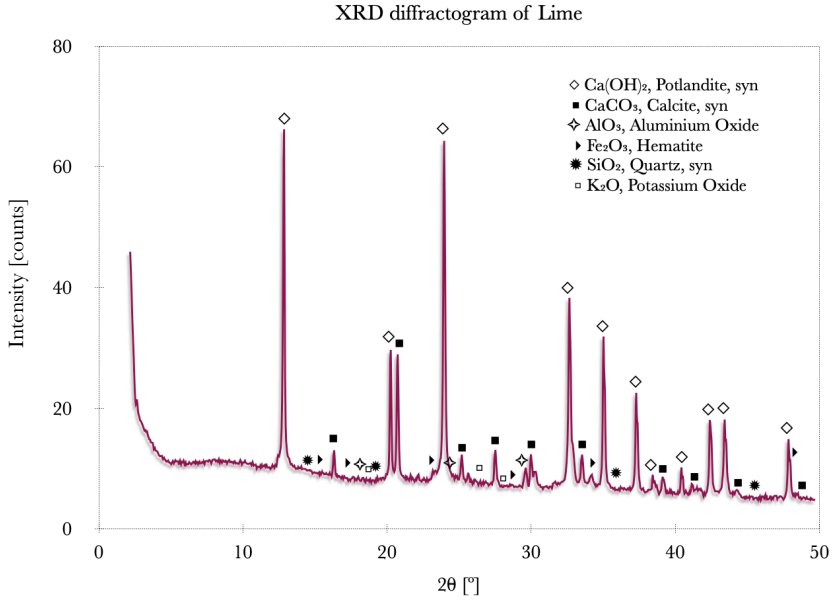

A2-3 *XRD diffractograms of lime used to prepare the mortar layers.*

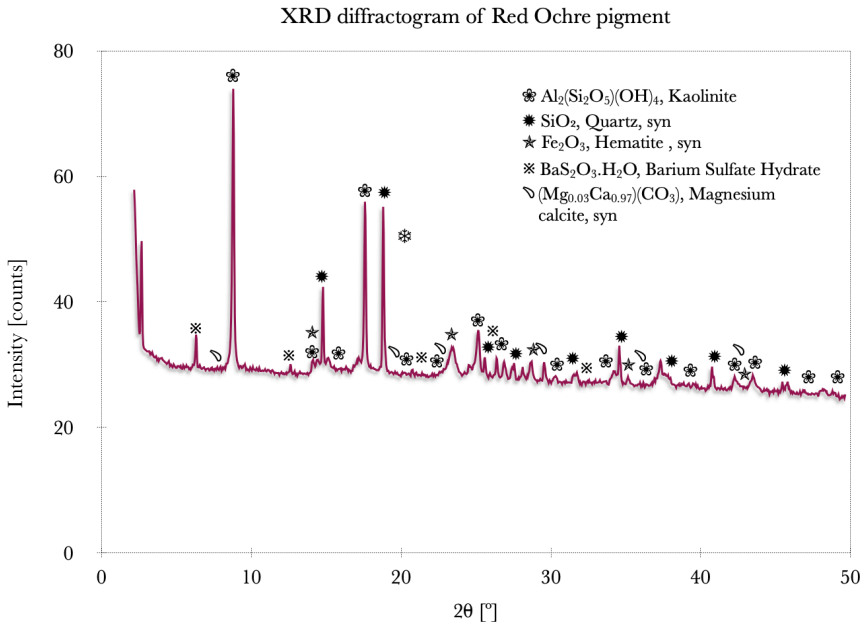

A2-4 *XRD diffractograms of the red ochre pigment.*

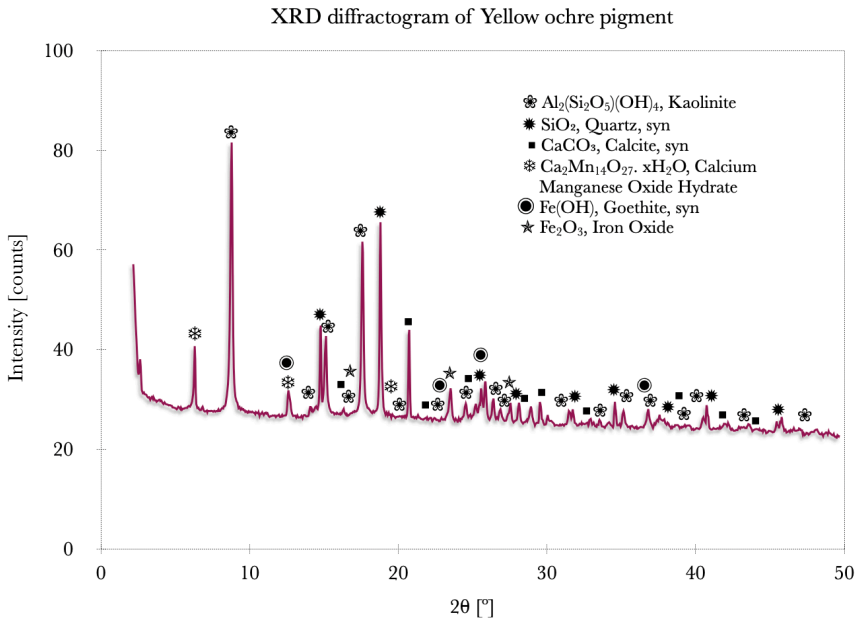

A2-5 *XRD diffractograms of the yellow ochre pigment.*

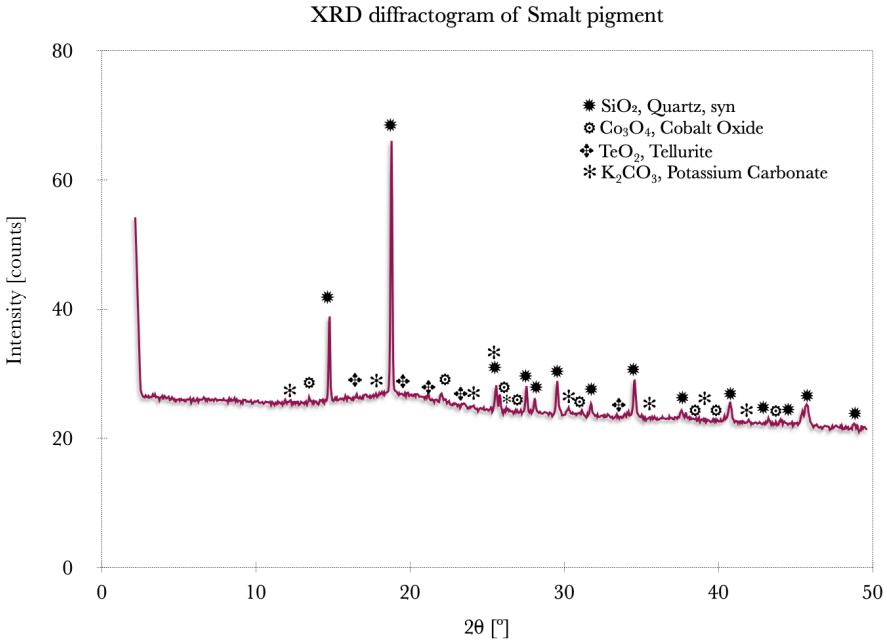

A2-6 *XRD diffractograms of the smalt pigment.*

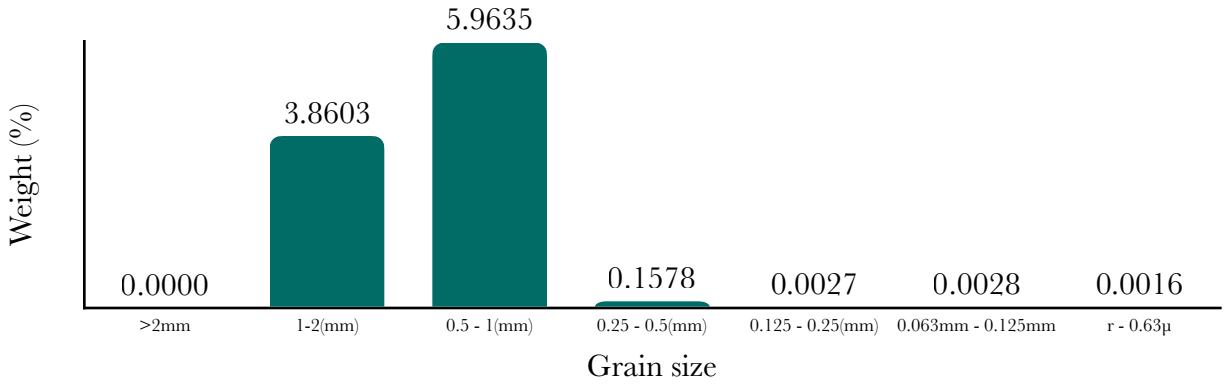

A2-7 *Grain-size distribution of the sand used for the arriccio mortar layer preparation with an error percentage of 0.23%.*

Appendix 3 Additional data concerning the characterization of the laboratory synthesized HERCULES nanolime.

A3-1. *Theoretical and actual yield data used for the calculation of the synthesis yield.*

	S1	S3	S4
Theorical mass (g)	7.4	3	3
Experimental mass (g)	3.2	1.6	1.1
Yield (%)	43.5	52.7	45.3

TGA analysis of the nanolimes

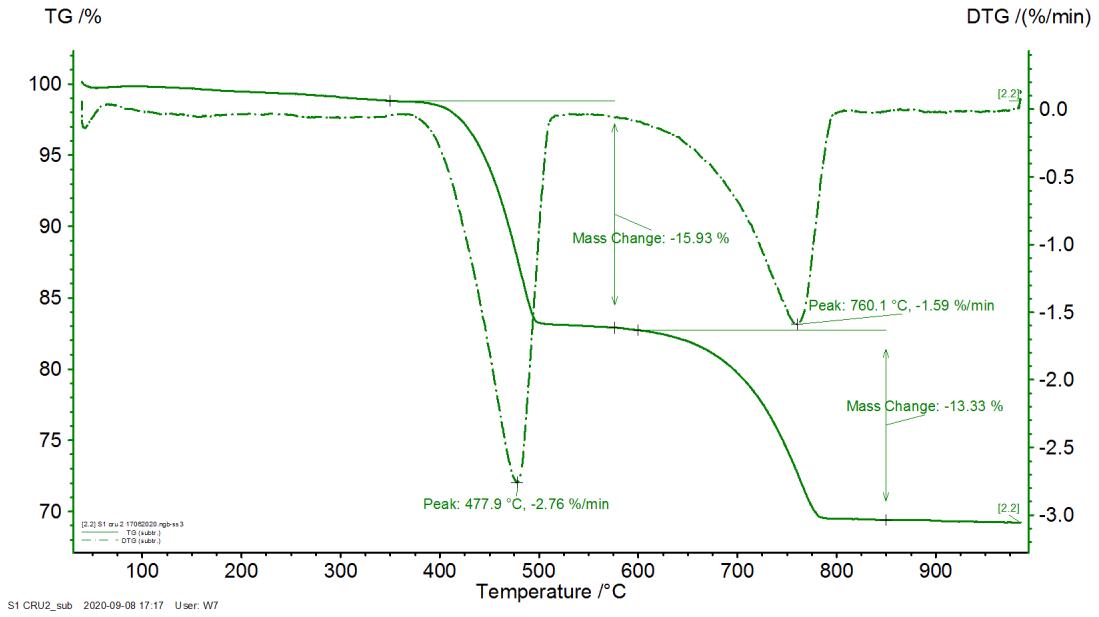

A3-2. *TGA-DTG results of HERCULES nanolime.*

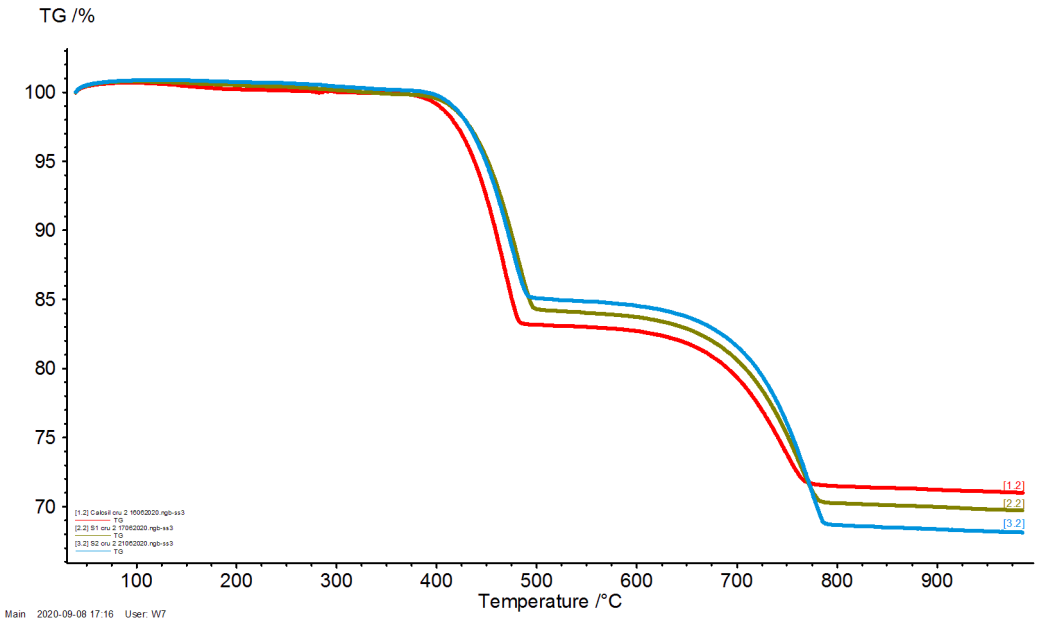

***A3-3**. TGA results of HERCULES nanolime (green and blue lines) in comparison to CaLoSiL® (red line).*

SEM images of tested HERCULES nanolime dispersions.

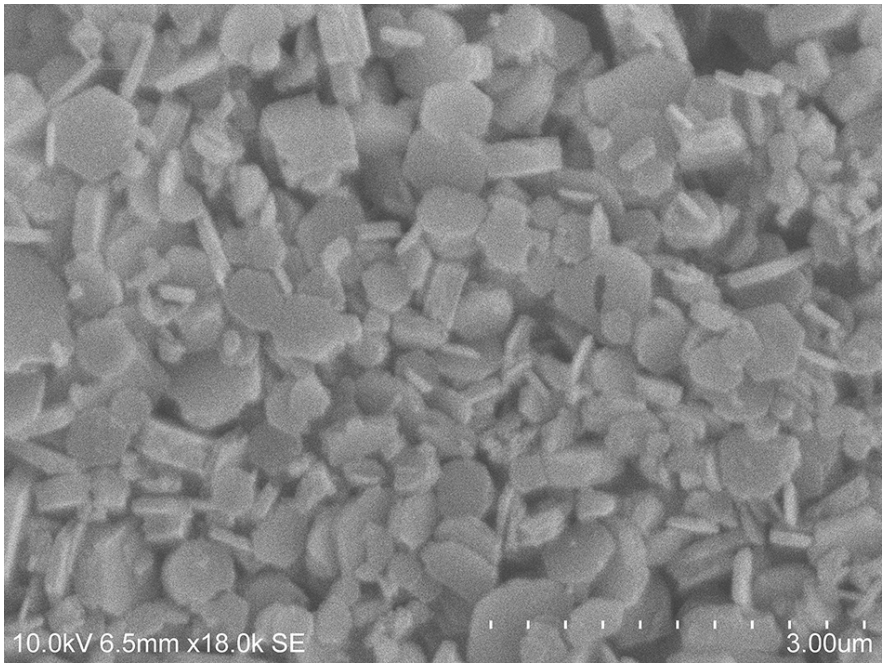

***A3-4.** SEM image of tested HERCULES nanolime dispersion in Acetone:2-Propanol (1:10).*

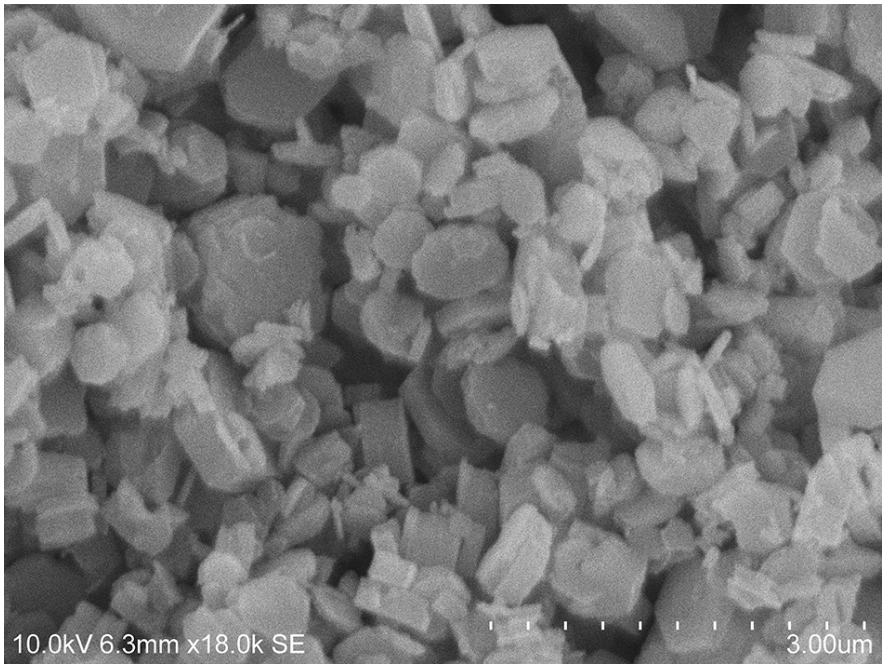

A3-5. *SEM image of tested HERCULES nanolime dispersion in Acetone.*

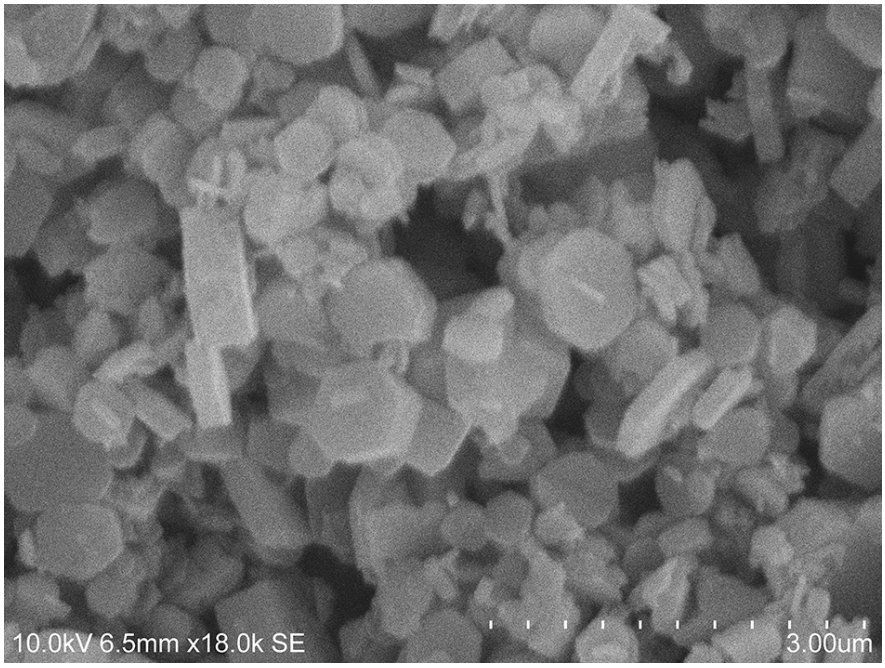

A3-6. *SEM image of tested HERCULES nanolime dispersions in H_2O:2-Propanol (1:10).*

Appendix 4 Additional data concerning the treatment evaluation.

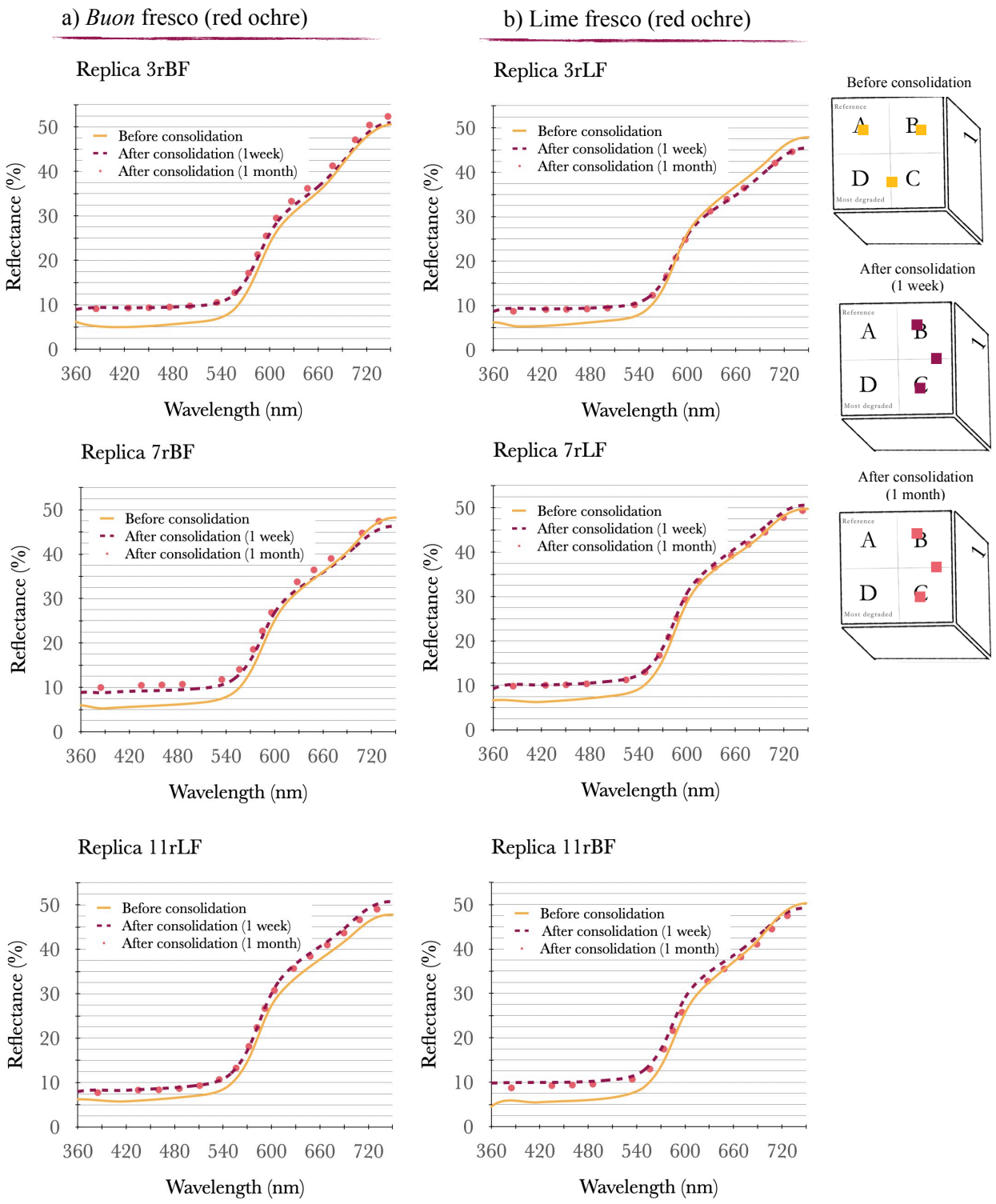

A4-1 *. Reflectance spectral curves of all red ochre replicas treated with HERCULES nanolime: a) Buon fresco replicas (left side): 3rBF, 7rBF, and 11rBF; and b) Lime fresco replicas (right side): 3rLF, 7rLF, and 11rLF.*

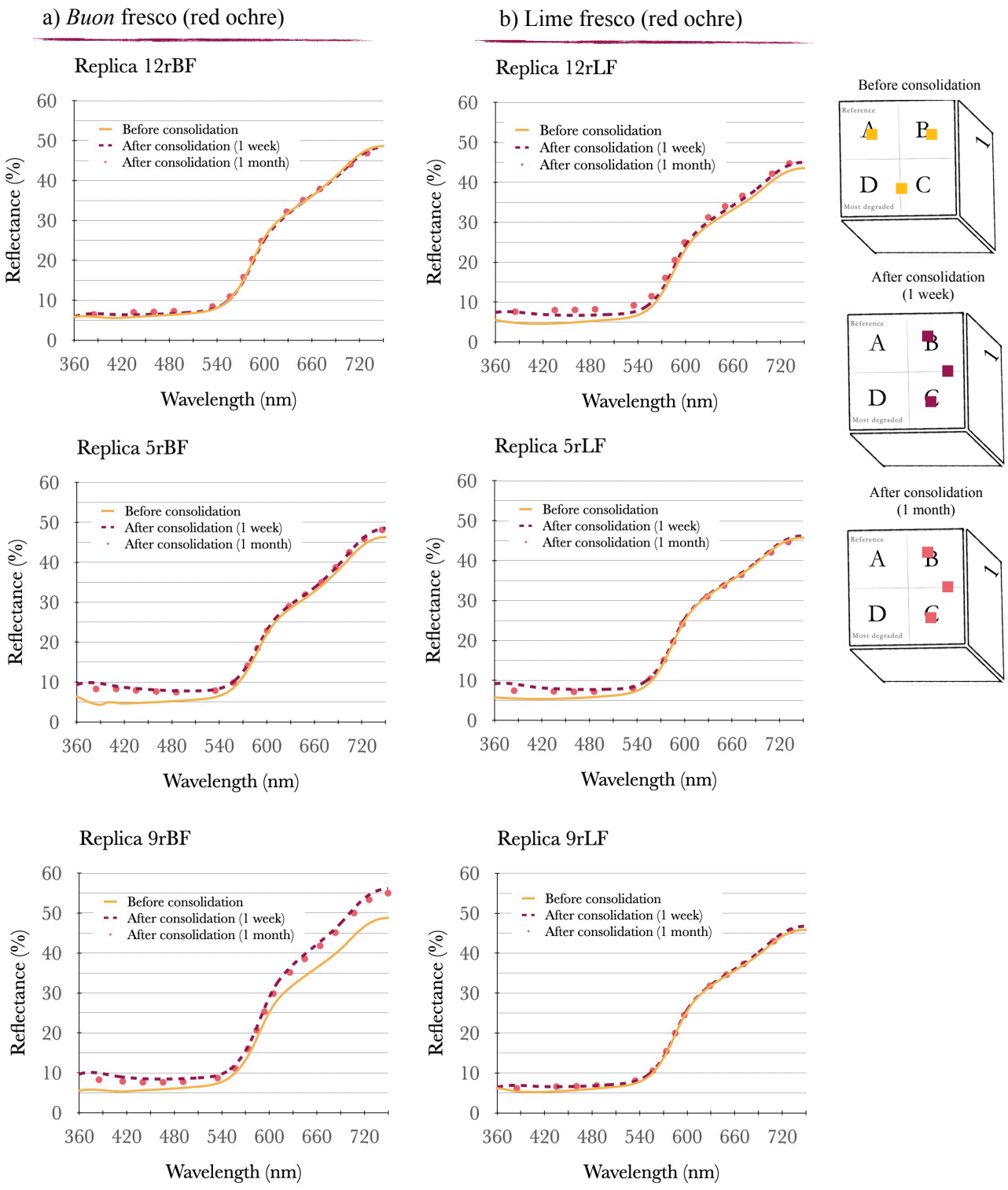

***A4-2**. Reflectance spectral curves of all red ochre replicas treated with CaLoSiL®: a) Buon fresco replicas (left side): 3rBF, 7rBF, and 11rBF; and b) Lime fresco replicas (right side): 3rLF, 7rLF, and 11rLF.*

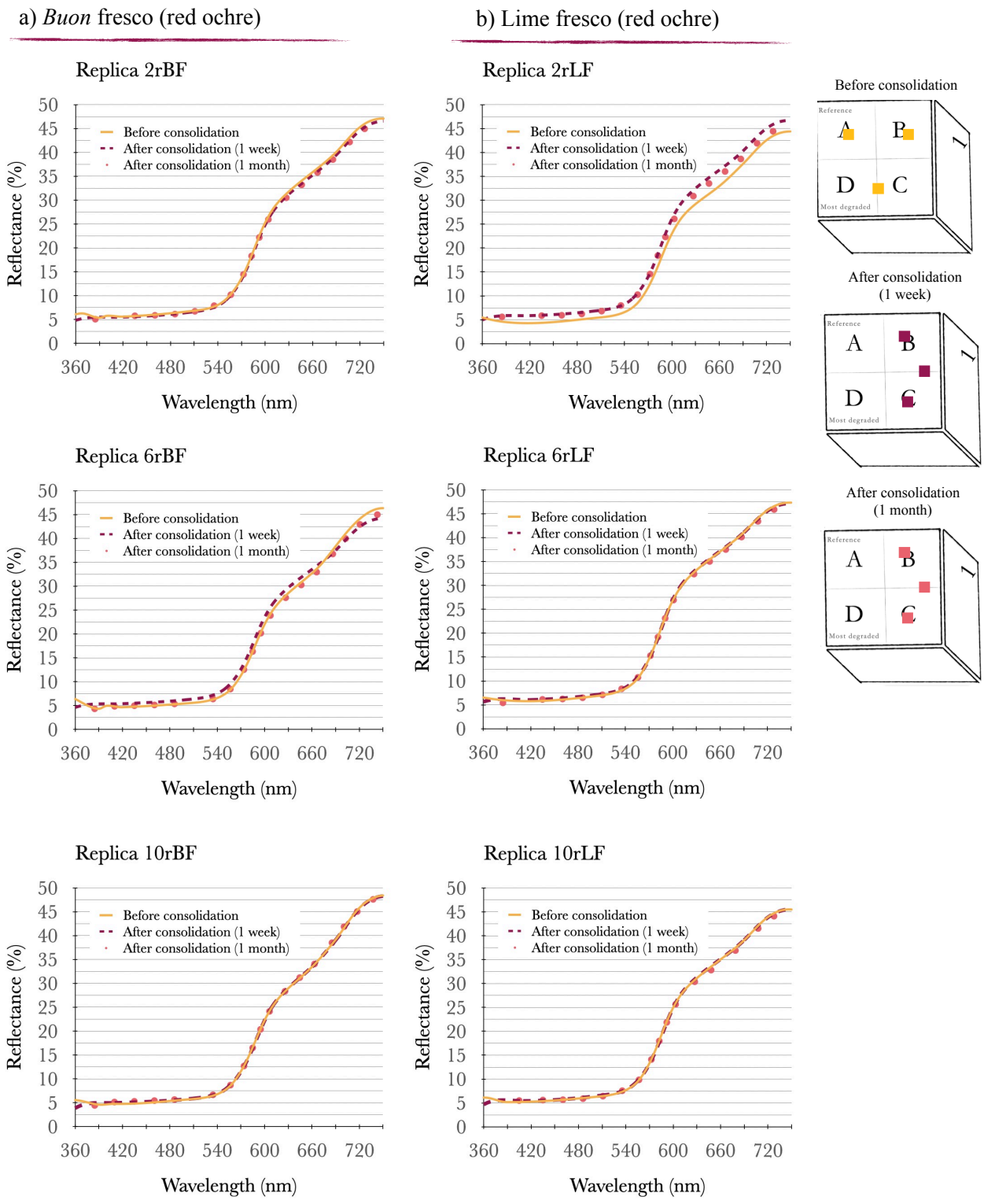

***A4-3**. Reflectance spectral curves of all red ochre replicas treated with Primal®: a) Buon fresco replicas (left side): 2rBF, 6rBF, and 10rBF; and b) Lime fresco replicas (right side): 2rLF, 6rLF, and 10rLF.*

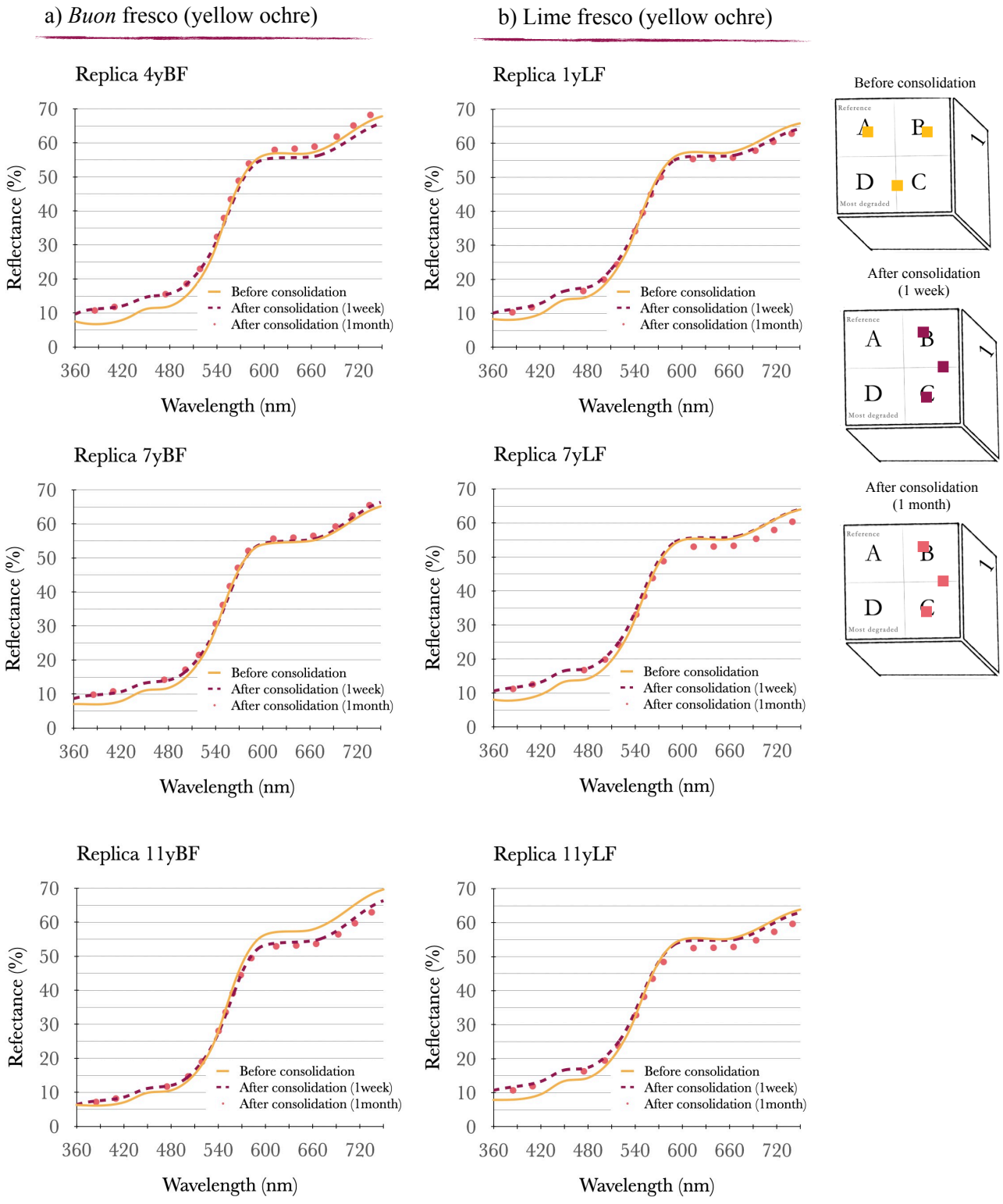

***A4-4**. Reflectance spectral curves of all yellow ochre replicas treated with HERCULES nanolime: a)Buon fresco replicas(left side): 3rBF, 7rBF, and 11rBF; and b) Lime fresco replicas(right side): 3rLF, 7rLF and 11rLF.*

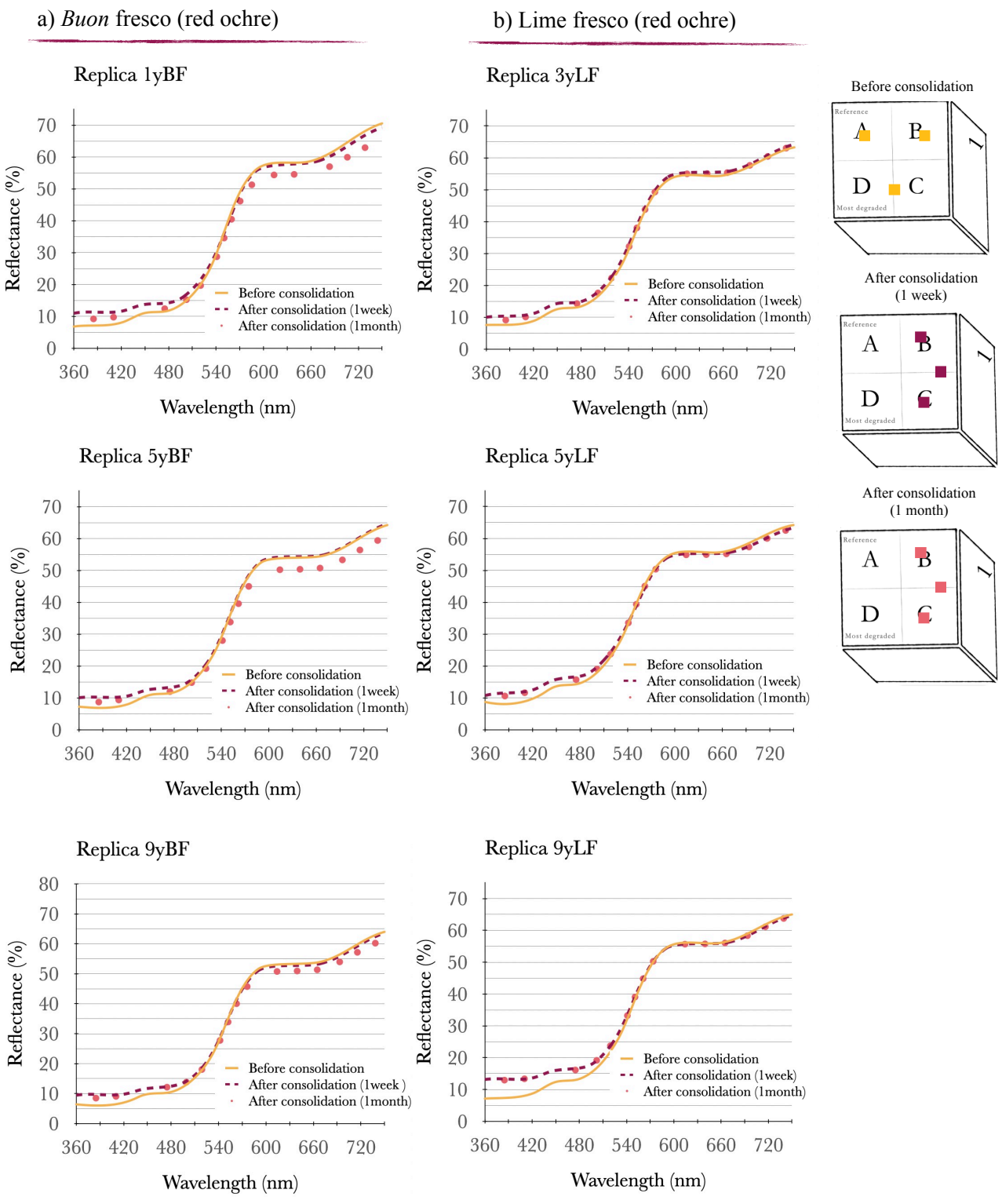

***A4-5**. Reflectance spectral curves of all yellow ochre replicas treated with CaLoSiL®: a)Buon fresco replicas (left side): 1yBF, 5yBF, and 9yBF; and b) Lime fresco replicas (right side): 3yLF, 5yLF, and 9yLF.*

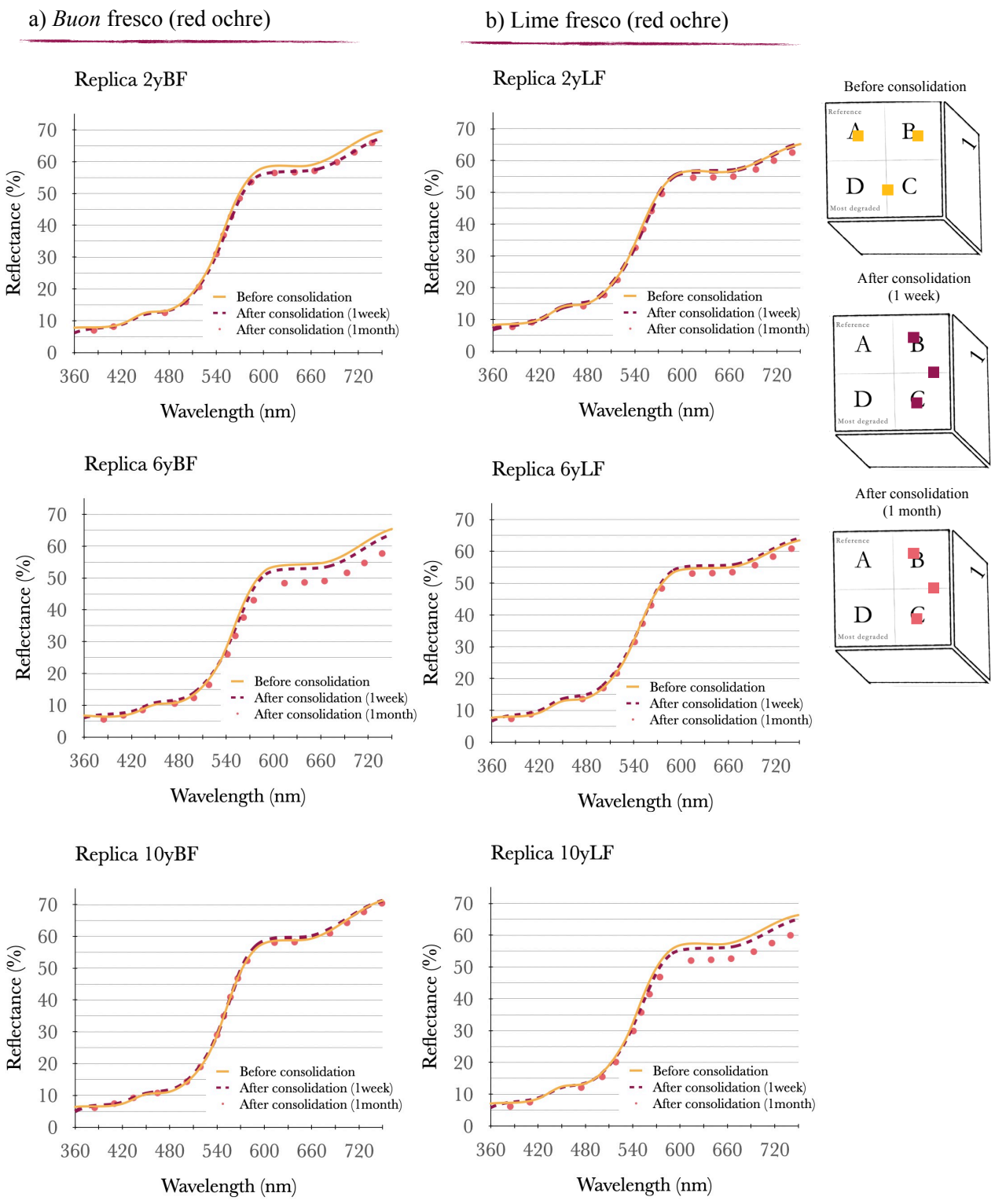

***A4-6**. Reflectance spectral curves of all yellow ochre replicas treated with Primal®: a) Buon fresco replicas (left side): 2yBF, 6yBF, and 10yBF; and b) Lime fresco replicas (right side): 2yLF, 6yLF, and 10yLF.*

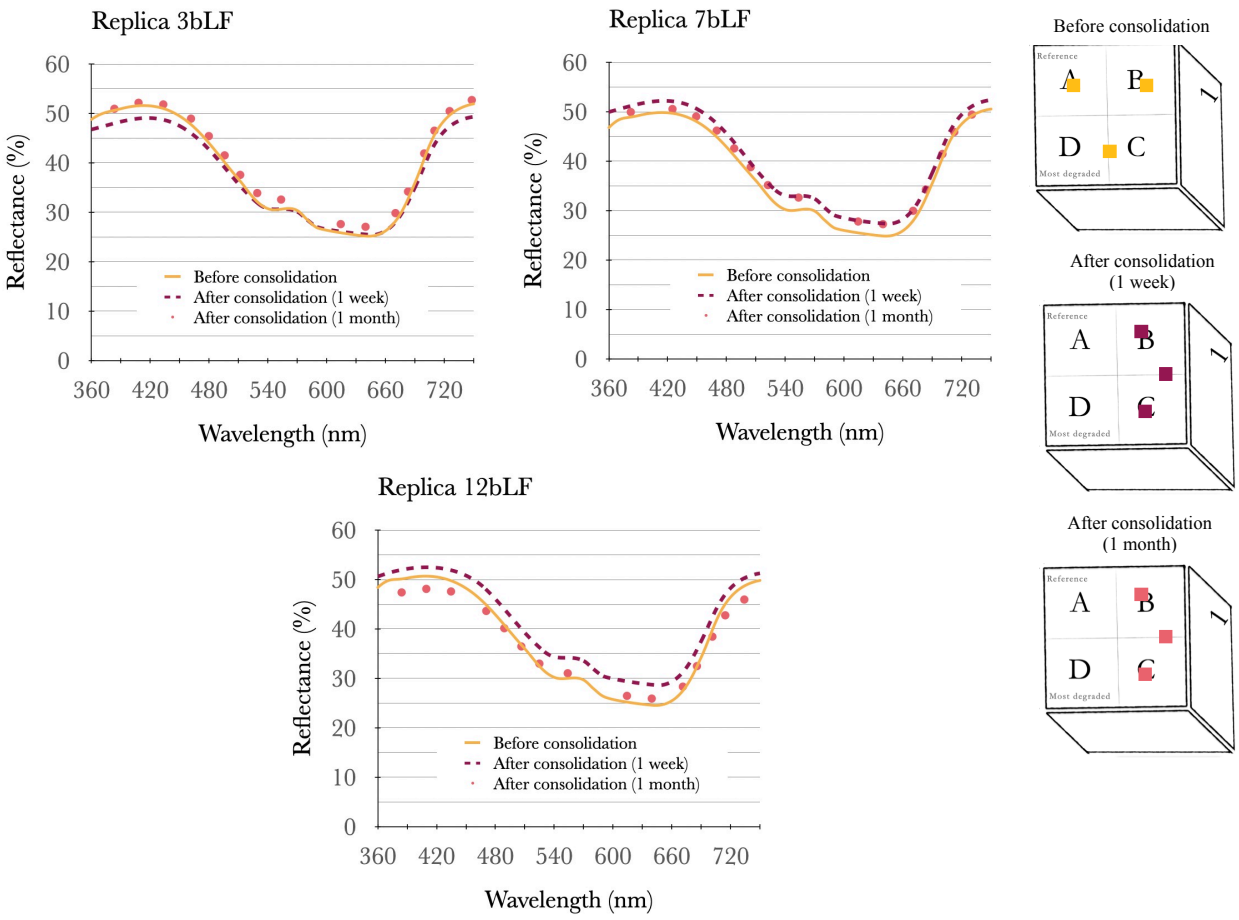

***A4-7**. Reflectance spectral curves of smalt replicas (3bLF, 7bLF, and 12bLF) treated with HERCULES nanolime.*

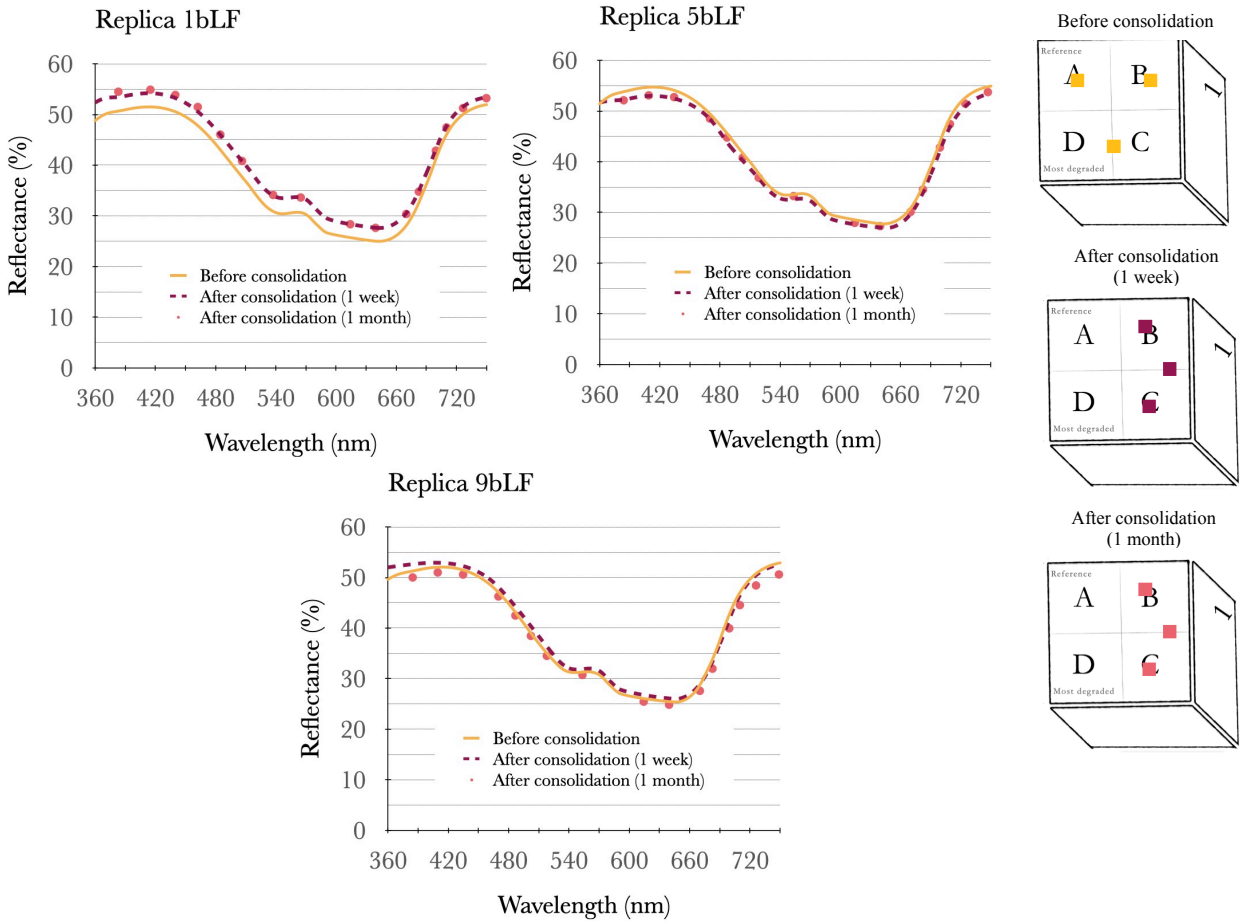

***A4-8**. Reflectance spectral curves of smalt replicas (1bLF, 5bLF, and 9bLF) treated with CaLoSiL®.*

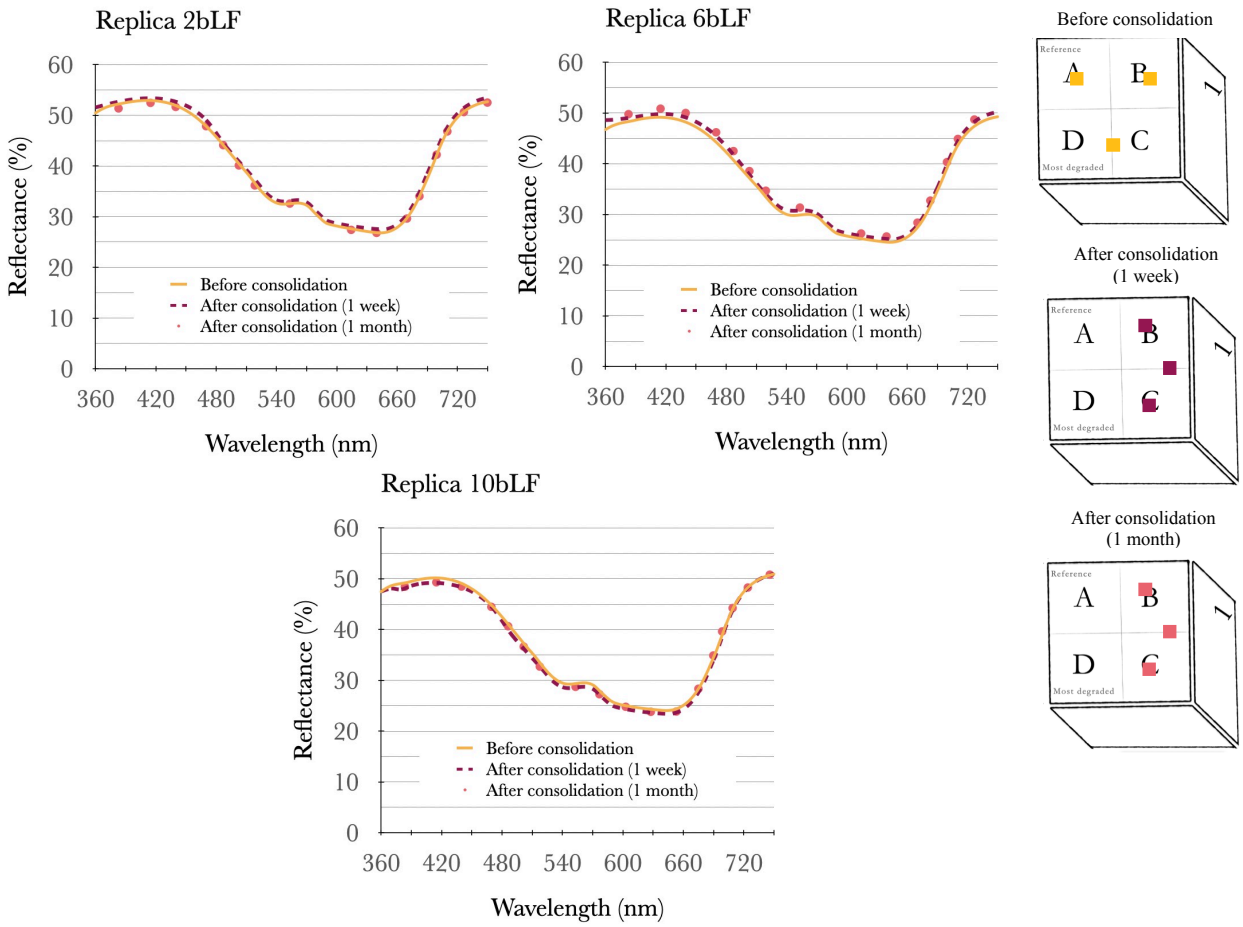

***A4-9**. Reflectance spectral curves of smalt replicas (1bLF, 5bLF, and 9bLF) treated with Primal®.*

Cross- sections

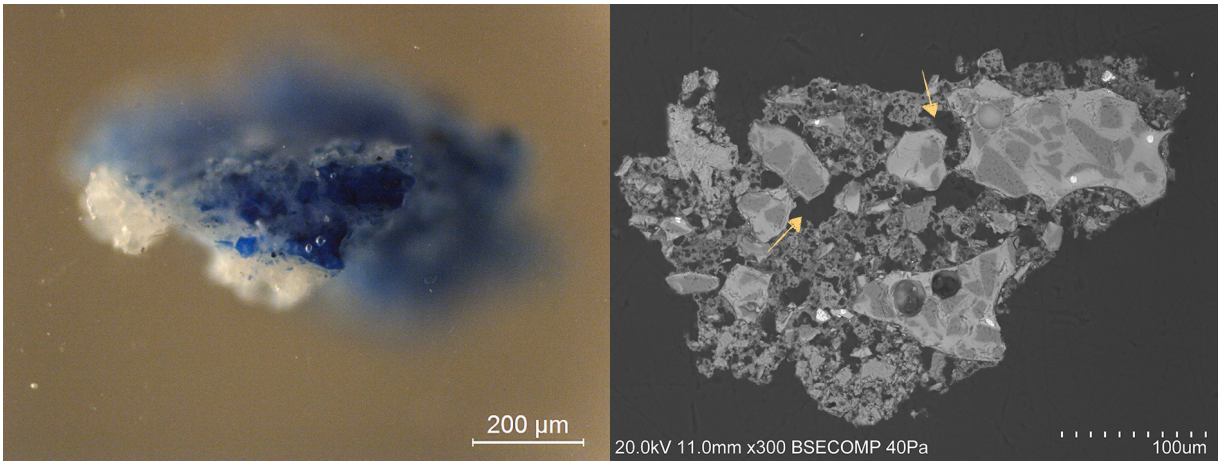

***A4-10.** Untreated reference; on the left OM picture (X100); on the right SEM image were its possible to observe loss of cohesion.*

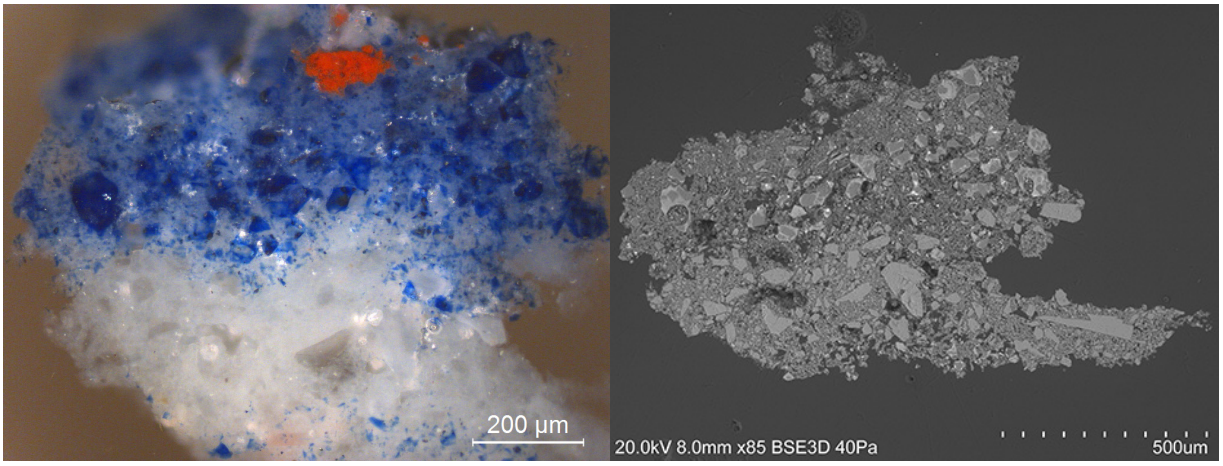

A4-11. *Treated with CaLoSiL® ; on the left OM picture (X500); on right SEM image were the general area of the cross-section is observed.*

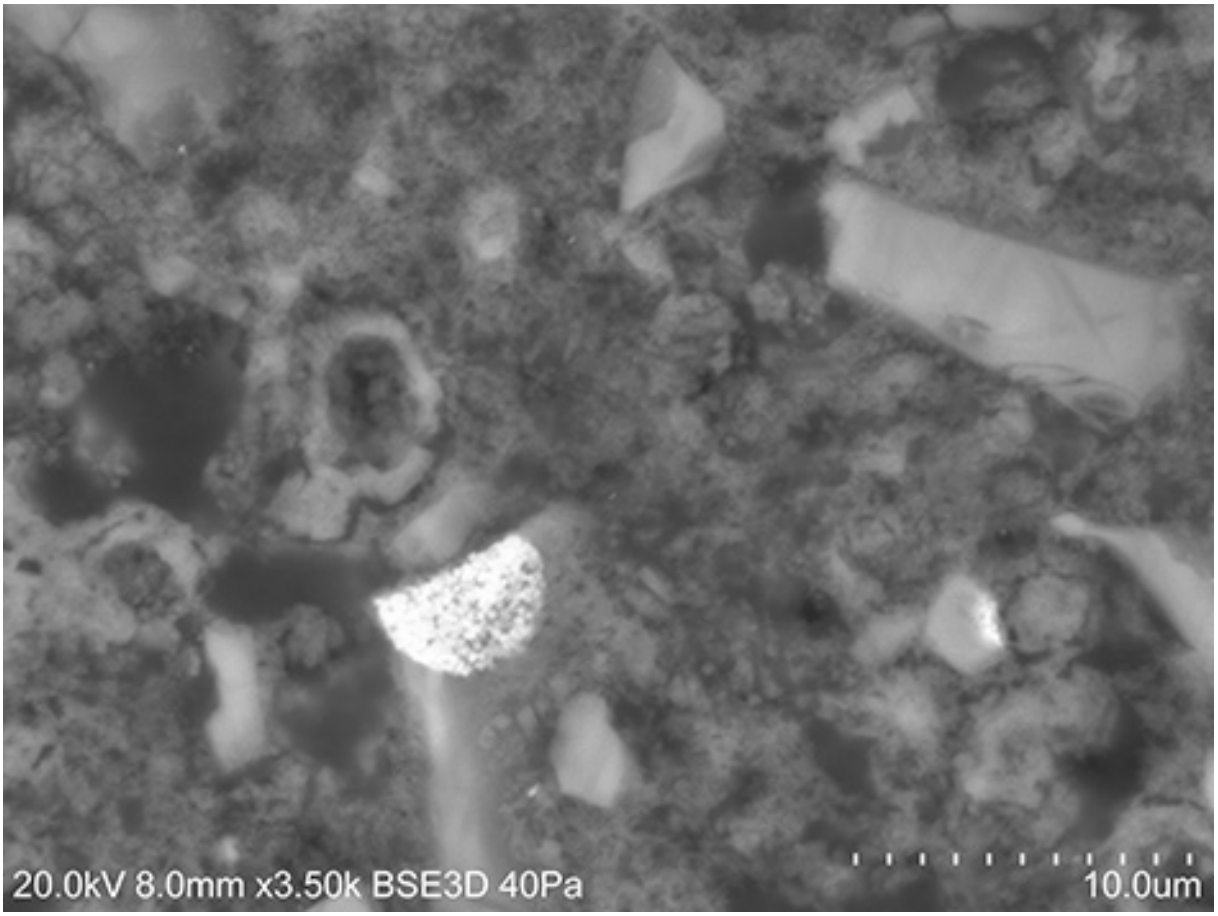

A4-12. *SEM image of the paint layer cross-section of replica 1bLF treated with CaLoSiL®. Where it is possible to observe the formation of a layer between pigment particles.*

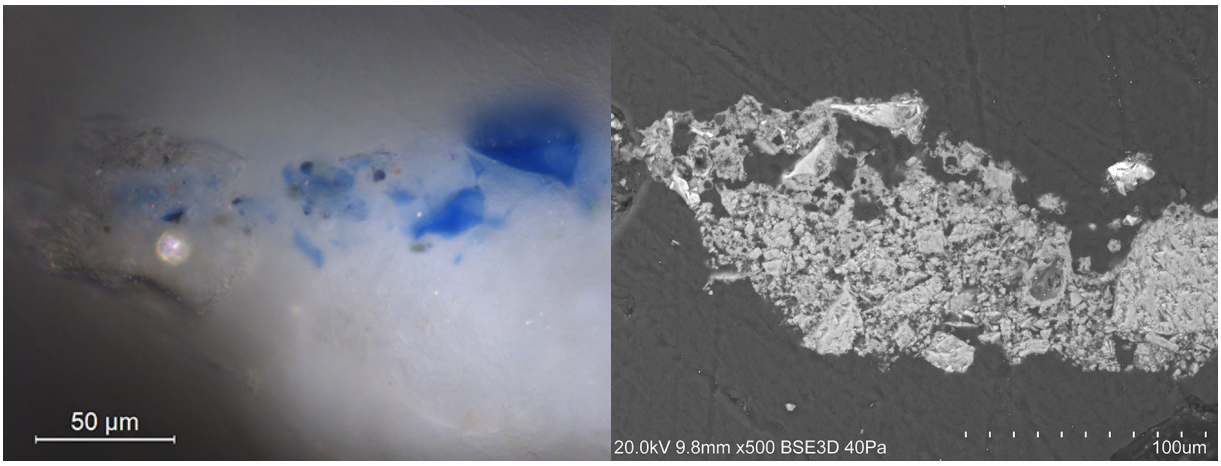

A4-13. *Treated with the HERCULES nanolime; on the left OM picture (X500); on right SEM image were the general area of the cross-section is observed (NPs were not observed).*